TECHNICAL REPORT STANDARD PAGE

1. Title and Subtitle
Correlation of Rut Depths Measured by the Profilers of LTRC and DOTD PMS
2. Author(s)
Qiming Chen and Zhongjie Zhang
3. Performing Organization Name and Address
Louisiana Transportation Research Center
4101 Gourrier Avenue
Baton Rouge, LA 70810
4. Sponsoring Agency Name and Address
Louisiana Department of Transportation and Development
P.O. Box 94245
Baton Rouge, LA 70804-9245

5. Report No.
FHWA/LA.23/681
6. Report Date
August 2023
7. Performing Organization Code
LTRC Project Number: 21-2P
SIO Number: DOTLT1000387
8. Type of Report and Period Covered
Final Report
November 2020 to May 2023
9. No. of Pages
153
10. Supplementary Notes
Conducted in Cooperation with the U.S. Department of Transportation, Federal Highway Administration
11. Distribution Statement
Unrestricted. This document is available through the National Technical Information Service, Springfield, VA 21161.
12. Key Words
Rut Depth, Full Profile, 5-Point, Correlation, Cracks

13. Abstract
This research study aimed at developing a correlation of rut depths measured with Louisiana Transportation Research Center's (LTRC's) profiler with a 5-point laser system and Department of Transportation and Development (DOTD) Pavement Management System's (PMS's) profiler with a scanning laser system. For this purpose, the transverse profile data collected in 2020 and 2021 at the eight pavement management control sites with flexible and composite pavement by both LTRC and Fugro road profilers were analyzed. Additionally, 25 sites were selected to represent the typical pavement conditions and characteristics of the Louisiana highway network.

Three repeat runs of LTRC's 5-point rut bar system were first made at six control sites and four selected sites. The correlations of the calculated rut depths indicated that the repeatability of LTRC's 5-point rut depth at the individual point level was not that good. However, averaging rut depths over 0.004-mile and 0.1-mile increments showed noticeable improvements of correlation, especially for average rut depths over 0.1 mile which achieved an overall correlation value of 0.90 and above.

The current rut algorithm of Roadware Vision causes incorrect measurements that include measurements in cracks, measurements outside wheel path, and failure of locating the point of maximum rut depth. LTRC's 5-point rut bar system cannot always capture the maximum rut depth for transverse profiles (missing the peak and valley). It can also be significantly affected by the edge drop off and grass for right wheel path (RWP) rut depth.

The correlations of average rut depths were higher than correlations of the left wheel path (LWP) and RWP. Averaging rut depths over 0.1-mile increment showed noticeable improvement of correlation between LTRC and Fugro road profilers. The results of t-tests showed that mean values of LTRC's 5-point rut depth and Fugro's full profile rut depth were statistically different at all scales (individual rut depth, 0.004-mile average rut depth, and 0.1-mile average rut depth). The t-tests also showed that the mean values of LTRC's and Fugro's 5-point rut depth were statistically differently at individual and 0.004-mile average level. However, with careful planning, the difference between the mean value of LTRC's 5-point rut depth and Fugro's 5-point rut depths at 0.1-mile average level could be statistically insignificant.

A standard operating procedure (SOP) was developed to standardize the process of collecting and compiling rutting data by LTRC at the network level and delivering them to DOTD engineers for conducting/supporting pavement management activities.

Project Review Committee

Each research project will have an advisory committee appointed by the LTRC Director. The Project Review Committee is responsible for assisting the LTRC Administrator or Manager in the development of acceptable research problem statements, requests for proposals, review of research proposals, oversight of approved research projects, and implementation of findings.

LTRC appreciates the dedication of the following Project Review Committee Members in guiding this research study to fruition.

LTRC Administrator/Manager

Zhongjie Zhang

Pavement and Geotechnical Research Administrator

Members

Christophe Fillastre

Mark Ordogne

Xingwei Chen

Jason Lacombe

Patrick Icenogle

Scott Nelson

Directorate Implementation Sponsor

Christopher P. Knotts, P.E.

DOTD Chief Engineer

Correlation of Rut Depths Measured by the Profilers of LTRC and DOTD PMS

By
Qiming Chen
Zhongjie Zhang

Louisiana Transportation Research Center
4101 Gourrier Avenue
Baton Rouge, LA 70808

LTRC Project No. 21-2P
SIO No. DOTLT1000387

conducted for
Louisiana Department of Transportation and Development
Louisiana Transportation Research Center

August 2023

Abstract

This research study aimed at developing a correlation of rut depths measured with Louisiana Transportation Research Center's (LTRC’s) profiler with a 5-point laser system and Department of Transportation and Development (DOTD) Pavement Management System's (PMS’s) profiler with a scanning laser system. For this purpose, the transverse profile data collected in 2020 and 2021 at the eight pavement management control sites with flexible and composite pavement by both LTRC and Fugro road profilers were analyzed. Additionally, 25 sites were selected to represent the typical pavement conditions and characteristics of the Louisiana highway network.

Three repeat runs of LTRC's 5-point rut bar system were first made at six control sites and four selected sites. The correlations of the calculated rut depths indicated that the repeatability of LTRC's 5-point rut depth at the individual point level was not that good. However, averaging rut depths over 0.004-mile and 0.1-mile increments showed noticeable improvements of correlation, especially for average rut depths over 0.1 mile which achieved an overall correlation value of 0.90 and above.

The current rut algorithm of Roadware Vision causes incorrect measurements that include measurements in cracks, measurements outside wheel path, and failure of locating the point of maximum rut depth. LTRC's 5-point rut bar system cannot always capture the maximum rut depth for transverse profiles (missing the peak and valley). It can also be significantly affected by the edge drop off and grass for right wheel path (RWP) rut depth.

The correlations of average rut depths were higher than correlations of the left wheel path (LWP) and RWP. Averaging rut depths over 0.1-mile increment showed noticeable improvement of correlation between LTRC and Fugro road profilers. The results of t-tests showed that mean values of LTRC's 5-point rut depth and Fugro's full profile rut depth were statistically different at all scales (individual rut depth, 0.004-mile average rut depth, and 0.1-mile average rut depth). The t-tests also showed that the mean values of LTRC's and Fugro's 5-point rut depth were statistically differently at individual and 0.004-mile average level. However, with careful planning, the difference between the mean value of LTRC's 5-point rut depth and Fugro's 5-point rut depths at 0.1-mile average level could be statistically insignificant.

A standard operating procedure (SOP) was developed to standardize the process of collecting and compiling rutting data by LTRC at the network level and delivering them to DOTD engineers for conducting/supporting pavement management activities.

Acknowledgments

This research project was funded by the Louisiana Department of Transportation and Development (DOTD) (SIO NO. DOTLT1000387) and the Louisiana Transportation Research Center (LTRC Project No. 21-2P). The contributions of Terrell Gorham and Biyuan Zheng are noteworthy.

Implementation Statement

A standard operating procedure (SOP) was developed to standardize the process of collecting and compiling rutting data by LTRC at the network level and delivering them to DOTD engineers for conducting/supporting pavement management activities.

Table of Contents

List of Tables

List of Figures

Introduction

Rutting is one of the major distresses observed in asphalt pavement. It is defined as the surface depression occurring in the wheel paths of roadways. Pavement rut is the accumulation of permanent deformation in all of the layers in a pavement structure. It is generally caused by consolidation or lateral movement of pavement materials or subgrade due to repeated traffic loading. Pavement ruts tend to hold water and cause vehicle hydroplaning, thus resulting in dangerous driving conditions and weather related accidents. Pavement rut also affects the pavement structure integrity. For these reasons, Louisiana Department of Transportation and Development (DOTD) regularly monitors the levels of rut depth in pavement. It is one type of distress data collected by DOTD's Pavement Management System (PMS). It is also a required performance measurement specified in the Highway Performance Monitoring System (HPMS).

Louisiana Transportation Research Center (LTRC) currently owns a road profiler, which uses a 5-point rut bar system for pavement rut depth measurements. In other words, LTRC's profiler uses point lasers to measure the elevation of the bar over the pavement surface at five different points across the lane. One laser is located in the center, one laser in each wheel path, and one wing laser on each side oriented at a 45˚ angle as shown in Figure 1.

The rut depth is obtained by drawing a line from the elevation at the left/right wing laser to the elevation at the center laser. The difference between the elevations of the bar over the line and over the pavement surface at the left/right wheel path is the rut depth for the left/right wheel path [1].

Figure 1. LTRC's road profiler

DOTD is currently contracting with Fugro to collect pavement rut depth data for its PMS. As shown in Figure 2, Fugro uses an automatic road analyzer (ARAN) equipped with a Pave3D system for the pavement profile data collection. The Pave3D system, which uses two scanning lasers as shown in Figure 2, utilizes the latest 3D laser scanning technology (i.e., the Laser Crack Measurement System (LCMS)). This scanning laser system is capable of acquiring high-resolution 3D range data (0.04 in. in the transverse direction with transverse width of 13 ft., i.e., 4096 points across the lane) at high speed (up to 62 mph) to create a detailed transverse profile for rutting calculations and has a depth accuracy of 0.02 in. [2].

Figure 2. Fugro's ARAN [2]

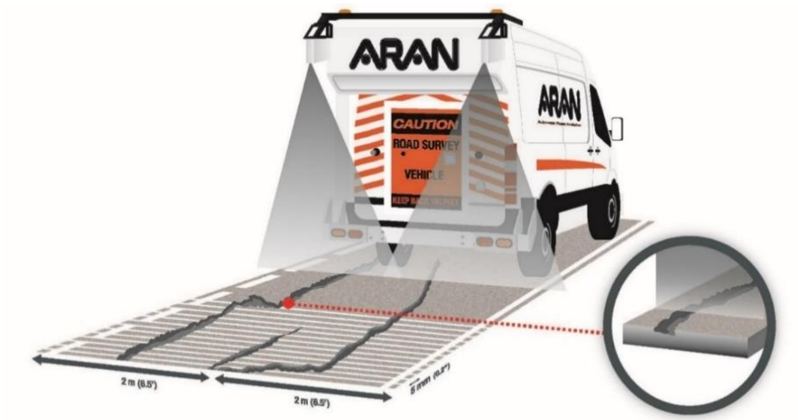

The blue profile in Figure 3 shows a typical transverse profile data collected by the Pave3D system. The rut depth directly estimated from the blue profile obviously would be affected by the anomalies, i.e., spikes abnormally higher or lower than the surrounding range data, thus resulting in unreasonable rutting values. The causes of anomalies include bottom of the crack, loose rocks on the pavement surfaces, vegetation, and so on. DOTD's PMS section had encountered this issue in the early stage when it converted to the scanning laser for the profile data collection. Various algorithms have been proposed in the literature to smooth the transverse profile (i.e., remove high-frequency variations resulting from the pavement surface texture, the noise, the anomalies, etc.). The proposed algorithms in the literature include median filter, discrete cosine transform, moving average, etc. The red line is the transverse profile after smoothing process.

Figure 3. LCMS profile data [3]

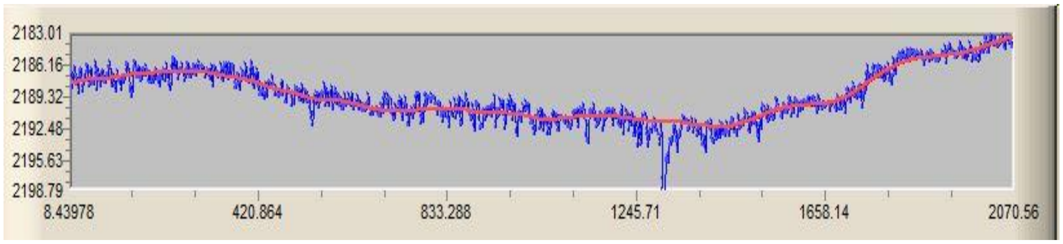

Based on the Vision rutting post processor settings presented by the Pavement Management Systems Section (Figure 4), the algorithm used to smooth the transverse profile in DOTD’s PMS is the moving average with a window size of five. A 1.8-m straightedge is simulated to calculate the rut depth after the transverse profile is smoothed.

Because of the difference in rut model and algorithm, it is obvious that the two systems will result in some differences of calculated rut depths. Pavement Management Systems Section of DOTD often requests LTRC to collect rutting data for the pavement management control sites and compare them with the data in DOTD’s PMS. The correlation of calculated rut depths between these two systems should be established for us to better understand the rutting data collected by LTRC and the rutting data in DOTD's PMS. It is also believed that, in the long run, LTRC is going to move towards the latest scanning laser technology. To ensure that the historical data can be kept for future referencing and a smooth transition, a good correlation is also necessary.

Figure 4. Vision's rutting post processor settings [4]

1. Profile Validity	
Maximum height	0.1
Maximum spacing	0.1
Minimum length	3
Percent of valid points	80
Validate Profile	True
2. Resample	
Profile Resample	None
3. Profile Smoothing	
Smooth Profile	MovingAverage
Window Length	5
4. Edge Detection	
Correct profile	True
Distace from center	1
Edge search	Full
Edge side	RightOnly
Mutliplier	2.5
Point separation	4
5. Ponding	
Calculate Ponding	False
6. Rut Boundaries	
Default Lane Width	3.048
Minimum Lane Width	2.2
Rut Search Range	PavementWidth
7. Rut Algorithm	
Edge length	1.8
Measurement line drop	Perpendicular
Method	StraightEdge
Search range	HalfLane
8. Selection Options	
Deviation	0.1
Selection	Optimal
9. Correct Transverse Profile	
Left Profile Rotate Angle	0
Right Profile Rotate Angle	0

Literature Review

The technologies to obtain pavement rutting measurements have evolved in the last decades from manual methods (e.g., straightedge method), to point-based rut bar systems (e.g., 5-point rut bar systems), then to 3D laser scanning systems (e.g., LCMS).

Manual Measurement Methods

The traditional manual method for measuring rut depth is by placing a straightedge across the rut as shown in Figure 5 and specified in ASTM 1703 [5]. A sufficient number of measurements should be made along the straightedge to determine the maximum distance between the straightedge and the pavement. The maximum distance is determined as the rut depth for the wheel path. Using a wire in place of a straightedge compensates for the curvature of the road surface. However, it requires two people to stretch the wire from the centerline to the shoulder while a third person measures the distance between the wire and the pavement [6]. Figure 6 compares the straightedge method and wire method. The straightedge and wire methods would produce the same results as long as the straightedge length is long enough to cover the same support points at the ends of the wheel path. However, the straightedge is generally placed only across a wheel path. Therefore, the straightedge and wire would provide different information for profile case 1 as shown in Figure 6. Because the manual methods are time-consuming, labor-intensive, and unsafe, especially on highways with high traffic volume, they are gradually being phased out and replaced with automated methods. As shown in Figure 6, there are two definitions for the rut depth: (1) perpendicular to the datum of the elevation measurements, or (2) perpendicular to the straightedge. Bennett and Wang estimated the difference in magnitude for both cases, concluding that the difference is not significant for the range of rut depth commonly found [7].

Figure 5. Straightedge method [5]

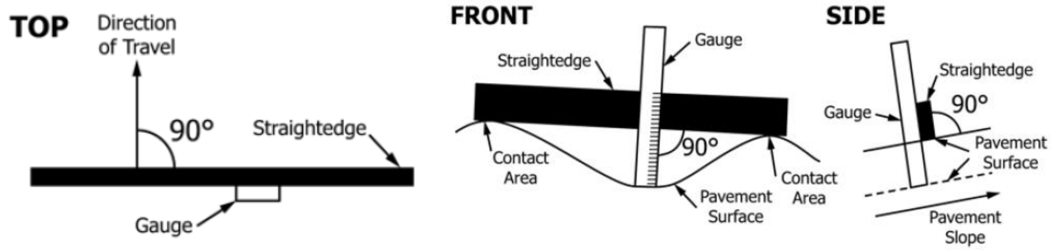

Figure 6. Comparison of straightedge and wire method

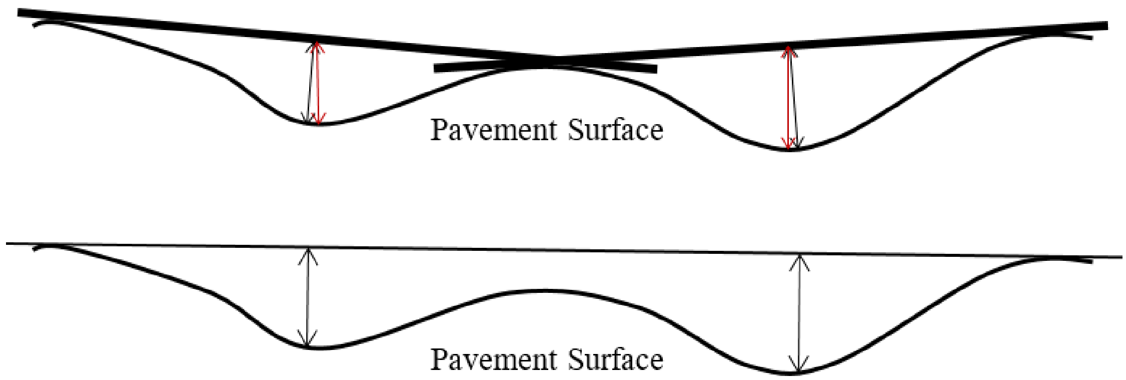

(a) Profile Case 1

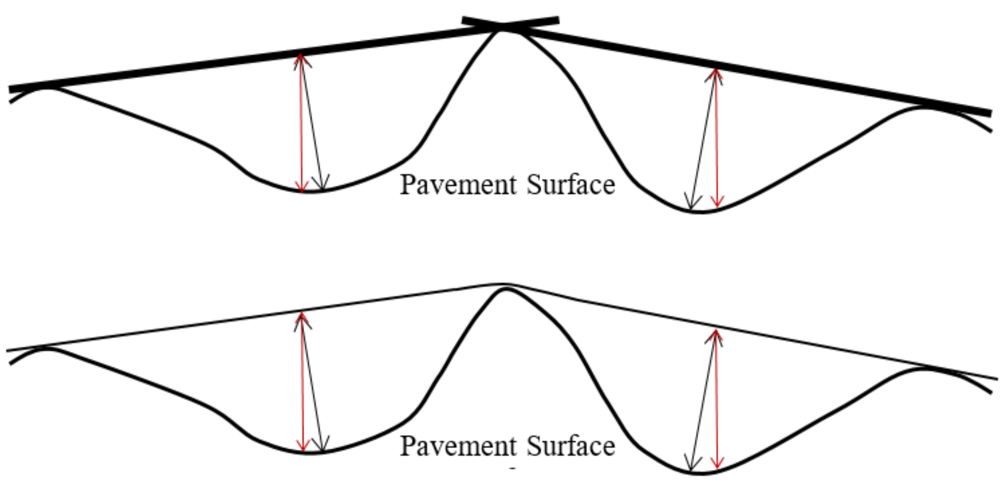

(b) Profile Case 2

Automated Measurement Methods

Point-Based Rut Bar Systems

A point-based rut bar system typically utilizes three or more point lasers/ultrasonic sensors mounted on a rut bar to profile the pavement surface in the transverse direction. Usually, the rut bar length is limited to approximately 10 ft. (3 m) for the sake of safety concerns [8]. In general, the rut depth measurement accuracy increases with the increasing number of sensors [9]. However, increasing the number of sensors would reduce sensor spacing. This reduction in spacing can result in signal interference for ultrasonic sensors. Lasers, which are much faster than ultrasonic sensors, are not affected by signal interference from adjacent sensors [6]. Another significant source of error in point-based rut bar system measurements is related to a limited number of points used to determine the maximum rut depth. Due to the wandering of a survey vehicle, the varying of lane widths, and the varying of rut shapes, the sensors may not locate exactly on the peaks and valleys of transverse profiles. As a result, the maximum rut depths are often underestimated [9]. Even with a 20 point-based rut bar system, a transverse profiler would still have about 150-200 mm between each ‘point’. These profiles are not detailed enough to detect defects like cracking, potholes, rut width, rut cross-sectional area, raveling, etc.

Figure 1 shows the configuration of a 5-point laser system. To cover the full-lane width, the wing lasers on both sides of the rut bar are tilted to a certain angle (typically 45 degrees) from the vertical as illustrated in Figure 1. As indicated in Figure 7, the transverse location of the rut bar and the rut shape can significantly affect the measurements, thus the rut depth computation. While the 5-point rut bar system configuration is able to capture the maximum rut depth for transverse profiles shown in Figure 7a and 7d, it cannot capture the maximum rut depth for transverse profiles shown in Figure 7b and 7c. The results reported in the literature showed that 5-point rut bar system can underestimate the pavement rut depth as much as 64% [9]. It is therefore recommended that the consistent transverse location of the rut bar should be ensured to avoid inconsistent rut depth measurements over time, and the mean rut depth values should be adjusted to reflect more realistic rut depth when 5-point rut bar system is used [1].

Figure 7. Pavement transverse profiles and point-based system configurations [9]

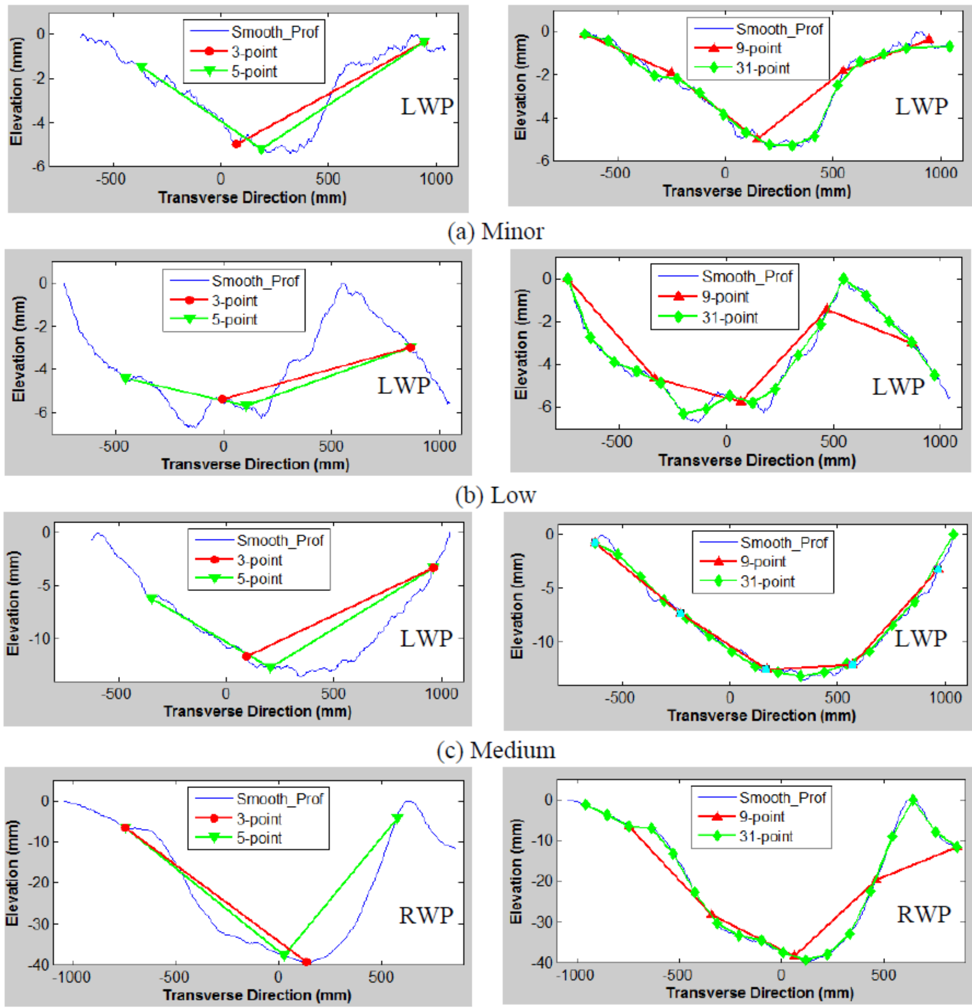

(a) Minor

(b) Low

(c) Medium

(d) High

3D Continuous Profile-Based Systems

3D Line Laser System. The 3D line laser system, also known as the camera-laser-based 3D scanner, is based on the triangulation principle, which is presented in Figure 8 [9]. Typically, a 3D line laser system consists of a laser line projector and a high speed camera. When collecting the 3D range data, the laser projector sheds a structured light (i.e., a laser line in the 3D line laser system) on top of the pavement surface, and the camera captures the laser line as an image at an angle. A sub-pixel peak detection algorithm is then employed to analyze the laser line image; find the sub-pixel location of the laser line; and convert the distortion of the laser line to the unevenness of the pavement's surface. Meanwhile, corresponding 2D intensity data are obtained. When the survey vehicle is moving, the 3D line laser system continuously scans the pavement surface and acquires range and intensity transverse profiles. The intensity profiles are used to restore the 2D intensity image of the pavement surface, and the range profiles are used to reconstruct essentially a continuous 3D pavement surface. The measurement range of such a 3D line laser system is determined by the intersection between the emitted laser line and the field of view of the digital camera.

Figure 8. Triangulation principle diagram

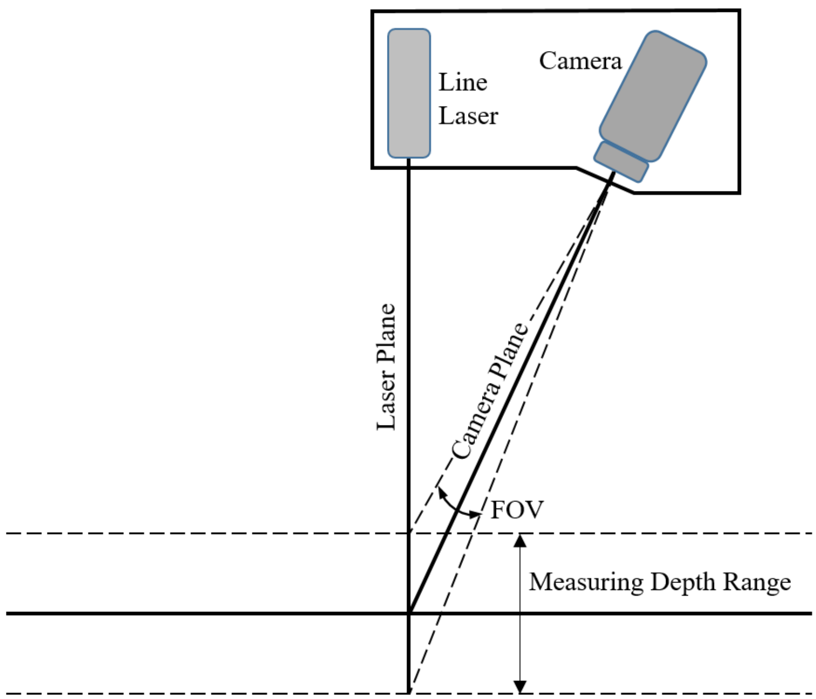

An example of such a system is the Pavemetrics' Laser Rutting Measurement System (LRMS) and LCMS, which were developed by National Optics Institute (INO) in Canada. The Pavemetrics' LCMS system can be used to obtain both crack and rut measurements. Table 1 summarize the specifications of LRMS and LCMS.

Table 1. Comparison of LRMS and LCMS

	LRMS	LCMS
Number of Laser Profiles	2	2
3D Points Per Profile	1280 points	4,160 points
Sampling Rate	30 or 150 profiles/s	5,600 profiles/s
Maximum Vehicle Speed	100 km/h	100 km/h
Transverse Width	4 m	4 m
Transversal Accuracy	+/-2 mm	+/-1 mm
Depth Range of Operation	500 mm (30 Hz) or 450 mm (150 Hz)	+/-125 mm
Depth Accuracy	+/-1mm	+/-0.25mm

The Pavemetrics's LRMS or LCMS hardware has been integrated into survey vehicles by many manufacturers such as Australian Road Research Board (ARRB), Dynatest, and Fugro. However, each manufacture has its own algorithms to process the collected data and compute rut depths. As a result, different survey systems, even with the same scanning lasers, can produce different rut depths for the same pavement section [6].

Point Laser Scanning Systems. The core of this measurement technology is phase-measurement laser radar (Ladar), which measures the distance to the pavement as the optical path is scanned transversely across the pavement by a rotating polygon (Figure 9). The laser sensor consists of a transmitter and a detector. A polygonal scan mirror with six sides changes the direction of the laser light while it rotates, thus scanning a line and generating the profile along the line six times per revolution of the polygon. At 10,000 RPM the system can generate up to 1000 scans/s. Figure 9 shows a typical configuration of the scanner. Depending on the pavement width that is needed to be measured, the height of scanner can be moved up or down. With a 90° field of view, the scan line length is equal to twice the polygon height (e.g., with scanner mounted 7 ft. above the pavement, it produces a profile 14 ft. wide).

Figure 9. Polygon scanner [10]

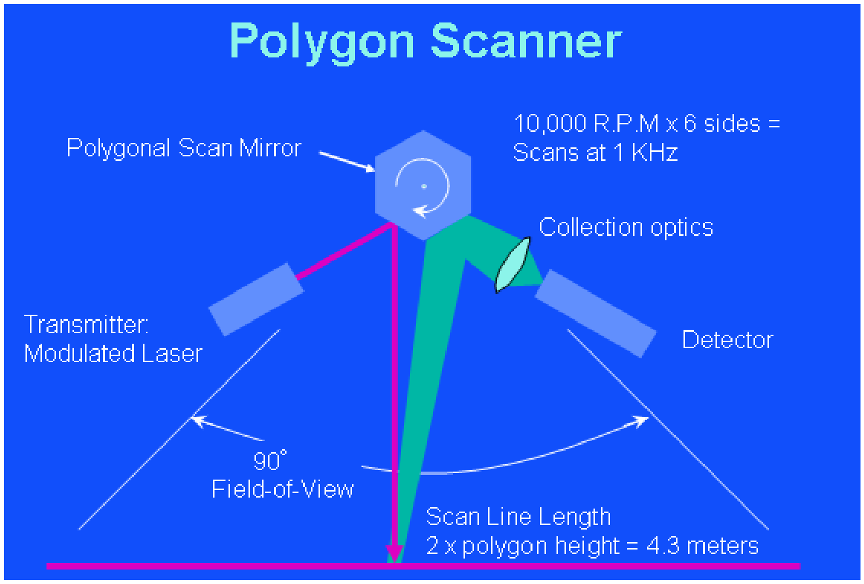

An example of such a system is the Pavement Profile Scanner (PPS), which was developed by the Phoenix Scientific Inc. Table 2 summarize the specifications of PPS.

Table 2. Specifications for PPS

	PPS
3D Points Per Profile	943 points
Sampling Rate	1,000 profiles/s
Maximum Vehicle Speed	100 km/h
Transverse Width	4.3 m
Transversal Resolution	+/-5 mm
Depth Accuracy	+/-0.15mm

For automated profile systems, three methods are mostly used to determine the rut depth: straightedge model, wire model, pseudo-rut model [10] [11].

Straightedge Model: The straightedge model simulates the manual method of placing a straightedge across the rut as specified in ASTM 1703. Different algorithms were developed to determine the rut depths from profile data by using this method [9]. They generally involve smoothing the transverse profile; identifying the support points of the straightedge; connecting the two support points; and determining the rut depth.

Wire Model: The wire model simulates a wire being stretched across the lane, as shown in Figure 6. It begins at a high point on one side of the profile and ends at another high point on the other side of the profile. The wire may get in contact with other high points in between. Rut depth is the difference in elevation between pavement surface and the wire.

Pseudo-Rut Model: The pseudo-rut model estimates rut depth based on the difference between the high points and low points. This method is commonly used with point-based rut bar systems, which have a limited number of sensors [e.g., for 3-point rut bar system, the rut depths for the wheel paths are calculated by taking the difference between the elevations of center laser (high point) and the wheel path lasers (low point) (Figure 10)].

Figure 10. 3-Point rut bar system

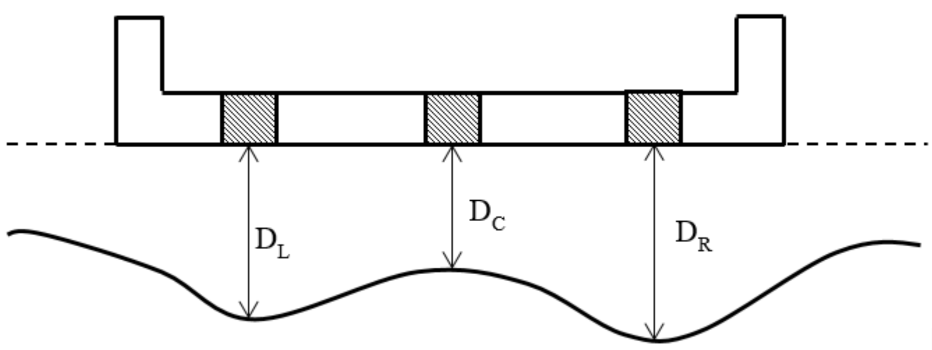

$$R_L = D_L - D_C;\ R_R = D_R - D_C$$

or $$R = (D_L + D_R)/2 - D_C$$

Objective

The objective of this research was to develop a correlation of rut depths measured with LTRC's profiler with a 5-point laser system and DOTD's PMS's profiler with a scanning laser system. A standard operating procedure (SOP) of pavement rutting data collection, compilation, and delivery by LTRC was developed so that DOTD pavement engineers can use LTRC data together with PMS data to evaluate the pavement performance and conduct/support pavement management activities.

Scope

Three repeat runs of LTRC 5-point rut bar system have been made at six control sites and four selected sites. The repeatability of LTRC's 5-point rut bar system was evaluated for all six control sites and four selected sites using the correlation of calculated rut depths.

The transverse profile data collected in 2020 and 2021 at the eight pavement management control sites with flexible and composite pavement by both LTRC and Fugro profilers were analyzed to obtain individual rut depth, average rut depth over 0.004 mile, and average rut depth over 0.1 mile. An additional 25 sites were selected to represent the typical pavement conditions and characteristics of the Louisiana highway network: (1) roads with varying rut depths; (2) roads with varying lane widths; (3) roads with varying quantity needed to fill ruts; and (4) roads with varying standard deviation for rutting. Average rut depth over 0.004 mile and 0.1 mile were obtained from both LTRC and Fugro transverse profile data.

Correlations were examined by constructing scatter plots of the rut depths from the profile data collected by LTRC's profiler versus the rut depths estimated from the profile data collected by Fugro's profiler. T-tests or paired t-tests were conducted to determine if there were a statically significant difference between the rut depth measured by LTRC's profiler and the rut depth measured by Fugro's profiler. The strengths of the relationship between the rut depths measured by LTRC's profiler and Fugro's profiler were evaluated using the correlation coefficients and R square values.

At the end, a standard operating procedure (SOP) was developed to standardize the process of collecting and compiling rutting data by LTRC and delivering them to DOTD engineers for subsequent actions, such as evaluating pavement performance and conduct/support pavement management activities.

Methodology

In this study, repeatability of LTRC 5-point rut bar system was checked. Both 2020 and 2021 rutting data from calibration control sites were analyzed. Additional rutting data were collected from selected homogeneous pavement sections and included in the analysis.

Project Selection

LA-PMS Calibration Control Sites

DOTD selects thirteen 0.5-mile long control pavement sites for calibration of the current DOTD PMS vendor's highway data collection system, or ARAN9000. Both 2020 and 2021 rutting data from eight calibration control sites with flexible or composite pavement were used for the comparison of rut depths measured by the profilers of LTRC and DOTD's PMS. Table 3 presents the general description of the calibration sites used for the comparison in this section.

Table 3. PMS calibration control sites

Control Site No.	Control Section	District	Route	Beginning Chainage	Ending Chainage	Pavement Type	Lane Width (ft.)
CS03	019-05	61	US0061	11	11.5	COM	12/12
CS06	060-04	61	LA0067	6.3	6.8	ASP	11/12
CS07	061-05	61	LA0010	3.5	4	ASP	11/10
CS08	250-01	61	LA0019	6.8	7.3	COM	11.6/12
CS09	250-01	61	LA0019	11.4	11.9	COM	11/12
CS10	255-02	61	LA0408	6.2	6.7	ASP	10/11
CS12	817-08	61	LA0946	4.3	4.8	COM	12/12
CS13	863-09	61	LA0964	0.2	0.7	ASP	11/12

Pavement Rutting Test Sections

To compare the profilers of LTRC and DOTD's PMS, 25 homogeneous pavement sections were selected based on 2019 PMS data, which represent the typical pavement conditions and characteristics of the Louisiana highway network. Various rut depth levels were taken into consideration during the selection of the sections. In addition, the lane width; quantity needed to fill ruts; and standard deviation for rutting are intended to represent most of the variables in the data collection process. During the data collection process, the research team found that one section was under construction and decided to remove it from data collection. Figure 11 shows the geographical location of the final 24 sections. The selected sections include 3 interstates, 3 US highways and 19 Louisiana state highways.

Figure 11. Geographical location of the selected pavement sections

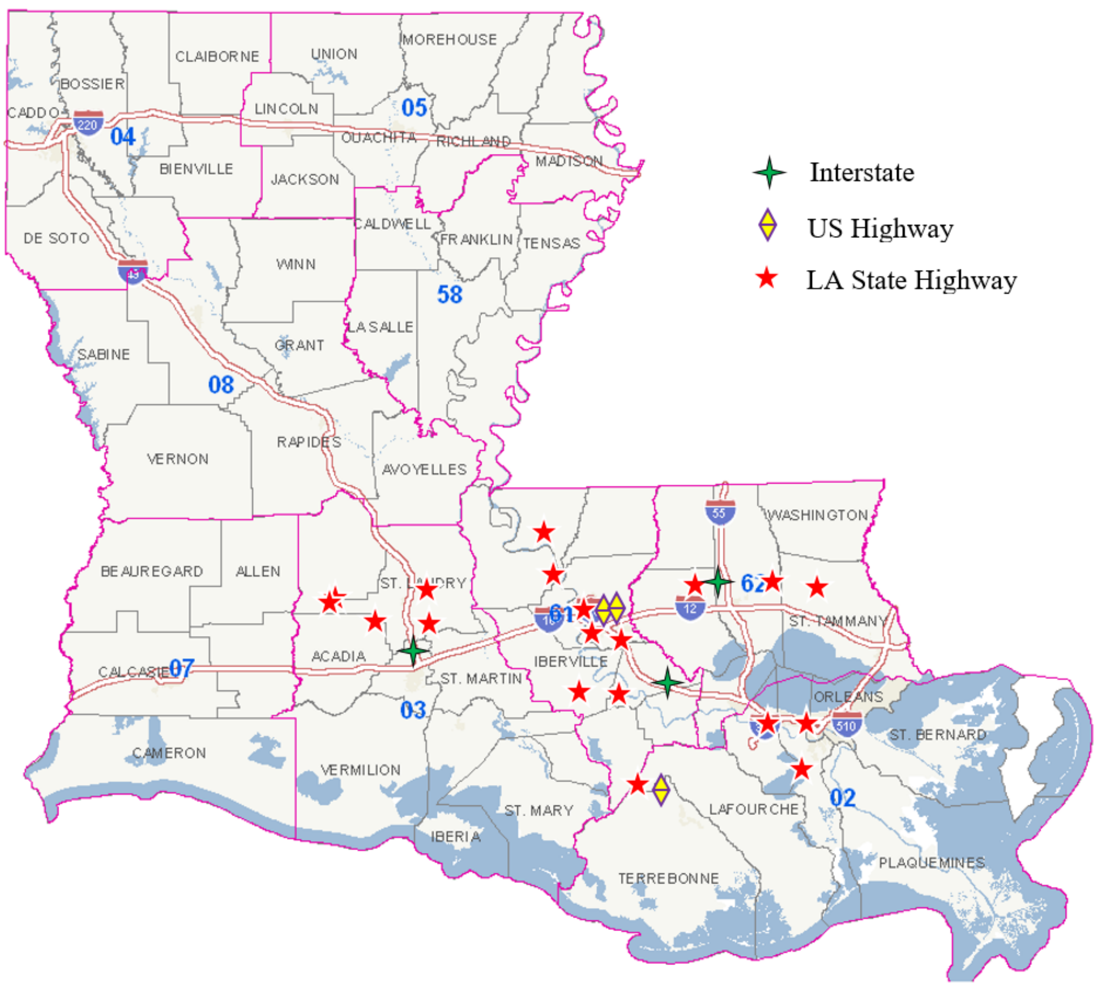

Table 4 shows the general description of the selected homogeneous pavement sections. The RL_AVE (Avg. Rutting in LWP); RR_AVE (Avg. Rutting in RWP); and R_AVE (Avg. Rutting in combined) columns represent the average rutting in LWP, RWP, and combined, respectively. Based on R_AVE (Avg. Rutting in Combined) values, the pavement sections are divided into four groups: 0 - 0.25 in.; 0.25 - 0.50 in.; 0.50 - 0.75 in.; and greater than 0.75 in.

Table 4. Selected pavement sections

Name	District	Route	From (logmile)	To (logmile)	Lane Width (ft.)	RL_AVE (Avg. Rutting in LWP)	RR_AVE (Avg. Rutting in RWP)	R_AVE (Avg. Rutting in combined)
826-10-1	02	LA0560	0.00	0.85	8	0.07	0.11	0.09
824-23-1	61	LA3001	0.00	0.89	9	0.13	0.16	0.15
226-01-1	61	LA0982	7.08	8.30	10	0.10	0.11	0.11
013-05-1	61	US0190	5.68	6.34	11	0.25	0.18	0.21
452-90-1	62	I-0055	21.73	32.17	12	0.31	0.15	0.23
852-30-1	62	LA1083	0.00	5.43	13	0.12	0.11	0.11
803-04-1	61	LA0945	0.31	1.46	9	0.30	0.40	0.35
269-02-1	62	LA0442	2.81	4.42	10	0.25	0.41	0.33
061-04-1	61	LA0010	0.76	4.12	10	0.29	0.31	0.30
257-04-1	61	LA0042	0.00	3.10	10	0.32	0.20	0.26
282-01-1	02	LA0048	0.00	2.09	11	0.33	0.21	0.27
013-05-1	61	US0190	1.23	5.68	11	0.33	0.25	0.29
803-25-1	61	LA0427	0.00	2.32	11	0.26	0.29	0.27
244-01-1	02	LA0020	6.50	7.44	12	0.29	0.22	0.26
424-07-1	02	US0090	16.74	18.72	12	0.25	0.28	0.27
450-12-2	61	I-0010	0.00	2.59	12	0.29	0.21	0.25
455-01-2	03	I-0049	1.50	2.18	12	0.26	0.25	0.26
081-01-1	03	LA0347	0.30	4.48	10	0.56	0.74	0.65
060-01-1	61	LA0067	1.24	1.86	11	0.57	0.57	0.57
203-01-1	03	LA0029	0.95	4.07	12	0.56	0.57	0.57
419-01-1	02	LA3021	0.00	0.70	12	0.55	0.56	0.56
849-10-1	03	LA0741	1.14	4.04	10	0.76	0.74	0.75
849-23-1	03	LA0091	1.70	2.41	12	1.12	0.98	1.05
208-01-1	03	LA0178	0.97	3.12	12	0.74	0.89	0.81

Rut Algorithm

LTRC's 5-Point Rut Bar System

LTRC's profiler uses point lasers to measure the elevation of the rut bar over the pavement surface at five different points across the lane. One laser is located in the center, one laser in each wheel path, and one wing laser on each side oriented at a 45° angle as shown in Figure 12.

Figure 12. Illustration of LTRC's 5-point rut bar system

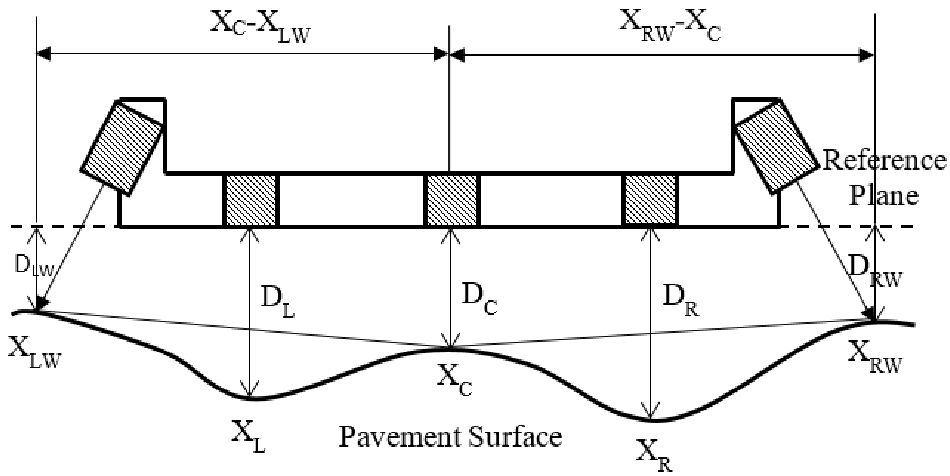

For LTRC's 5-point rut bar system, the collected elevation data can be used to estimate the rut depth using pseudo-rut model as follows [9]:

$$R_L = D_L - \frac{D_{LW} + D_C}{2}$$

$$R_R = D_R - \frac{D_C + D_{RW}}{2}$$

Where R_L, R_C, and R_R are the rut depth in the LWP, center, and RWP, respectively; D_L, D_C, and D_R are the elevation of the bar over the pavement surface at the LWP, center, and RWP, repectively; D_{LW} and D_{RW} are the elevation of the bar over the pavement surface determined by the left wing and right wing lasers.

Straight edge model can also be used to estimate the rut depth from the collected elevation data as follows [12]:

$$R_L = D_L - (m_L X_L + c_L)$$

$$R_R = D_R - (m_R X_R + c_R)$$

Where $m_L = \frac{(D_C - D_{LW})}{(X_C - X_{LW})}$; $c_L = D_{LW} - mX_{LW}$; $m_R = \frac{(D_{RW} - D_C)}{(X_{RW} - X_C)}$; $c_R = D_{RW} - mX_{RW}$

DOTD's PMS Vendor's Laser Cracking Measurement System

DOTD's PMS vendor's road profiler uses LCMS to collect high-resolution transverse profile (4000+ points per profile) and covers a 13 ft. (4m) pavement width. It can collect 5,600 profiles/s but only deliver 25 profiles for each 0.1 mile. Fugro uses its 'Vision' software and the supporting algorithm to estimate the rut depth from the collected elevation data. In 'Vision" software, the rut depth can be either estimated from the full transverse profile or resampled profile (three points, five points, etc.). For full transverse profile, the transverse profile in DOTD's PMS is first smoothed using the moving average with a window size of five. A 10 ft. lane width is used unless actual lane is smaller, and then the actual lane width is used. A 1.8-m straightedge is then simulated to calculate the rut depth, which is the maximum distance perpendicular to the straightedge. For a 5-point resampled profile, the location of each of 5 points from the center of the transverse profile was set up to match LTRC's 5-point rub bar system (i.e., X_{LW}= 61.32 in., X_L=34.53 in., X_C=0.00 in., X_R=34.57 in., and X_{RW}=61.93 in.). Straightedge model is then used to estimate the rut depth. The transverse profile explorer of Roadware Vision, a custom designed software from Fugro, allows the user to view the transverse profile graphically one at a time. The transverse profile explorer can also display the smoothed profile, straightedge line, rut depths, rut depth locations, rut boundary, curb/drop off, etc. The rut processor analysis settings have incorporated previous research findings to improve accuracy of rutting calculations and to eliminate/minimize the errors caused by cracks, missed wheel path, double measurement in the same wheel path, and elevated edge off roadway [13].

Discussion of Results

Repeatability of LTRC 5-Point Rut Bar System

Three repeat runs of LTRC's 5-point rut bar system have been made at six control sites (CS). A typical result is presented in Figure 13 for both wheel paths. DOTD reports rutting data in PMS using the average rut depth over 0.1 mile, which is usually calculated from 25 readings, i.e., every 0.004 mile within 0.1 mile. Typical three-run rut depth data over 0.004-mile and 0.1-mile average are shown in Figure 14 and Figure 15, respectively. As can be seen from these figures, no matter at what scales, the similar trend is observed in three runs for both left and right wheel path rut depth data. A small shifting of the rutting profile is also noted in some of three repeated runs. The repeatability of LTRC's 5-point rut bar system is evaluated using the cross-correlation of calculated rut depths, and the results are presented in Table 5 for all points, 0.004-mile interval data, and 0.1-mile interval data. As can be seen from the table, the correlation value improves when averaging the rut depth data over longer length of pavement.

Three repeat runs of LTRC's 5-point rut bar system have also been made at four selected sites. Typical three-run rut depth data for each individual point, over 0.004-mile average, and over 0.1-mile average are shown in Figure 16, Figure 17, and Figure 18, respectively. Again, the repeatability of LTRC's 5-point rut bar system is evaluated using the cross-correlation of calculated rut depths, and the results are presented in Table 6 for all points, 0.004-mile interval data, and 0.1-mile interval data. A similar trend observed at control sites was observed here except for the RWP rut depth of control section 226-01. The correlation coefficient for RWP rut depth of control section 226-01 is very low. By further looking into the rut depth data of each individual run, it is found that there are many abnormal spikes for 0.004-mile interval data at control section 226-01, as shown in Figure 19. Site visit suggests that this is due to the narrow lane (10 ft. wide) and grass at the edge of the roadway as shown in Figure 20.

An overall correlation value of 0.90 and above is achieved on 0.1-mile interval data for both data sets.

Figure 13. Profiles of continuous rut depth for CS07

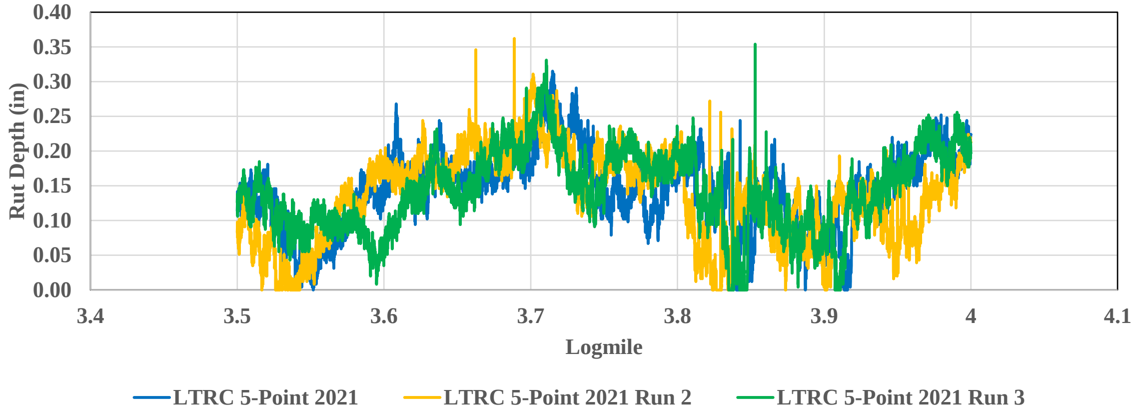

(a) LWP

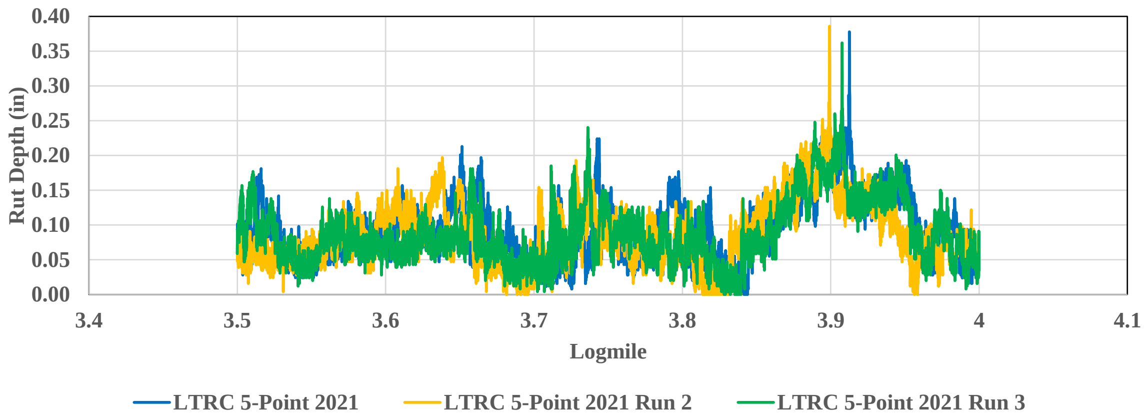

(b) RWP

Figure 14. Profiles of 0.004-mile interval rut depth for CS07

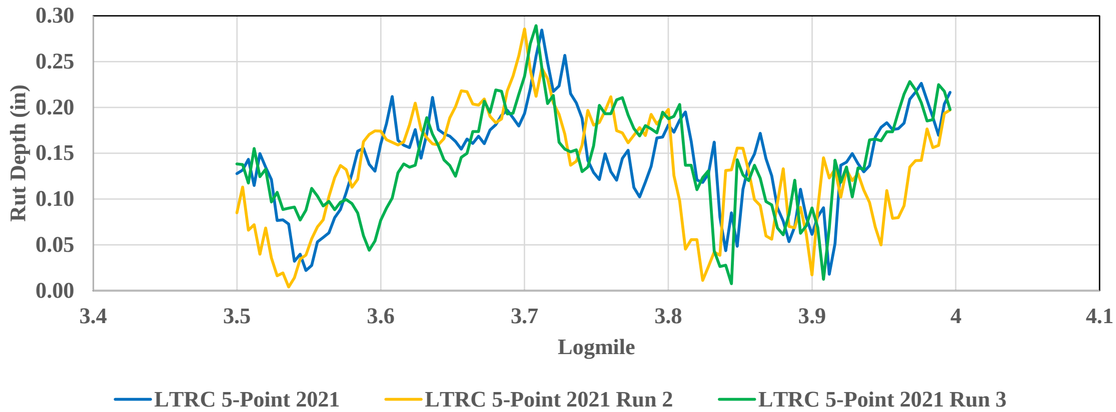

(a) LWP

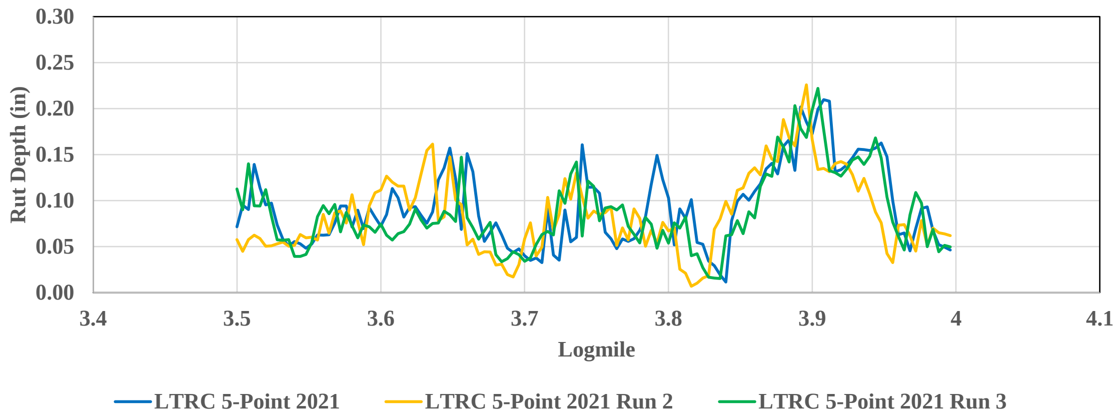

(b) RWP

Figure 15. 0.1-mile rut depths for CS07

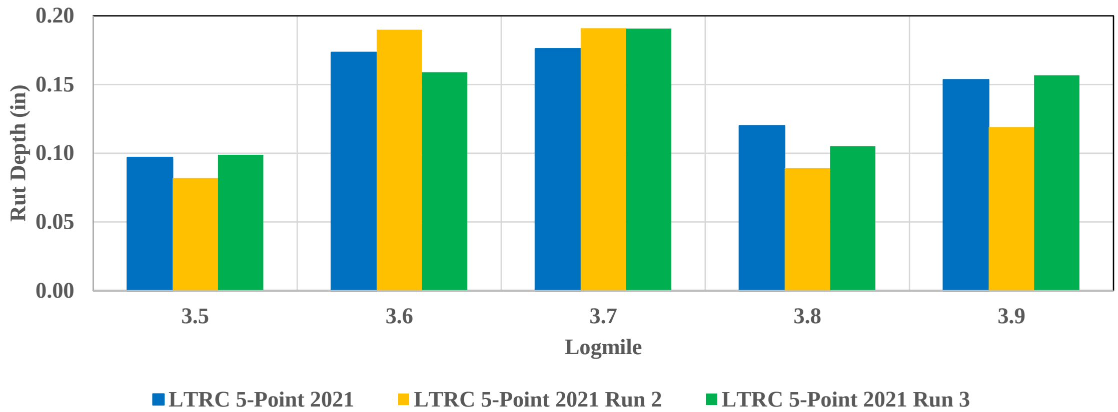

(a) LWP

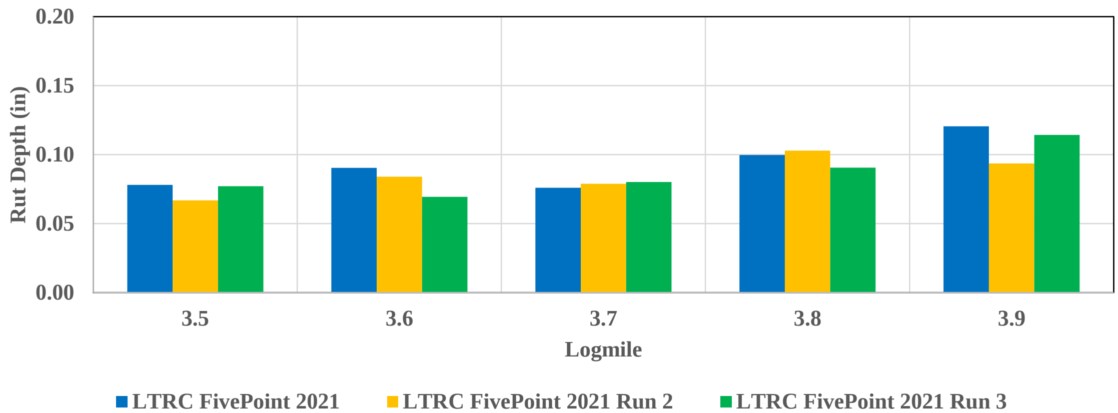

(b) RWP

Figure 16. Profiles of continuous rut depth for CS 424-07

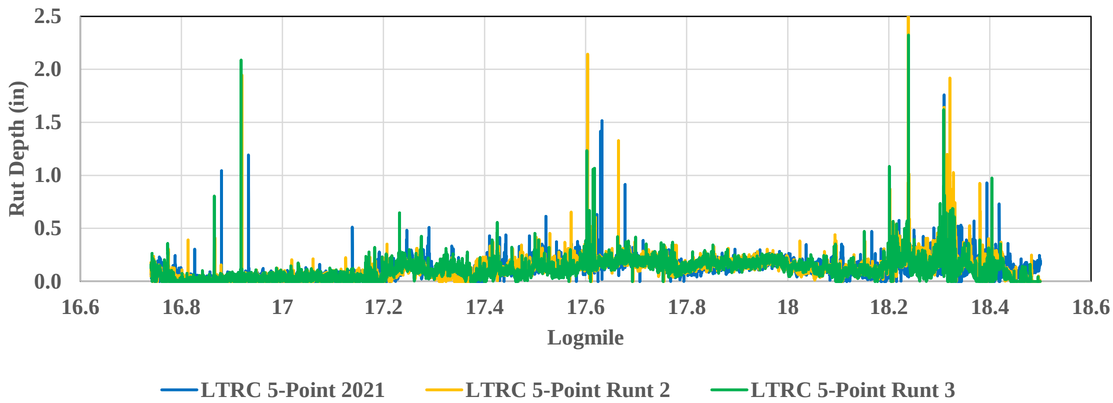

(a) LWP

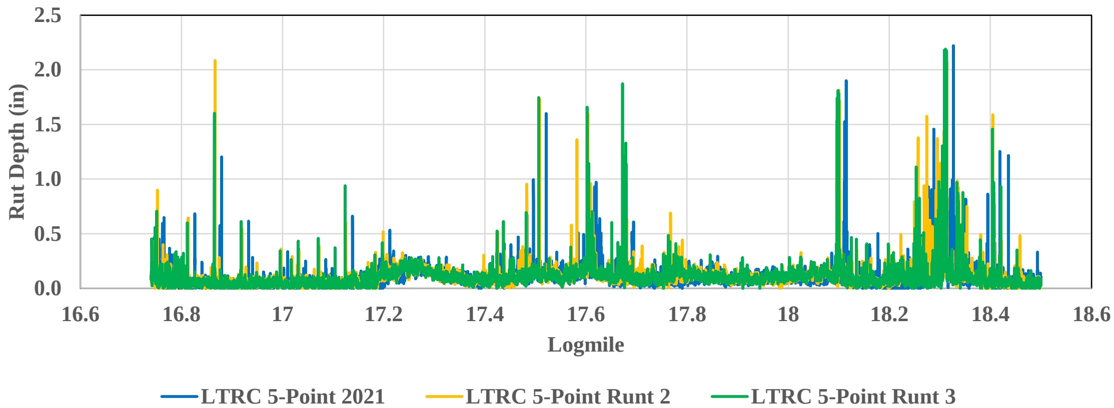

(b) RWP

Figure 17. Profiles of 0.004-mile interval rut depth for CS 424-07

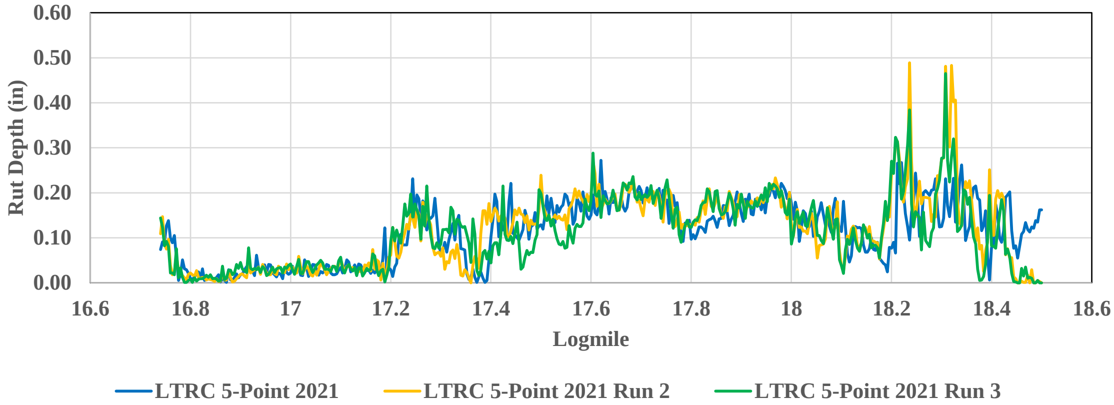

(a) LWP

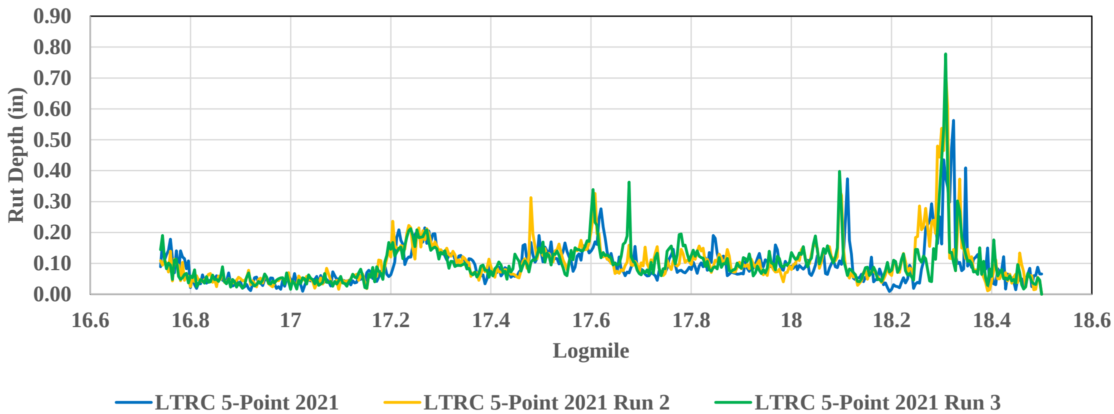

(b) RWP

Figure 18. 0.1-mile rut depths for CS 424-07

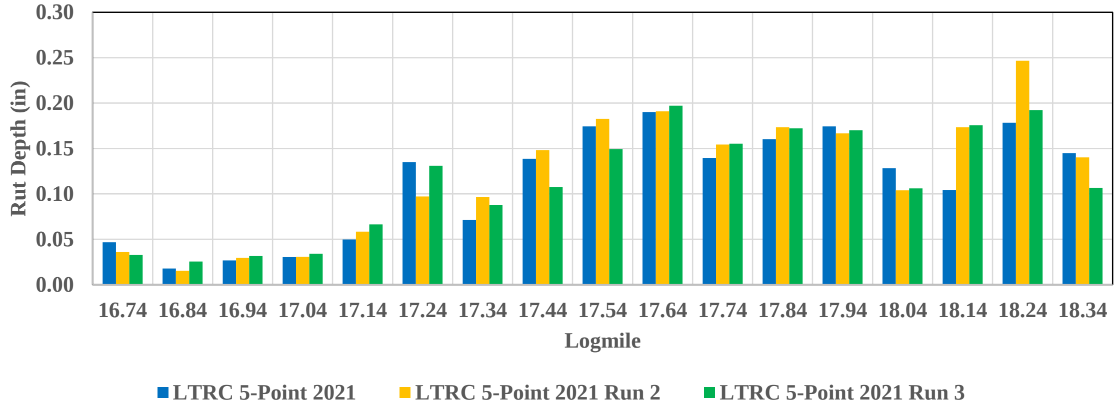

(a) LWP

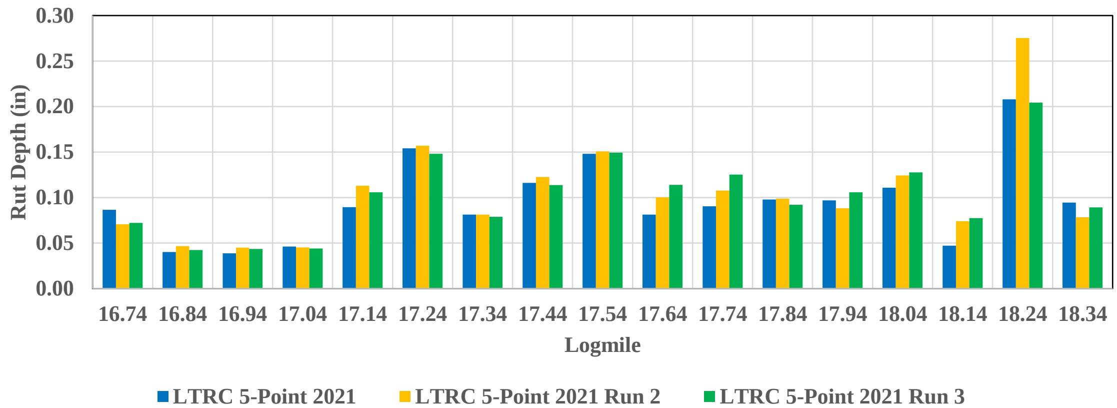

(b) RWP

Table 5. Correlation of three runs for control sites

	LWP Correlation			RWP Correlation		
	Points	0.004-mile interval	0.1-mile interval	Points	0.004-mile interval	0.1-mile interval
CS03	0.46	0.54	0.65	0.49	0.80	0.91
CS06	0.65	0.82	0.98	0.34	0.56	0.92
CS07	0.53	0.58	0.92	0.54	0.64	0.72
CS08	0.59	0.70	0.98	0.50	0.60	0.88
CS09	0.42	0.72	0.99	0.27	0.56	0.92
CS13	0.47	0.61	0.63	0.36	0.53	0.69
All	0.67	0.79	0.94	0.56	0.74	0.95

Table 6. Correlation of three runs for selected sites

	LWP Correlation			RWP Correlation		
	Points	0.004-mile interval	0.1-mile interval	Points	0.004-mile interval	0.1-mile interval
226-01	0.63	0.82	0.99	0.39	0.50	0.38
803-04	0.63	0.72	0.97	0.40	0.52	0.87
244-01	0.72	0.78	0.96	0.61	0.72	0.98
424-07	0.53	0.73	0.93	0.37	0.64	0.95
All*	0.65	0.75	0.94	0.45	0.59	0.90

*CS 226-01 is not included

Figure 19. Profiles of continuous RWP rut depth for CS226-01

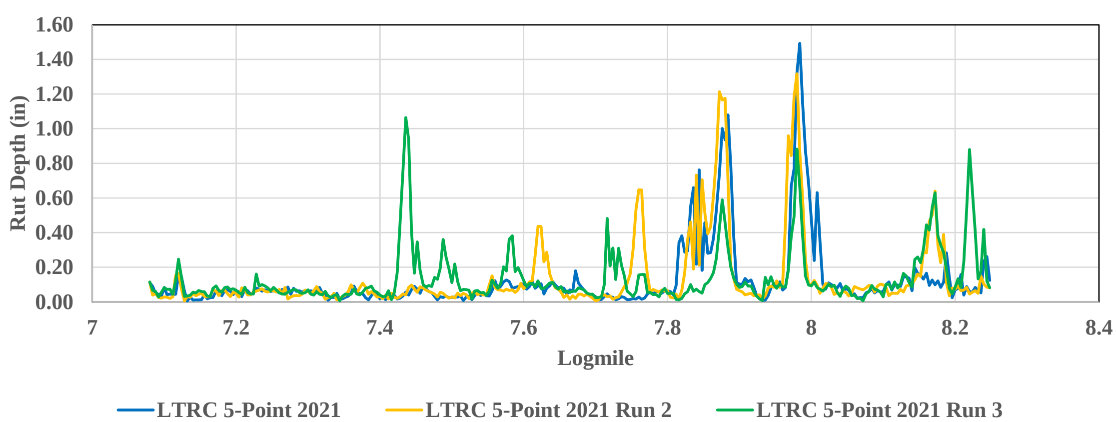

Figure 20. Right-of-way image for CS226-01

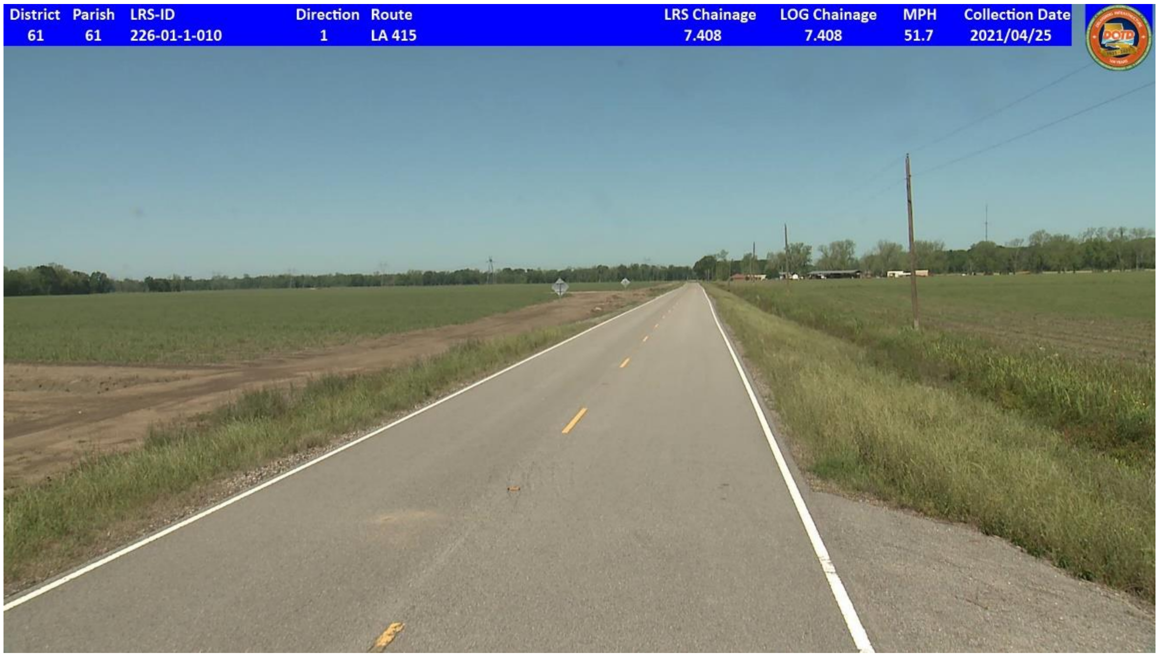

Control Sites Data Sets

For the eight calibration control sites, the transverse profiles collected by Fugro were obtained from DOTD’s pavement management system engineers. The vendor’s scanning laser system is capable of acquiring 4096 points across 13-ft. wide lane (i.e., a transverse resolution of 0.04 in.). The delivered data, however, showed that the average transverse spacing between points is about 0.12 in., i.e., each 13-ft. wide profile consist of about 1270 points. The Transverse Profile Explorer of Fugro's Roadware Vision allows viewing both acquired and smoothed profiles. Note that the Vision algorithms are proprietary to Fugro, Inc., and, therefore, are not readily accessible.

For LTRC’s 5-point rut bar system, negative rut depths are reported as zero. Note that the algorithm to estimate the rut depth for LTRC's 5-point rut bar system is proprietary to Dynatest and it cannot be controlled by the user. To be consistent with this practice, when calculating rut depth from Fugro's 5-point resampled profile, “Map To Zero” option was selected for negative rut.

Usually, the profile is collected at 1 ft. interval, but there are some small variations between LTRC’s and Fugro's profile system. Therefore, the number of profiles collected at each control site by LTRC's profile system is different than those collected by Fugro's profile system. In addition, it is noted that there is small difference in number of profiles collected by LTRC's profile system in 2020 and 2021.

Individual Rut Depth

A histogram was created for the Fugro full profile rut depth, Fugro 5-point rut depth, and LTRC 5-point rut depth (Figure 38 to Figure 43 in Appendix). These histograms show that a significant amount of zeroes are seen in both Fugro and LTRC 5-point rut depths (i.e., 5-point rut depth calculations can provide negative value).

The standard deviations of rut depths are pooled across all control sites to obtain a value for both 2020 and 2021 data. The correlation of variance (COV) is calculated by dividing the mean by the pooled standard deviation. These values are used to examine the variability associated with locations of rut depth. The COVs of 5-point rut depths, no matter if estimated from LTRC's 5-point rut bar system or Fugro's 5-point resamples profile, are generally higher than that of the rut depths estimated from Fugro's full profile (Table 7, Table 8, Table 9, and Table 10). The higher COV values for Fugro's 5-point resamples profile indicate that rut depth location varies across stations and have significant effect on the calculated rut depth. It is also noted that the LWP rut depth data has much higher variation than RWP rut depth data for LTRC's 5-point rut bar system, while it is the opposite for Fugro's 5-point resample profile for 2020 data. The reason is unknown.

Table 7. Variation of 2020 rut depth data for all control sites

	LTRC 5-Point System			Fugro 5-Point Resampled Profile			Fugro Full Profile		
	LWP	RWP	Avg.	LWP	RWP	Avg.	LWP	RWP	Avg.
No. of Points	2,640×8 =21,112			2,681×8 =21,440			2,681×8 =21,440		
Mean	0.0418	0.110	0.0761	0.102	0.0315	0.0666	0.192	0.166	0.179
STD	0.0479	0.0481	0.0371	0.0691	0.0525	0.0476	0.0784	0.0749	0.0583
COV(%)	114.6	43.6	48.7	68.0	166.8	71.4	40.8	45.0	32.5

Table 8. COV of 2020 rut depth data for each individual control site

	LTRC 5-Point System			Fugro 5-Point Resampled Profile			Fugro Full Profile		
	LWP	RWP	Avg.	LWP	RWP	Avg.	LWP	RWP	Avg.
CS03	192.6	24.0	32.8	52.6	844.8	52.7	26.6	32.4	21.0
CS06	127.5	56.1	66.3	63.1	162.4	68.5	48.5	54.4	39.0
CS07	37.9	34.8	25.9	55.1	121.5	56.6	18.4	26.5	14.6
CS08	243.8	39.9	45.1	89.4	840.7	92.3	46.5	46.8	38.0
CS09	134.5	48.6	48.0	44.5	170.0	50.9	40.7	39.8	29.8
CS10	84.8	54.9	50.7	49.3	203.2	60.8	28.2	33.6	24.4
CS12	520.7	21.7	23.6	116.5	250.2	105.3	39.3	30.3	28.0
CS13	84.6	35.0	38.6	100.0	78.8	70.4	23.7	25.3	18.9

Table 9. Variation of 2021 rut depth data for all control sites

	LTRC 5-Point System			Fugro 5-Point Resampled Profile			Fugro Full Profile		
	LWP	RWP	Avg.	LWP	RWP	Avg.	LWP	RWP	Avg.
No. of Points	2,667×8 =21,328			2,681×8 =21,440			2,681×8 =21,440		
Mean	0.0795	0.0794	0.0795	0.0859	0.0942	0.090	0.216	0.194	0.205
STD	0.0596	0.0570	0.0432	0.0690	0.0748	0.0543	0.0945	0.0770	0.0663
COV(%)	75.0	71.7	54.4	80.3	79.4	60.3	43.7	39.8	32.3

Table 10. COV of 2021 rut depth data for each individual control site

	LTRC 5-Point System			Fugro 5-Point Resampled Profile			Fugro Full Profile		
	LWP	RWP	Avg.	LWP	RWP	Avg.	LWP	RWP	Avg.
CS03	107.8	51.1	62.6	75.8	117.9	68.7	27.3	30.9	21.8
CS06	89.8	84.6	68.3	66.8	110.8	63.3	58.3	50.0	42.8
CS07	39.0	49.4	28.0	40.9	38.1	26.9	17.5	27.1	14.0
CS08	114	58.2	64.8	119.0	135.2	98.6	47.4	40.4	34.4
CS09	60.1	93.7	51.0	196.4	157.9	131.0	37.8	33.9	26.9
CS10	56.1	117.9	64.0	56.3	83.7	54.7	33.3	37.4	28.1
CS12	210.4	19.9	22.4	158.7	77.6	69.8	28.2	25.6	20.5
CS13	57.5	35.0	32.1	80.4	36.9	37.0	22.9	23.5	17.8

Scatterplots were created to compare Fugro full profile rut depth and its 5-point rut depth (Figure 21 and Figure 22). In general, the 5-point rut depth values are smaller than the full profile rut depths. It is also observed from the figures that the 5-point rut depth values are significantly lower than the full profile rut depths at some locations. To pinpoint the cause of this large discrepancy, scatterplots were created for each control site separately (Figure 44 to Figure 59 in Appendix). It is found that these large discrepancies were mostly from CS06. Pavement image data show that cracks are prevalent at this site. Throughout the use of the Roadware Vision software, many incorrect measurements in cracks/joints are noticed (Figure 23).

Figure 21. Scatterplot of Fugro's full profile rut depth vs. Fugro's 5-point rut depth in 2020

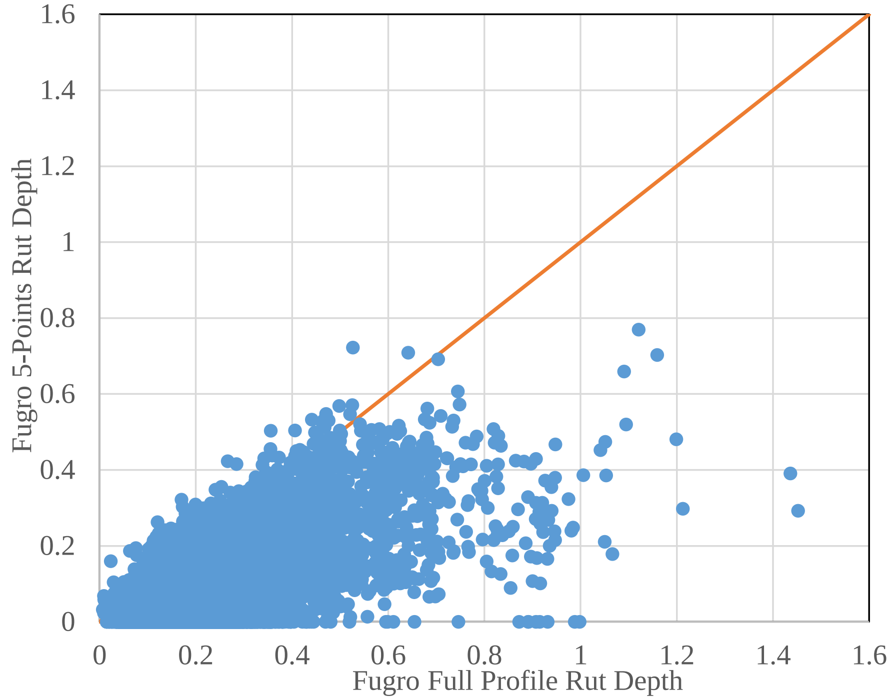

(a) LWP

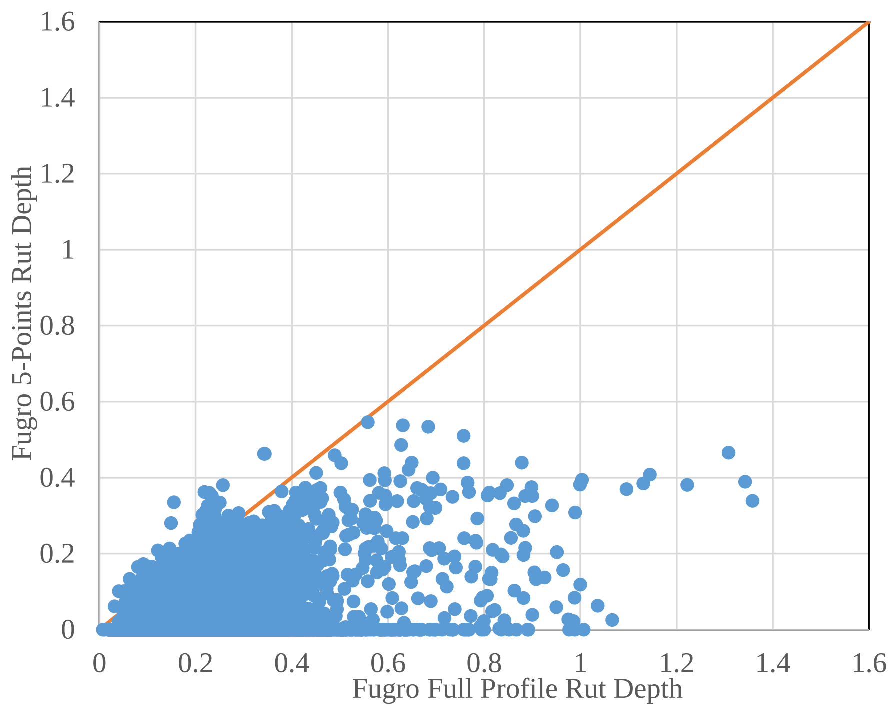

(b) RWP

Figure 22. Scatterplot of Fugro's full profile rut depth vs. Fugro's 5-point rut depth in 2021

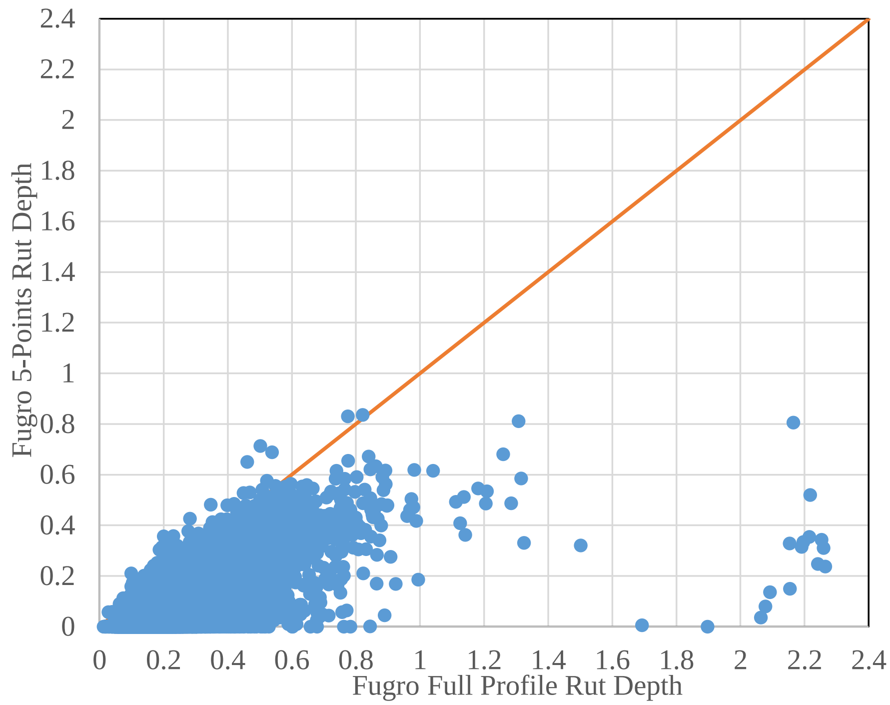

(a) LWP

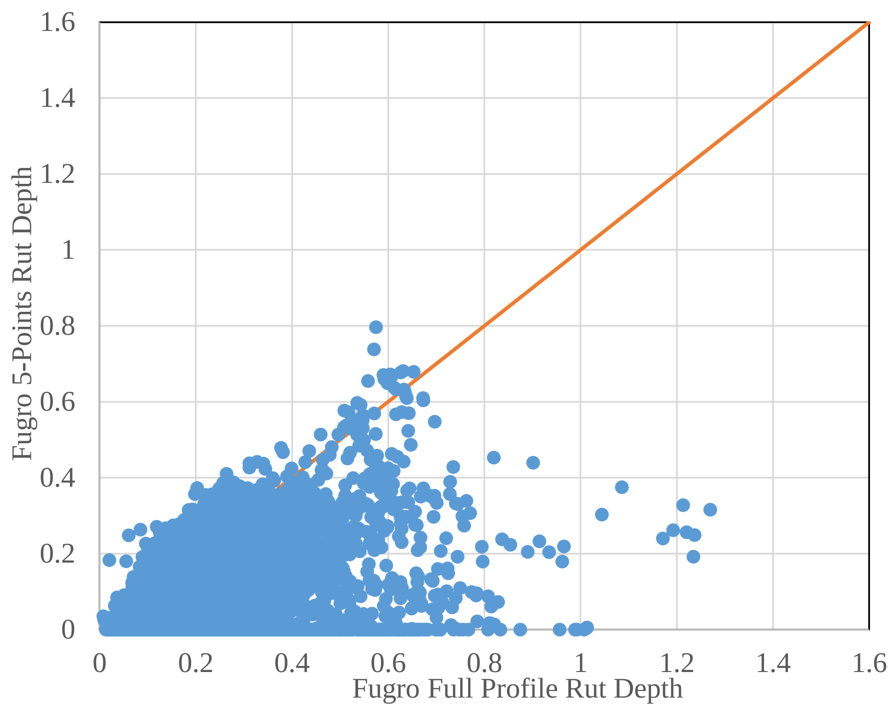

(b) RWP

Figure 23. Measurement in cracks/joints for full profile rut depth

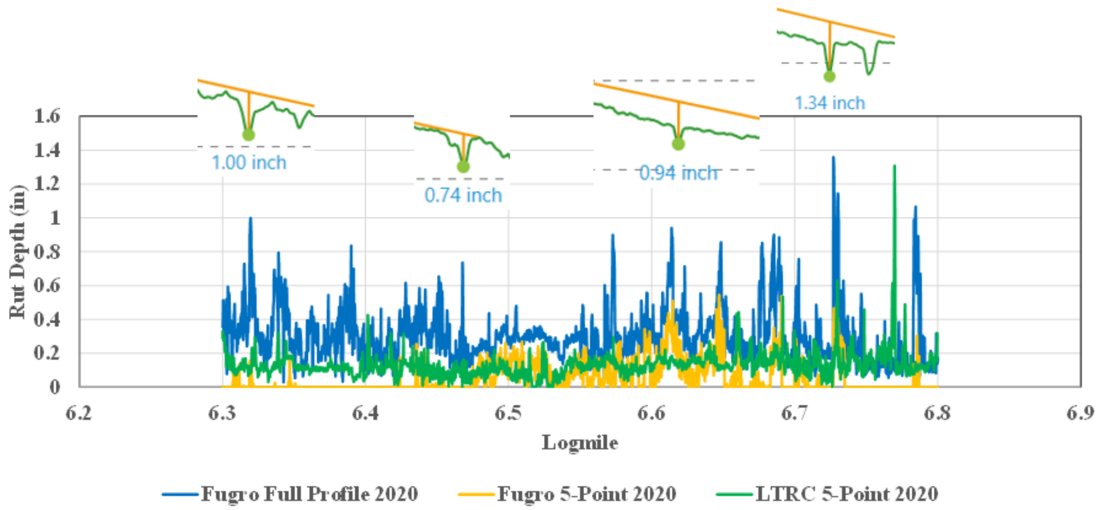

(a) CS06

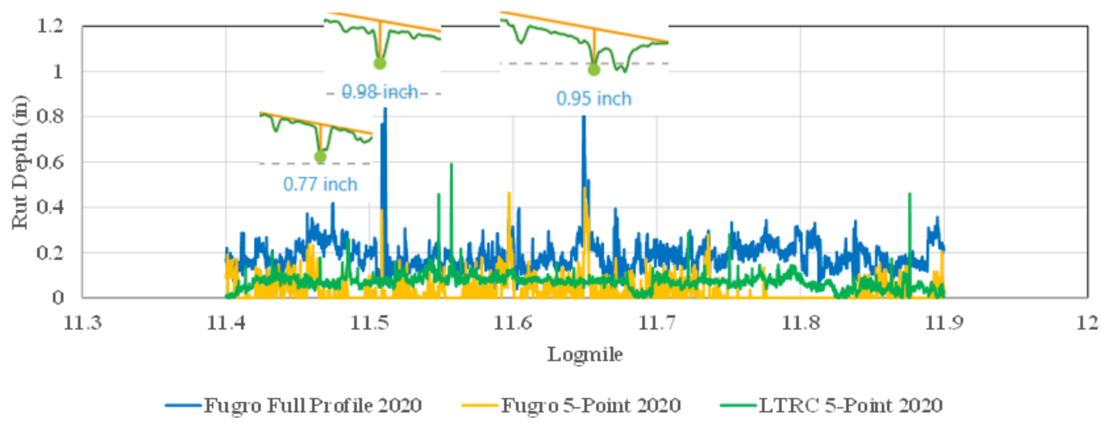

(b) CS09

Per DOTD's PMS, rutting is defined as a contiguous longitudinal surface depression in the wheel path. DOTD's PMS defines the wheel path as two longitudinal paths centered approximately 34 inches in each direction from the centerline of the analysis lane, each measuring 36 inches in width (Figure 24). The wheel path definition in AASHTO R85-18 is similar (Figure 25). Measurement outside the wheel path is also observed in some cases (Figure 26), especially for the pavement with longitudinal joint.

Figure 24. Wheel path definition in DOTD PMS

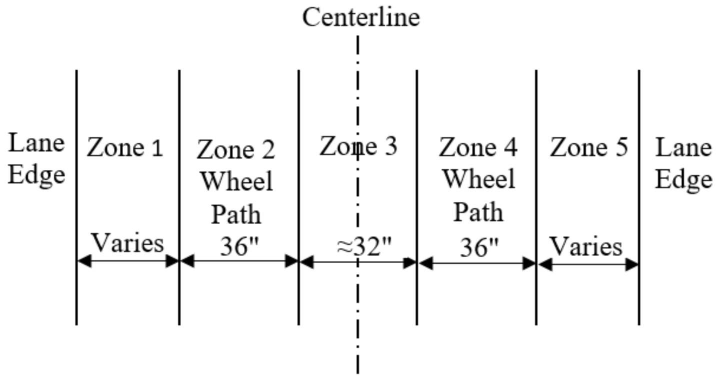

Figure 25. Wheel path definition in AASHTO R 85-18

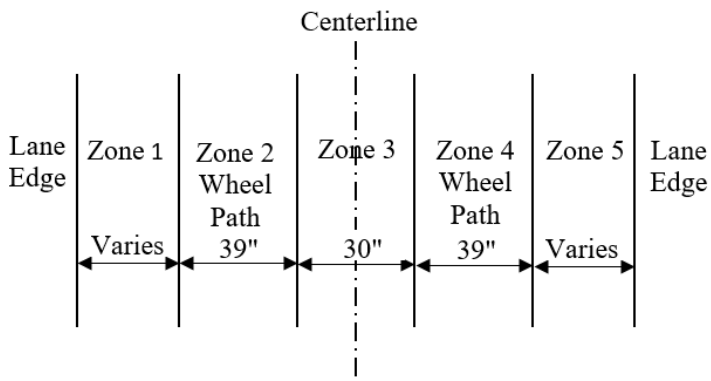

Figure 26. Measurement outside the wheel path for Fugro's full profile rut depth

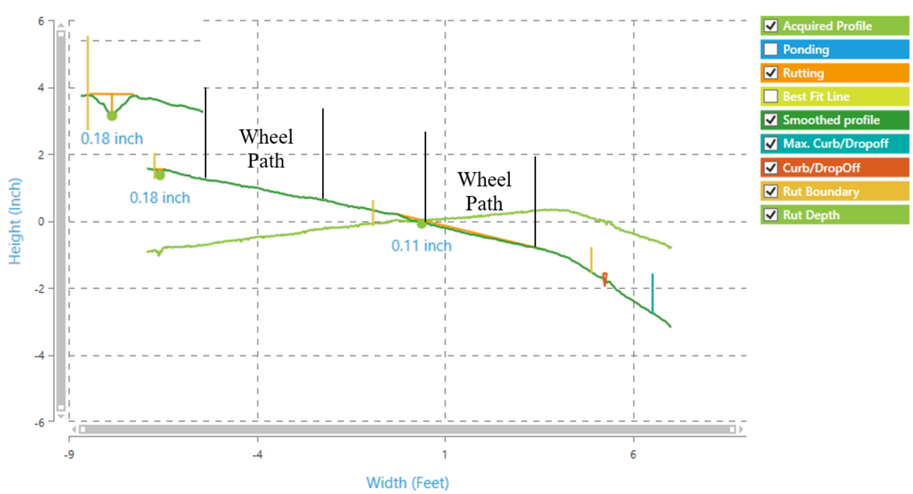

It is also noticed that the rut algorithm of Roadware Vision can fail to locate the point of maximum rut depth, as shown in Figure 27.

Figure 27. Failure of locating the maximum rut depth point for Fugro's full profile rut depth

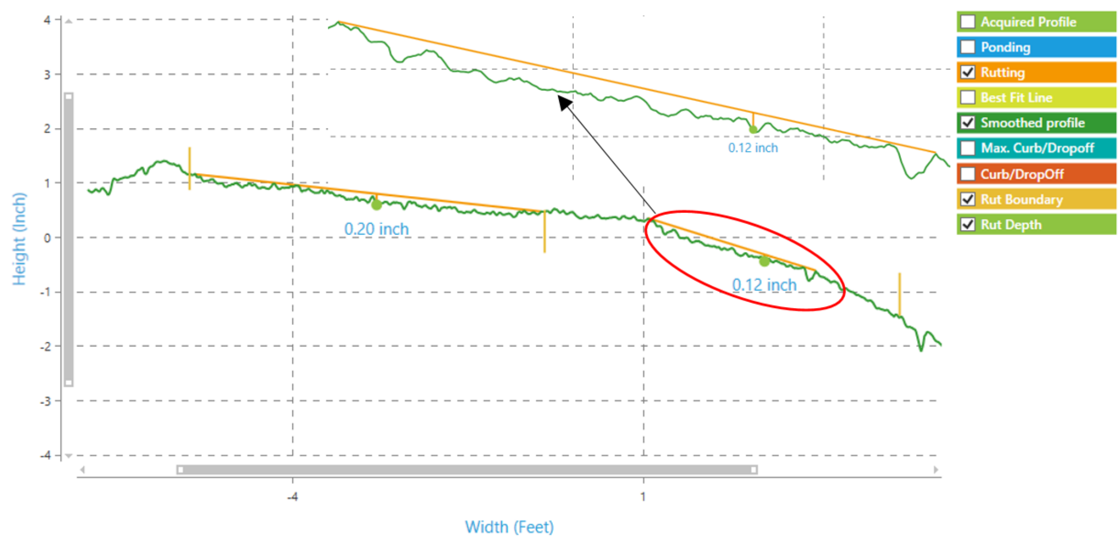

Due to fixed sensor location, 5-point rut depth cannot always capture the maximum rut depth for transverse profiles as shown in Figure 28 for LWP rut depth (missing the peak and valley); 5-point rut depth can also be significantly affected by the edge drop off/grass as shown in Figure 28 for RWP rut depth.

Figure 28. Missed maximum rut depth and edge drop off/grass effect for 5-point rut depth

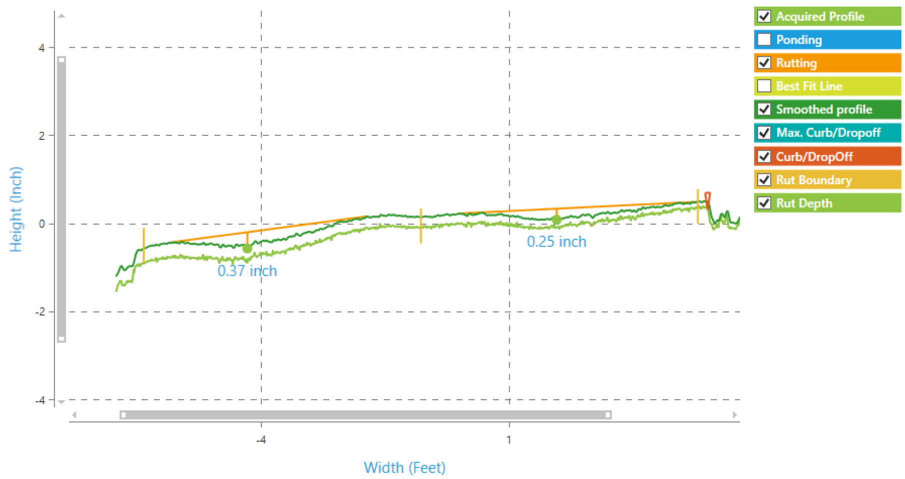

(a) Full Profile Rut Depth

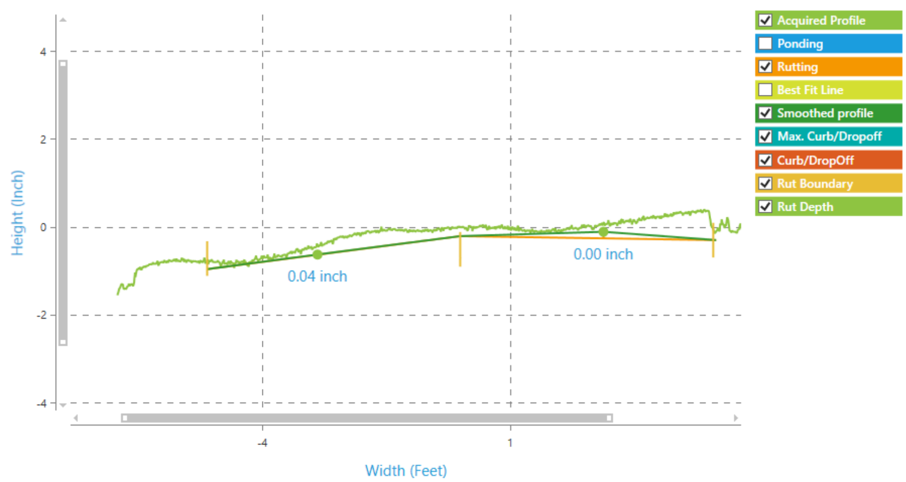

(b) 5-Point Rut Depth

Comparisons are made among Fugro's full profile rut depth, Fugro's 5-point rut depth, and LTRC's 5-point rut depth (Figure 60 to Figure 75 in Appendix). Statistical t-tests support that there were statistically significant differences (Table 11 and Table 12), indicating that the different measurement techniques do not provide the same estimate of individual rut depth.

Table 11. Statistical t test of LTRC's 5-point rut depths versus Fugro's full profile and 5-point rut depths for control sites (2020)

	LTRC 5-Point System			Fugro 5-Point Resampled Profile			Fugro Full Profile		
	LWP	RWP	Avg.	LWP	RWP	Avg.	LWP	RWP	Avg.
No. of Points	21120	21120	21120	21448	21448	21448	21448	21448	21448
p value from t test	-	-	-	0	0	1.6E-73	0	0	0

Table 12. Statistical t test of LTRC's 5-point rut depths versus Fugro's full profile and 5-point rut depths for control sites (2021)

	LTRC 5-Point System			Fugro 5-Point Resampled Profile			Fugro Full Profile		
	LWP	RWP	Avg.	LWP	RWP	Avg.	LWP	RWP	Avg.
No. of Points	21336	21336	21336	21448	21448	21448	21448	21448	21448
p value from t test	-	-	-	3.65E-15	6.49E-79	9.35E-61	0	0	0

Average rut depth over 0.004 mile

Histograms were created for the 0.004-mile average rut depth data (Figure 76 to Figure 81 in Appendix). These histograms show that amount of zero values (percentage wise) for average 5-point rut depths over 0.004 mile is much less than that for the individual rut depths, but they are still significant. The rut depth data average for over 0.004 mile across all control sites are shown in Figure 29 and Figure 30 for 2020 and 2021, respectively. The effect of cracks on rut depth is still significant for 0.004-mile average. It is also interesting to note that both LTRC's and Fugro's 5-point rut depth is significantly lower than Fugro's full profile rut depth at CS12 for LWP. Further review of the data in Roadware Vision indicates that measurement outside the wheel path in longitudinal joints happened frequently in LWP. Better match between LTRC's and Fugro's 5-point rut depths is observed in 2021 data than in 2020 data.

Table 13 and Table 14 include the mean, standard deviation, correlation coefficient, and *p* values of the paired t-test for 0.004-mile average rut depth data. CS06 is excluded here due to prevalent cracks at this site. The correlation coefficients between Fugro's 5-point rut depths and LTRC's 5-point rut depths are consistent for 2020 and 2021 data. The results of the paired t-tests yields statistically significant differences. However, the difference between 2021 Fugro's 5-point rut depths and 2021 LTRC's 5-point rut depths is much less significant as compared to other cases.

Figure 29. Profiles of 0.004-mile interval rut depth for all control sites in 2020

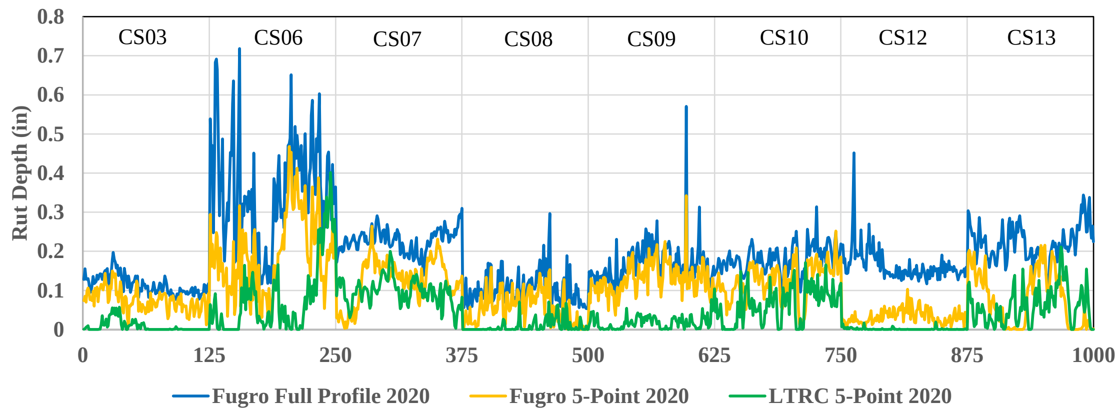

(a) LWP

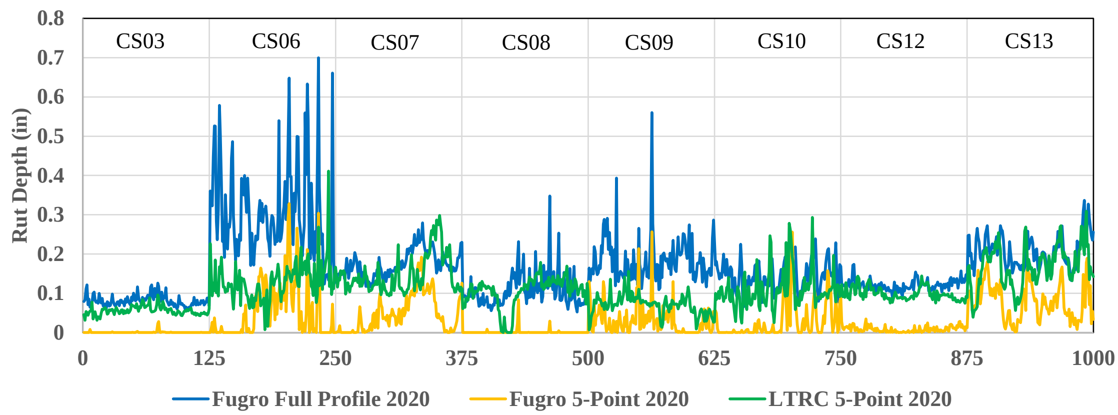

(b) RWP

Figure 30. Profiles of 0.004-mile interval rut depth for all control sites in 2021

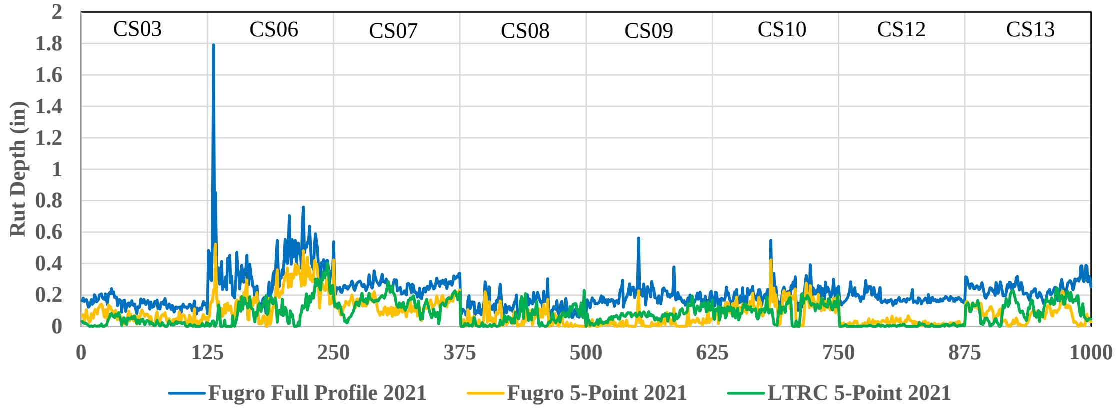

(a) LWP

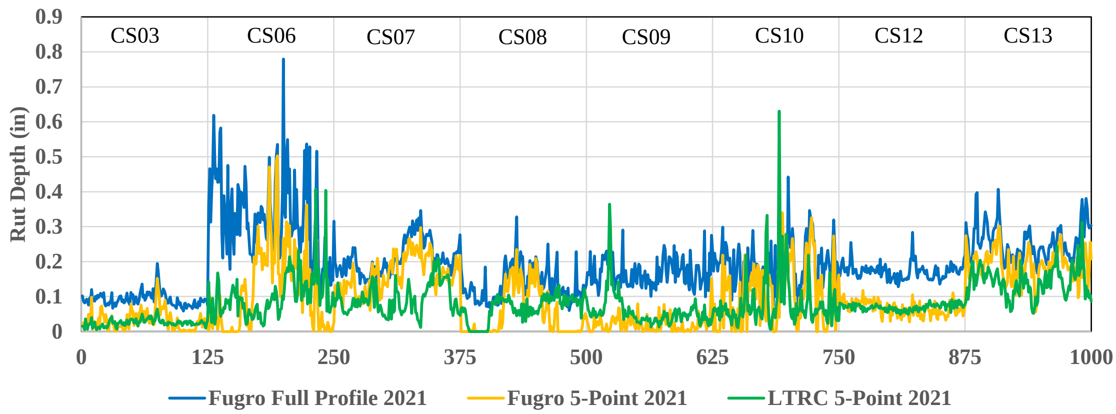

(b) RWP

Table 13. Correlation of LTRC's 5-point rut depths versus Fugro's full profile and 5-point rut depths for control sites (0.004-mile average) (2020)

	LTRC 5-Point System			Fugro 5-Point Resampled Profile			Fugro Full Profile		
	LWP	RWP	Avg.	LWP	RWP	Avg.	LWP	RWP	Avg.
No. of Points	875	875	875	875	875	875	875	875	875
Mean	0.0364	0.108	0.0720	0.0885	0.0282	0.0584	0.169	0.146	0.158
STD	0.0297	0.0381	0.0263	0.0464	0.0348	0.0322	0.0395	0.0376	0.0297
COV(%)	81.7	35.4	36.5	52.4	123.3	55.2	23.4	25.7	18.8
Correlation	-	-	-	0.507	0.431	0.574	0.383	0.466	0.450
R^2	-	-	-	0.119	0.247	0.196	0.287	0.205	0.358
p value from paired t test	-	-	-	2.1E-113	6.1E-239	2.73E-19	0.000	9.14E-72	1.2E-301

Table 14. Correlation of LTRC's 5-point rut depths versus Fugro's full profile and 5-point rut depths for control sites (0.004-mile average) (2021)

	LTRC 5-Point System			Fugro 5-Point Resampled Profile			Fugro Full Profile		
	LWP	RWP	Avg.	LWP	RWP	Avg.	LWP	RWP	Avg.
No. of Points	875	875	875	875	875	875	875	875	875
Mean	0.0740	0.0764	0.0752	0.0693	0.0907	0.0800	0.193	0.175	0.184
STD	0.0445	0.0436	0.0316	0.0424	0.0514	0.0361	0.0450	0.0443	0.0342
COV(%)	60.2	57.1	42.0	61.3	56.6	45.2	23.3	25.3	18.6
Correlation	-	-	-	0.429	0.468	0.572	0.457	0.475	0.565
R^2	-	-	-	0.183	0.319	0.397	0.243	0.349	0.400
p value from paired t test	-	-	-	0.0398	6.32E-09	0.0051	4.6E-273	6.1E-239	0

Average rut depth over 0.1 mile

Histograms were also created for the 0.1-mile average rut depth data (Figure 82 to Figure 87 in Appendix). These histograms show that zero values for 0.1-mile average 5-point rut depths, though significantly less in amount (percentage wise) than for the 0.004-mile average rut depths, can still be computed. Figure 31 and Figure 32 present the average rut depth data for over 0.1 mile across all control sites for 2020 and 2021, respectively. The apparent effect of cracks on rut depths at CS06 is still there for 0.1-mile average data. The aforementioned issue for CS12 is also still there for 0.1-mile average rut depth data.

Figure 31. Profiles of 0.1-mile interval rut depth for all control sites in 2020

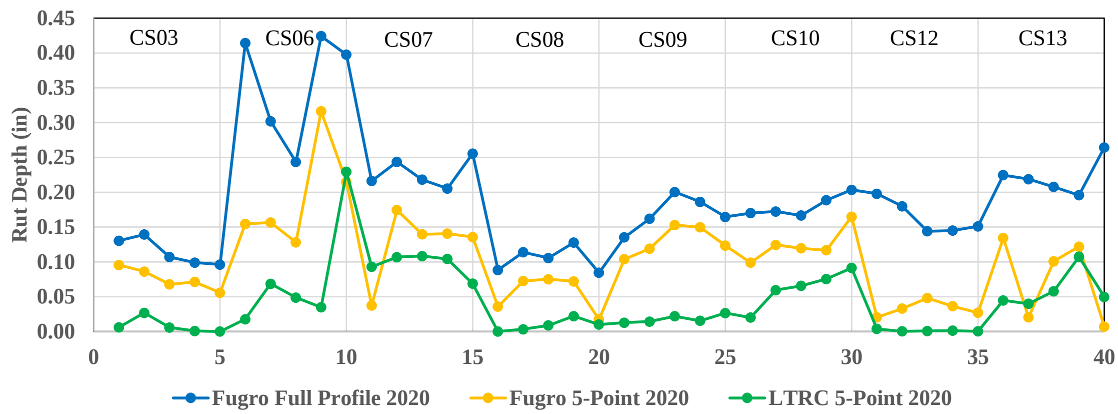

(a) LWP

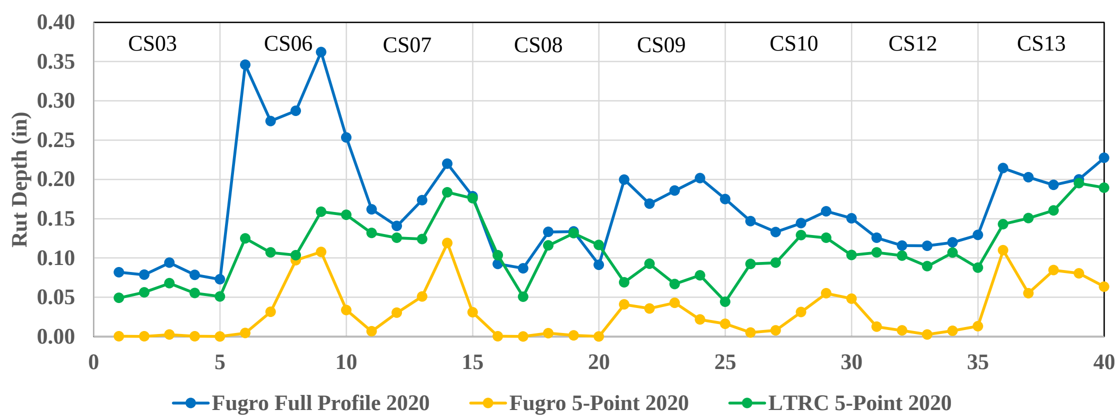

(b) RWP

Figure 32. Profiles of 0.1-mile interval rut depth for all control sites in 2021

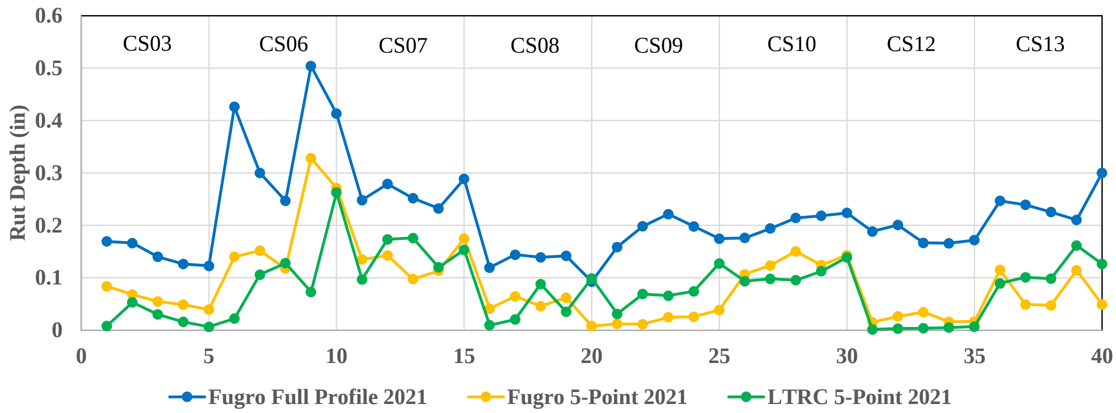

(a) LWP

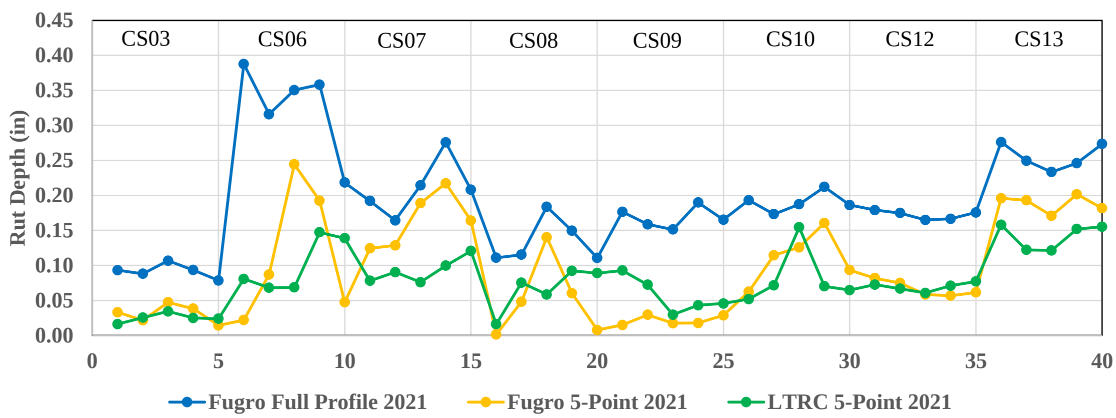

(b) RWP

Table 15 and Table 16 include the mean, standard deviation, correlation coefficient, and *p* values of the paired t-test for 0.1-mile average rut depth data. Again, CS06 is excluded here. The correlation for 0.1-mile average rut depth data is much improved as compared to 0.004-mile average rut depth data. The results of the paired t-tests yield *p* values greater than 0.05 for 2021 LTRC's and Fugro's 5-point rut depths. It means that the difference between 2021 LTRC's 5-point rut depths and 2021 Fugro's 5-point rut depths is not statistically significant. In other words, 0.1-mile average of LTRC's and Fugro's 5-point rut depth shows a stronger relationship than individual point or 0.004-mile average of LTRC's and Fugro's 5-point rut depth.

Table 15. Correlation of LTRC's 5-point rut depths versus Fugro's full profile and 5-point rut depths for control sites (0.1-mile average) (2020)

	LTRC 5-Point System			Fugro 5-Point Resampled Profile			Fugro Full Profile		
	LWP	RWP	Avg.	LWP	RWP	Avg.	LWP	RWP	Avg.
No. of Points	35	35	35	35	35	35	35	35	35
Mean	0.0364	0.108	0.0720	0.0885	0.0282	0.0584	0.169	0.146	0.158
STD	0.0167	0.0211	0.0148	0.0343	0.0206	0.0237	0.0216	0.0169	0.0146
COV(%)	45.9	19.6	20.6	38.8	73.1	40.7	12.8	11.5	9.3
Correlation	-	-	-	0.555	0.669	0.554	0.693	0.629	0.737
R^2				0.309	0.448	0.307	0.480	0.396	0.543
p value from paired t test	-	-	-	1.08E-08	1.71E-16	0.0206	9.14E-22	6.75E-07	4.8E-18

Table 16. Correlation of LTRC's 5-point rut depths versus Fugro's full profile and 5-point rut depths for control sites (0.1-mile average) (2021)

	LTRC 5-Point System			Fugro 5-Point Resampled Profile			Fugro Full Profile		
	LWP	RWP	Avg.	LWP	RWP	Avg.	LWP	RWP	Avg.
No. of Points	35	35	35	35	35	35	35	35	35
Mean	0.0740	0.0764	0.0752	0.0693	0.0907	0.0800	0.193	0.175	0.184
STD	0.0284	0.024	0.0188	0.0224	0.0304	0.0198	0.0235	0.0228	0.0168
COV(%)	38.4	31.5	25.0	32.3	33.6	24.8	12.2	13.0	9.1
Correlation	-	-	-	0.636	0.737	0.797	0.670	0.770	0.800
R^2				0.404	0.543	0.636	0.449	0.593	0.640
p value from paired t test	-	-	-	0.536	0.0778	0.364	9.23E-18	3.43E-18	1.08E-21

Selected Sites Data Sets

For the 24 selected pavement rutting test sections, the 0.004-mile and 0.1-mile average rut depth data are obtained from DOTD's pavement management system engineers

Average rut depth over 0.004 mile

The histograms were created for the average Fugro's full profile rut depth and LTRC's 5-point rut depth over 0.004 mile for selected sites (Figure 88 to Figure 89 in Appendix). These histograms again show a great amount of zero values. Scatterplots were created to compare Fugro's full profile rut depth and LTRC's 5-point rut depth (Figure 33). In general, the LTRC's 5-point rut depth values are smaller than the Fugro's full profile rut depths. The figures show that, at some locations, the Fugro's full profile rut depths are significantly higher than the LTRC's 5-point rut depth values. It is also observed that the LTRC's 5-pont rut depths can also be significantly higher than Fugro's full profile rut depths in some cases, especially on RWP. To pinpoint the causes of this large discrepancy, scatterplots were created for each selected site separately (Figure 90 to Figure 113 in Appendix). It is found that much higher Fugro's full profile rut depth values mostly occurred in the group of sites with reported PMS R_AVE value of 0.5-0.75 in and greater than 0.75 in. PMS image data show that cracks are prevalent at those sites (i.e., the high rut depth values reported in PMS are probably most due to measurements in cracks, not the actual rutting in pavement). Also, much higher LTRC's 5-point rut depth values mostly occurred in pavement sections with narrow lane width (≤10 ft.), in which LTRC's 5-point rut bar system significantly overestimated the rut depth due to grasses at the edge of the roadway. Figure 34 presents the rut depth data average over 0.004 mile across all the selected sites. Lots of spikes were observed along the Fugro's full profile rut depth profile which were probably due to the measurements in cracks.

Table 17 includes the mean, standard deviation, correlation coefficient, and *p* values of the paired t-test for 0.004-mile average rut depth data. The pavement sections with large rut depth discrepancies caused by aforementioned measurement issues of both systems were excluded. The variation of LTRC's 5-point rut depth data for the selected sites is consistent with that for the control sites. On the other hand, the variation of Fugro's full profile rut depth data for the selected sites is higher than that for the control sites. The correlations between Fugro's full profile rut depths and LTRC's 5-point rut depths at the selected sites are similar to those obtained from control sites. The results of the paired t-tests again show a statistically significant differences between the 0.004-mile average Fugro's full profile rut depth and LTRC's 5-point rut depth.

Figure 33. Scatterplot of Fugro's full profile rut depth vs. Fugro's 5-point rut depth for selected sites

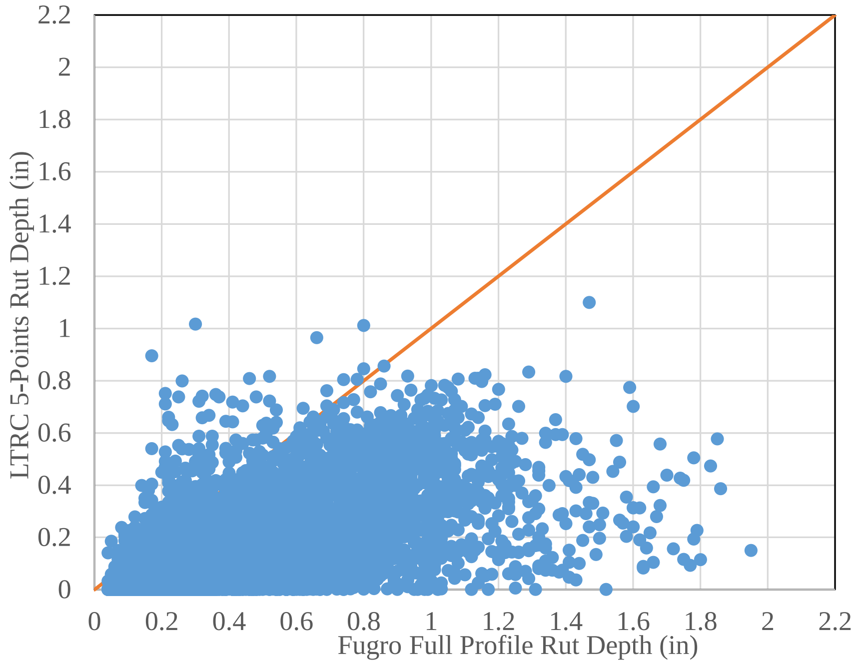

(a) LWP

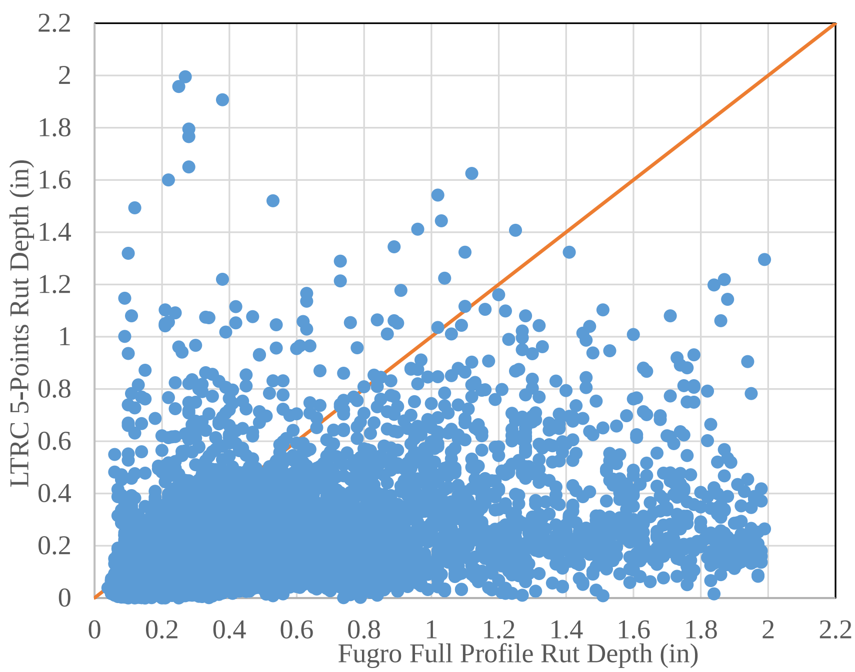

(b) RWP

Figure 34. Profiles of 0.004-mile interval rut depth for all selected sites

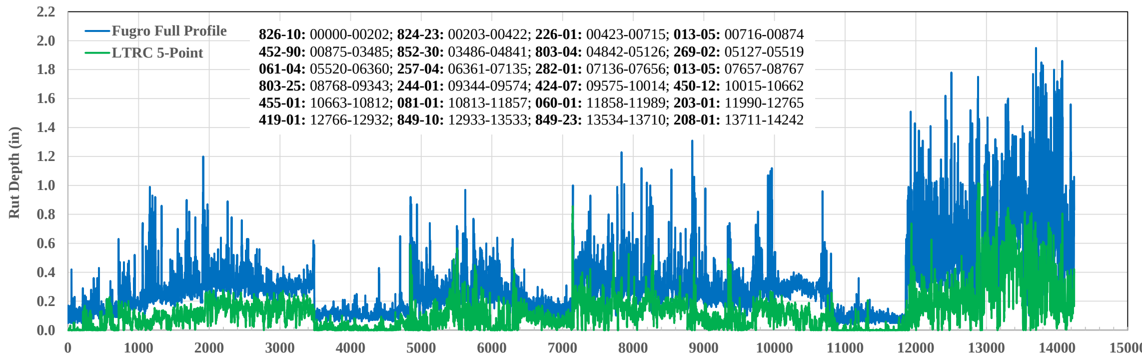

(a) LWP

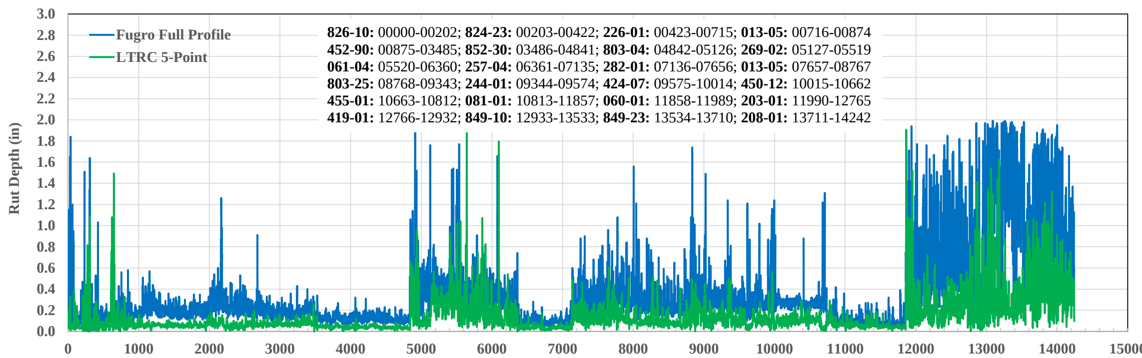

(b) RWP

Table 17. Correlation of LTRC's 5-point rut depths versus Fugro's full profile rut depth for selected sites (0.004-mile average)

	LTRC 5-Point System			**Fugro Full Profile**		
	LWP	RWP	Avg.	LWP	RWP	Avg.
No. of Points	7803	7803	7803	7803	7803	7803
Mean	0.104	0.0882	0.0961	0.276	0.230	0.253
STD	0.0642	0.0515	0.0478	0.102	0.106	0.0864
COV(%)	61.8	58.4	49.7	36.9	46.0	34.1
Correlation	-	-	-	0.474	0.402	0.499
R^2	-	-	-	0.225	0.162	0.249
p value from paired t test	-	-	-	0	0	0

Average rut depth over 0.1 mile

Histograms of the average Fugro's full profile rut depth and LTRC 5-point rut depth over 0.1 mile for the selected sites are presented in Figure 114 to Figure 115 in Appendix. These histograms show that only a few zero values is computed for LTRC's 0.1-mile average 5-point rut depths. Figure 35 presents the rut depth data over 0.1-mile average across all selected sites. The effect of cracks on rut depths is apparent in groups of sites with PMS R_AVE value of 0.5-0.75 in and greater than 0.75 in. It is also interesting to note that for control section 081-01, LTRC's 0.1-mile average 5-point rut depths are near zero. Further research indicates that this section was rehabilitated with overlay in 2020 so near zero rut depth values is expected. The rut depth value computed by the Fugro's full profile may be due to the same issue as observed in CS12.

Table 18 presents the mean, standard deviation, correlation coefficient, and *p* values of the paired t-test for 0.1-mile average rut depth data. The pavement sections with large rut depth discrepancies caused by aforementioned measurement issues of both systems were excluded. The similar patterns observed in 0.004-mile average rut depth data were observed here again in 0.1-mile average rut depth data.

Figure 35. Profiles of 0.1-mile interval rut depth for all selected sites

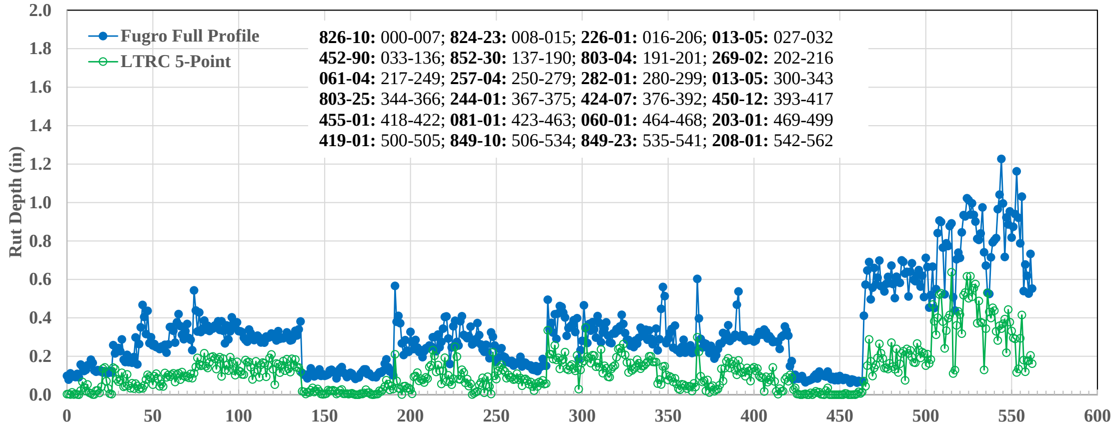

(a) LWP

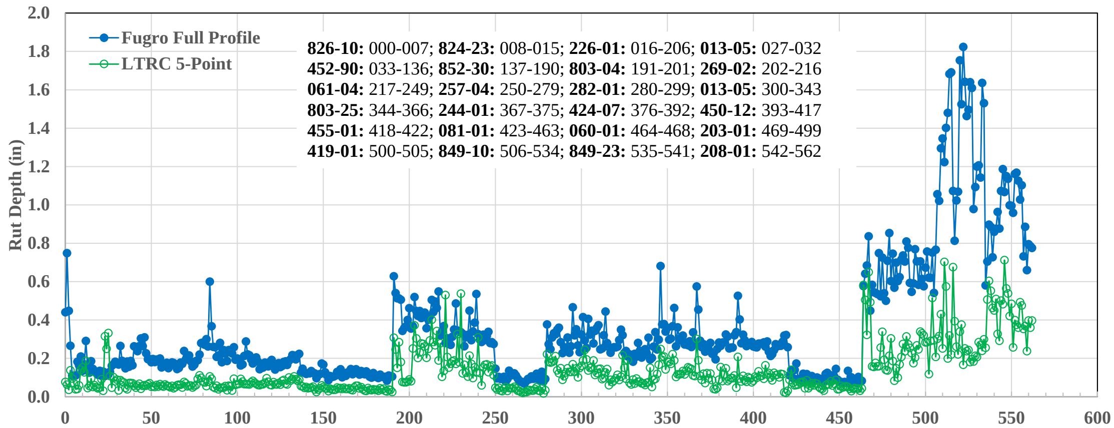

(b) RWP

Table 18. Correlation of LTRC's 5-point rut depths versus Fugro's full profile rut depth for selected sites (0.1-mile average)

	LTRC 5-Point System			Fugro Full Profile		
	LWP	RWP	Avg.	LWP	RWP	Avg.
No. of Points	307	307	307	307	307	307
Mean	0.104	0.0875	0.0959	0.276	0.230	0.253
STD	0.0453	0.0304	0.0322	0.0611	0.0587	0.0523
COV(%)	43.4	34.7	33.6	22.2	25.6	20.7
Correlation	-	-	-	0.718	0.722	0.761
R^2	-	-	-	0.516	0.521	0.579
p value from paired t test	-	-	-	4E-133	4E-121	3E-143

Remarks

As shown in both control sites and selected sites, the cracks have significant effect on computed Fugro's full profile rut depths at pavement sections where cracks are prevalent (i.e., the high rut depth values reported at those pavement sections in PMS are most probably due to measurements in cracks, not the actual rutting in pavement). In this case, when pavement condition is evaluated, double penalty may be applied. Figure 36 shows pavement image and rutting index for CS849-10. As can be seen from the figure, the rutting index fluctuates year to year due to measurements in cracks. The following formula is used by the Department to calculate the pavement condition index (PCI) for flexible pavement:

$$PCI = MAX\{MIN(RNDM, ALCR, PTCH, RUFF, RUT), [AVG(RNDM, ALCR, PTCH, RUFF, RUT) - 0.85STD(RNDM, ALCR, PTCH, RUFF, RUT)]\}$$

where, RNDM is the random cracking index; ALCR is the alligator cracking index; PTCH is the patch index; RUFF is the roughness index; RUT is the rutting index; and STD is the standard deviation.

Table 19 presents the calculated PCI in 2021 at several chainages. If we replace rut index of 2021 with the average of 2019 and 2021 rut index, the rating of pavement condition can be changed from poor to fair.

Figure 37 shows pavement image and rut index for CS 849-23. As can be seen from the figure, the rut index improved from around 25 in 2019 to around 50 in 2021. The review of PMS data indicated that large cracks were filled with asphalt patch materials. Table 20 presents the calculated PCI in 2022 at several chainages. If we replace rut index of 2021 with that of 2019, the rating of pavement condition can be moved towards near poor condition.

Figure 36. Pavement images and rut index profiles for CS849-10

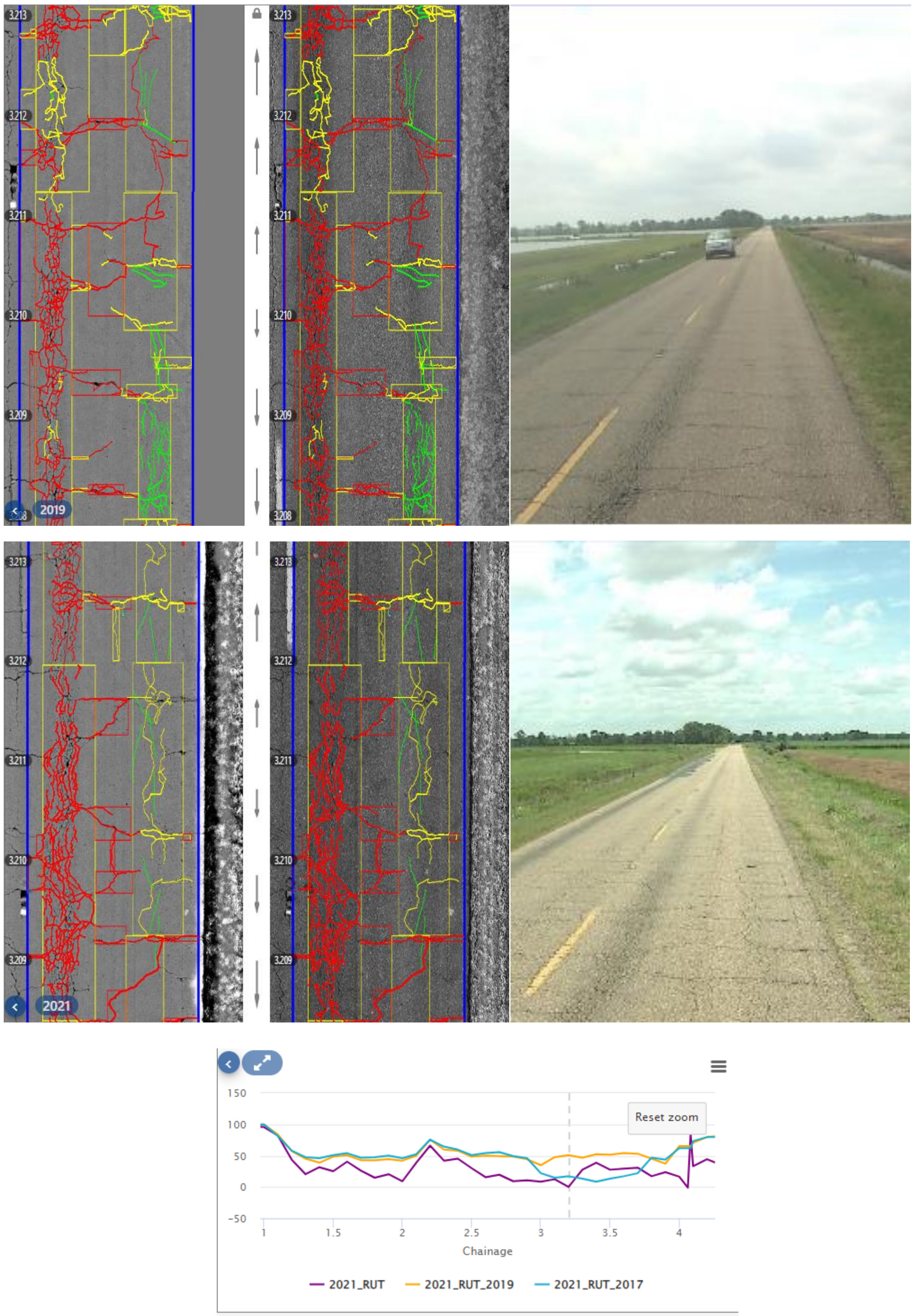

Table 19. Calculated pavement conditions for CS849-10

Chainage	**2.0**	**2.8**	**3.0**	**3.2**
2021 RNDM	55.4	50.6	49.4	49.9
2021 ALCR	31	41.7	43.8	50.3
2021 PTCH	100	100	100	100
2021 RUFF	78.4	76.6	70.4	78.2
2021 RUT	9.2	9.2	8.4	0
2021PCI	27.3	29.3	28.6	27.1
2019 RUT	42	48.4	34.8	59.8
PCI*	34.1	37.8	34.5	40.7

*Calculated based on the average of 2019 and 2021 rut index.

Figure 37. Pavement images and rut index profiles for CS849-23

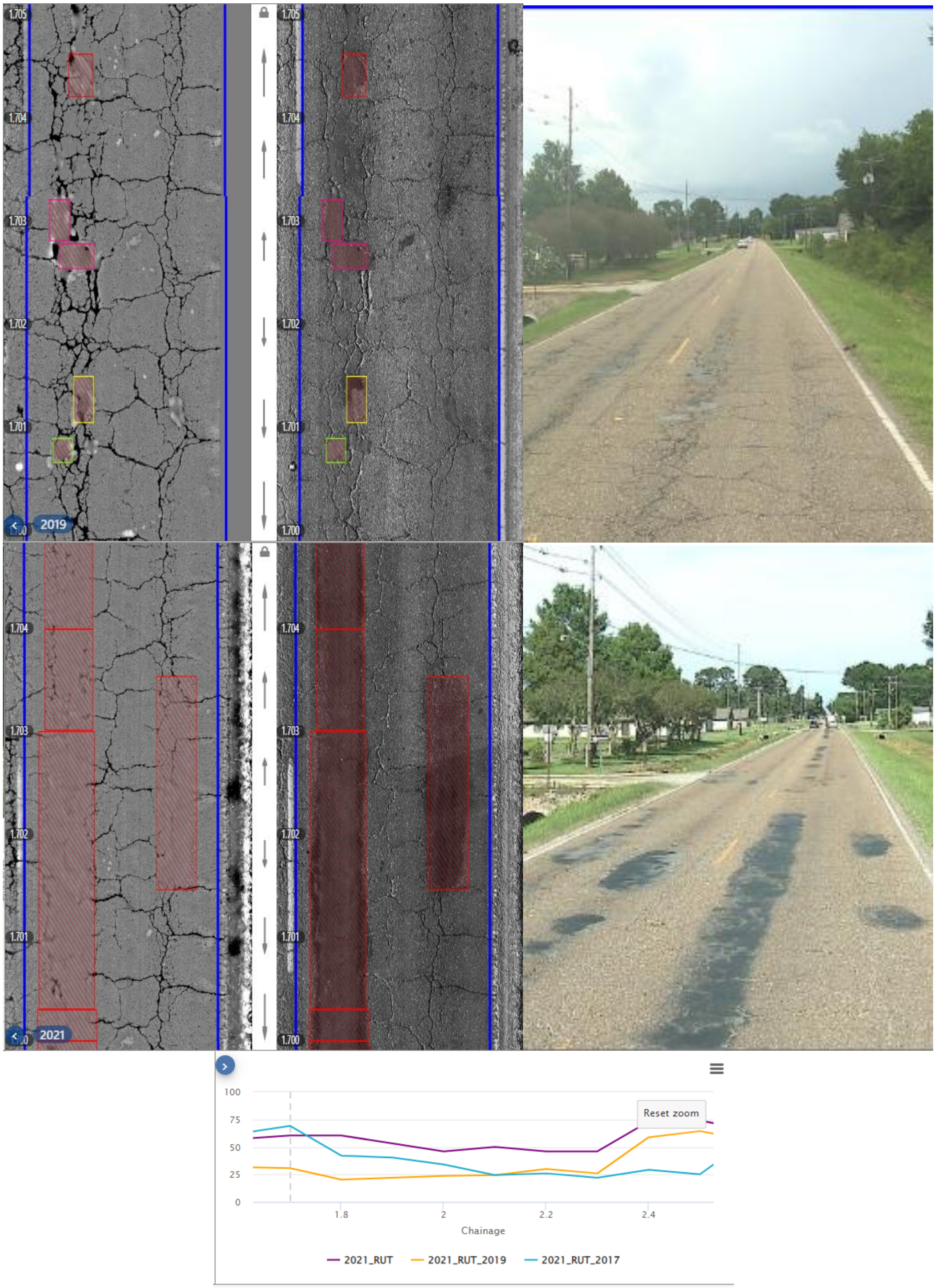

Table 20. Calculated pavement conditions for CS 849-23

Chainage	1.7	1.8	2.0
2021 RNDM	53.1	53.5	61.7
2021 ALCR	55.9	50.8	54.1
2021 PTCH	51.5	48.4	49.1
2021 RUFF	60.6	49.6	41.8
2021 RUT	60.4	60.4	46
2021PCI	53.1	48.9	44.8
2019 RUT	30.8	20.4	23.6
PCI*	41.7	34.2	35.1

*Calculated based on the rut index of 2019

Conclusions

The Pavement Management Systems Section of DOTD often requests LTRC to collect rutting data for the pavement management control sites and compare them with the data from the Vendor. The correlation of calculated rut depths between these two systems should be established for us to better understand the rutting data collected by LTRC and the rutting data in the DOTD PMS.

- Averaging rut depths over 0.004-mile and 0.1-mile increments show noticeable improvement of repeatability of LTRC's 5-point rut bar system, especially for average rut depths over 0.1 mile, which achieved an overall correlation value of 0.90 and above.
- The current algorithm of Roadware Vision causes incorrect measurements that include measurements in cracks, measurements outside wheel path, and the failure of locating the point of maximum rut depth.
- LTRC's 5-point rut bar system cannot always capture the maximum rut depth for transverse profiles (missing the peak and valley). It can also be significantly affected by the edge drop off and grass for RWP rut depth.
- The correlations of average rut depths were higher than those for the LWP and RWP. Averaging rut depths over 0.1-mile increment showed noticeable improvement of correlation between LTRC's and Fugro's road profiler.
- The results of t-tests showed that mean values of LTRC's 5-point rut depth and Fugro's full profile rut depth were statistically different at all scales (individual rut depth, 0.004-mile average rut depth, and 0.1-mile average rut depth).
- The t-tests indicated that the mean values of LTRC's and Fugro's 5-point rut depth was statistically different at individual and 0.004-mile average level, however, with careful planning, the difference between the mean value of LTRC's 5-point rut depth and Fugro's 5-point rut depths at 0.1-mile average level could be statistically insignificant.
- For pavement sections that cracks are prevalent, the cracks have significant effect on computed Fugro's full profile rut depths with the current algorithm of Roadware Vision. In this case, including rut index in pavement condition index computation can possibly create double penalty issue.

Recommendations

The following standard operating procedure (SOP) is recommended for using LTRC's 5-point rut bar system to collect rutting data to support pavement management activities.

1. Site Selections:

1.1. The control site selected for rutting verification should be at least 11 ft. wide.

1.2. The control site in which cracks are prevalent should be excluded from rut depth comparison

2. Preparation:

2.1 The accuracy of distance measuring instrument (DMI) should be checked at least at one section with at least 1000 ft. in length.

2.1.1 This test should be performed before the LTRC's 5-point rut bar system obtains rutting data at the control sites.

2.1.2. A section of at least 1000 ft. in length shall be selected on North Line Road near LTRC's pavement research facility. Clearly marking the starting and ending points of the test section, measure the distance between the starting and ending points with a measurement tape.

2.1.3. At least three auto-triggered runs at the low (30 mph) and high test speeds (50 mph) shall be conducted.

2.1.4. Compute the absolute difference between the DMI readings and the distance of the section tested. The average of the absolute difference for both the high-speed and low-speed runs must be less than 0.15 percent.

2.2 LTRC's 5-point rut bar system repeatability should be checked at least at six control sites.

2.2.1 Three repeat runs of the LTRC system shall be made at each selected control site. Data collection shall be automatically triggered at the starting location of the section.

2.2.2 Evaluate repeatability using the cross-correlation of the rut depth. Calculate the cross-correlation value of each site. On each site, cross-correlate each of the three rut depth profiles to each of the remaining two. The cross-correlation for each site is the average of three values. The repeatability cross-correlation is the average of cross-correlation value of each site. A repeatability cross-correlation of 0.40, 0.6, and 0.85 or greater is required for individual rut depth, 0.004-mile average rut depth, and 0.1-mile average rut depth, respectively. A lower repeatability cross-correlation may be acceptable for the individual site.

3. Data Collection and Report

3.1 Since control sites are short sections (0.5 mile), it would be better to make sure start and end points are triggered with a cone or some other means of ensuring the start/end locations are accurate.

3.2 Care shall be taken to ensure the center of the rut bar is as close to the centerline of the lane as possible during data collection.

3.2 Data shall be collected at 1 ft. interval.

3.2 The rut depth data shall be reported in 0.1 mile and sent to pavement management engineer.

3.3 It is recommended that LTRC's 5-point rut depth data be compared to Fugro's 5-point rut depth data with the following settings in Roadware Vision to match LTRC's 5-point rut bar system (X_{LW}=1.557528 m, X_L=0.877062 m, X_C=0.0 m, X_R=0.878078 m, and X_{RW}=1.573022 m) as shown in Figure 12.

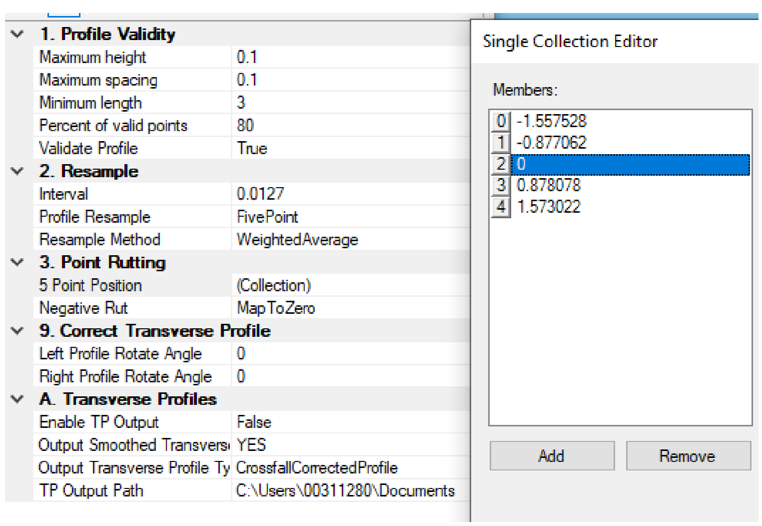

Acronyms, Abbreviations, and Symbols

Term	Description
AASHTO	American Association of State Highway and Transportation Officials
ARAN	Automatic Road Analyzer
ARRB	Australian Road Research Board
ASTM	American Society for Testing and Materials
cm	Centimeter
COV	Coefficient of Variation
CS	Control Site/Control Section
DMI	Distance Measuring Instrument
DOTD	Louisiana Department of Transportation and Development
FHWA	Federal Highway Administration
ft.	foot (feet)
HPMS	Highway Performance Monitoring System
in.	inch(es)
INO	National Optics Institute
LCMS	Laser Crack Measurement System
LRMS	Laser Rutting Measurement System
LTRC	Louisiana Transportation Research Center
LWP	Left Wheel Path
mm	Millimeter
mph	Mile per Hour
PCI	Pavement Condition Index
PMS	Pavement Management System
PPS	Pavement Profile Scanner
RWP	Right Wheel Path
SOP	Standard Operating Procedure

References

[1] A. Simpson, "Characterization of Transverse Profiles," FHWA Publication NO. FHWA-RD-01-024, Turner-Fairbank Highway Research Center, McLean, VA, 1975.

[2] Fugro, "pave3d-system-brochure_2," Fugro, 2013. [Online]. Available: https://www.fugro.com/docs/default-source/media-resources/pavement-management/pave3d-system-brochure_2.pdf?sfvrsn=4. [Accessed 12 August 2020].

[3] C. Fillastre, *What's New in Pavement Management,* Baton Rouge, LA: Presentation to LTRC, Pavement Management Systems, Louisiana Department of Transportation and Development, 2017.

[4] C. Fillastre, *Pavement Management System,* Baton Rouge, LA: Presentation to LTRC, Pavement Management Systems, Louisiana Department of Transportation and Development, 2018.

[5] ASTM, "Standard Test Method for Measuring Rut-Depth of Pavement Surfaces Using a Straightedge," ASTM E1703/E1703M-10 (Reapproved 2015), American Society for Testing and Materials (ASTM), West Conshohocken, PA, 2015.

[6] P. A. Serigos, J. A. Prozzi, B. H. Nam and M. R. Murphy, "Field Evaluation of Automated Rutting Measuring Equipment," FHWA/TX-12/0-6663-1, Texas Department of Transportation, Austin, TX, 2012.

[7] C. R. Bennett and H. Wang, "Harmonizing Automated Rut Depth Measurements," Transfund New Zealand Research Report, 2002.

[8] K. McGhee, "Automated Pavement Distress Collection Techniques: A Synthesis of Highway Practice," NCHRP Synthesis 334, National Coorperative Highway Research Program (NCHRP), Transportation Research Board, Washington, D.C., 2004.

[9] F. Li, "A Methodology for Characterizing Pavement Rutting Condition Using Emerging 3D Line Laser Imaging Technology," Ph.D. thesis. Department of Civil

Engineering, Georgia Institute of Technology, 2012.

[10] H. Wang, "Development of Laser System to Measure Pavement Rutting," Master thesis. Department of Civil and Environmental Engineering, University of South Florida, 2005.

[11] B. R. Hoffman and S. M. Sargand, "Verification of Rut Depth Collected with the INO Laser Rut Measurement System (LRMS)," FHWA/OH-2011/18, Ohio Department of Transportation, Columbus OH, 2011.

[12] R. S. Walker, S. Wright and W.-M. Kuo, "Real Time Instrumentation For Pavement Rut Measurements," Texas Department of Transportation, Austin, TX, 1995.

[13] P. Icenogle and G. Keel, "PMS Rutting," Internal Report, Louisiana Transportation Research Center, Baton Rouge, LA, 2003.

Appendix

Figure 38. Histograms of Fugro's full profile rut depths (individual) for all control sites in 2020

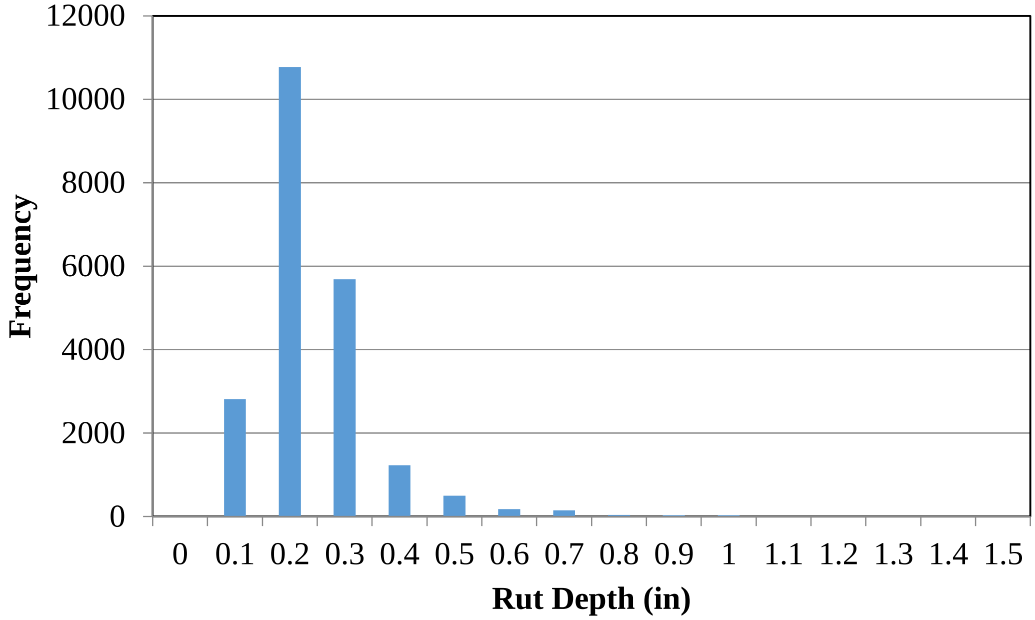

(a) LWP

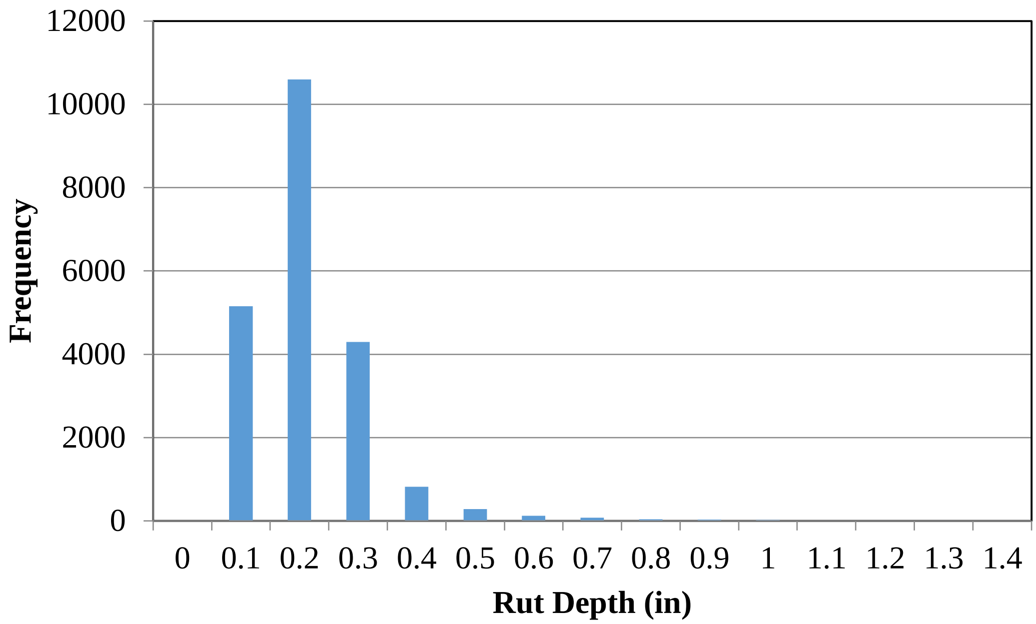

(b) RWP

Figure 39. Histograms of Fugro's 5-point rut depths (individual) for all control sites in 2020

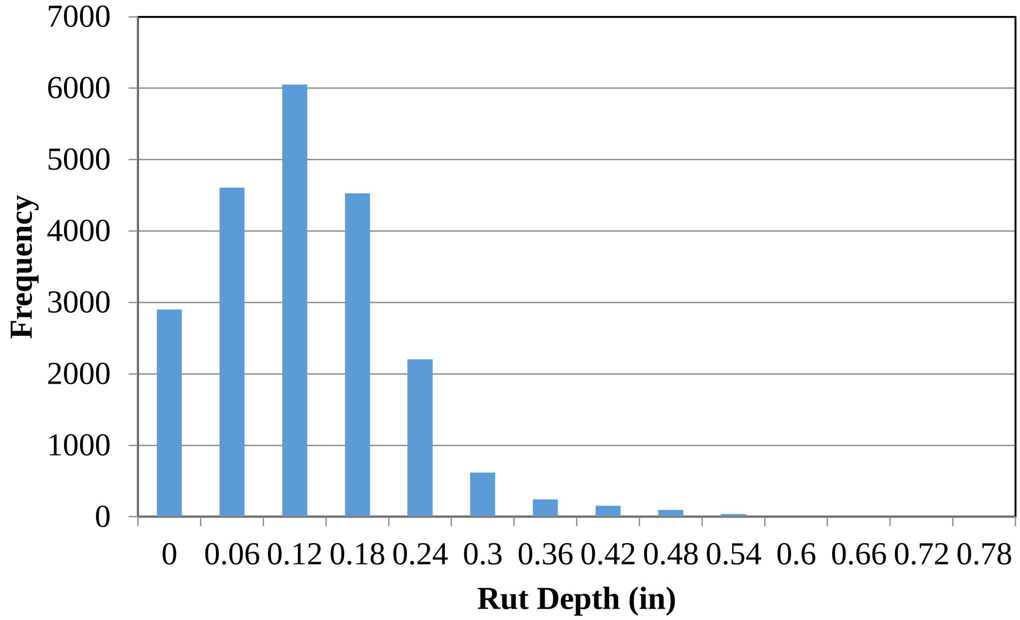

(a) LWP

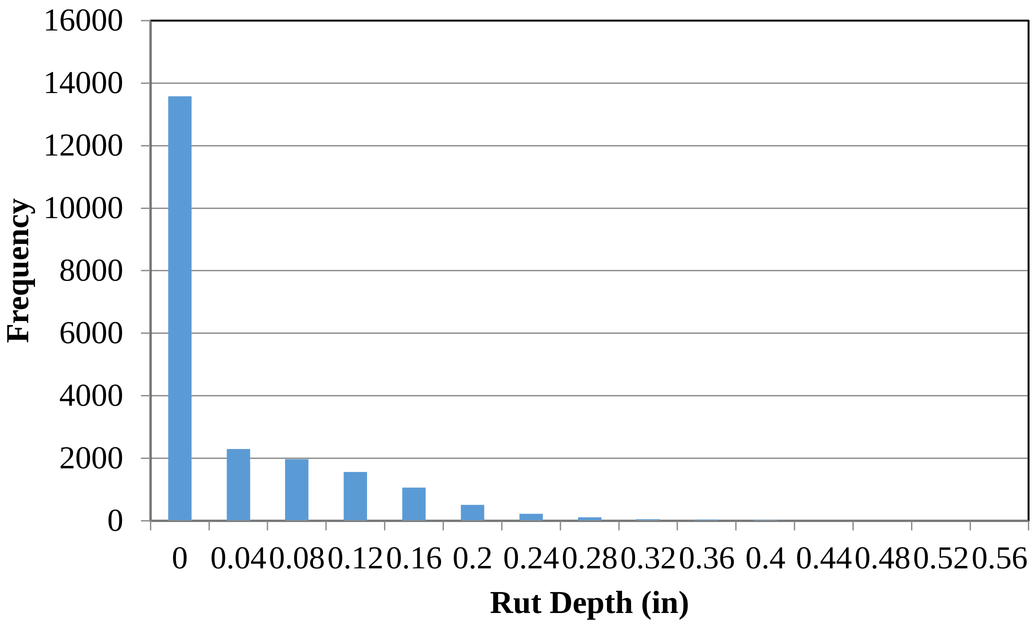

(b) RWP

Figure 40. Histograms of LTRC's 5-point rut depths (individual) for all control sites in 2020

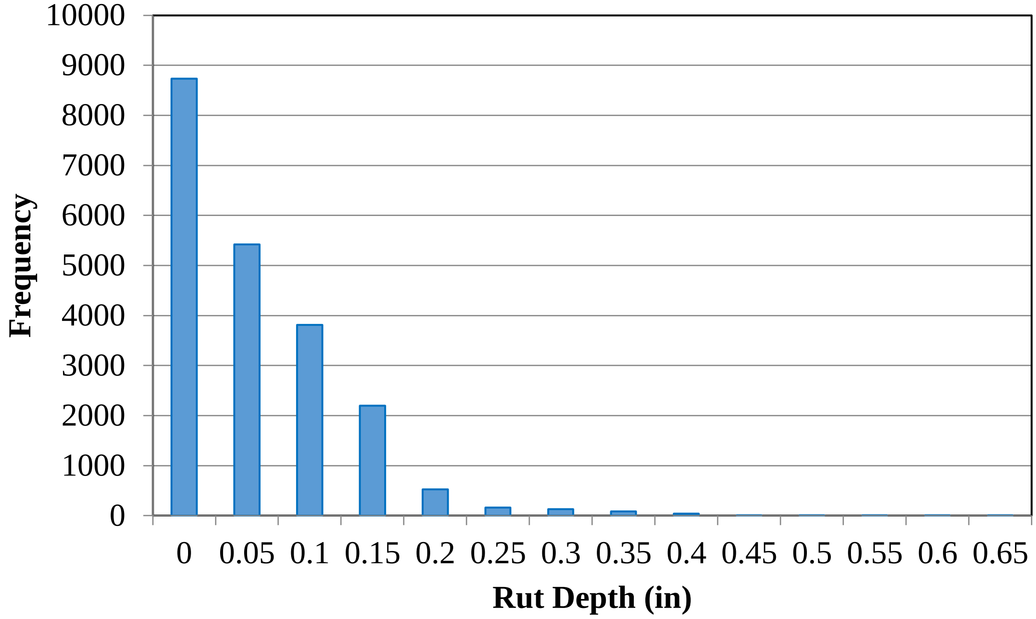

(a) LWP

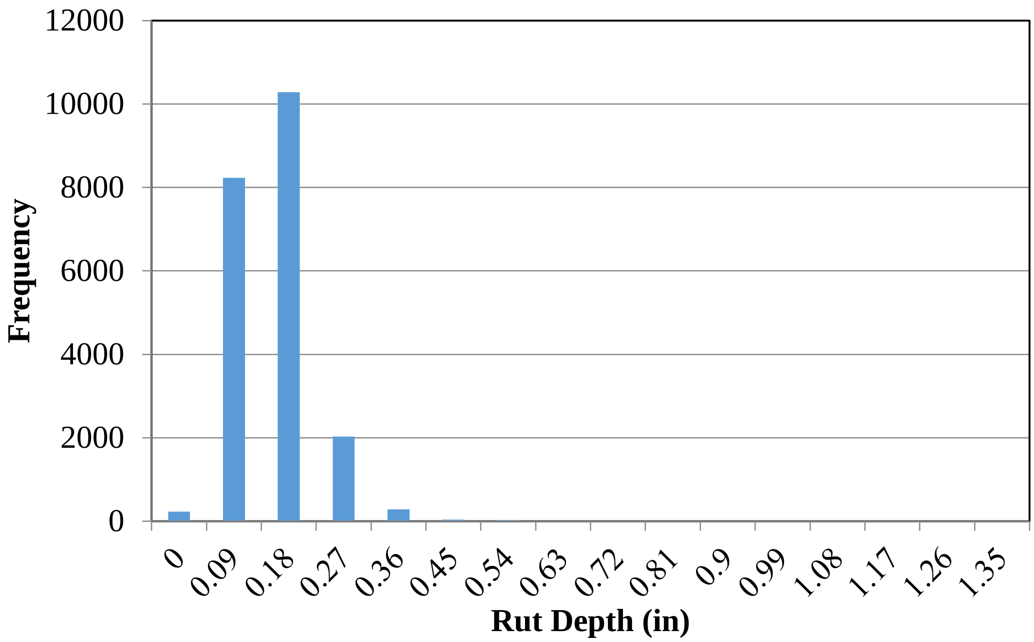

(b) RWP

Figure 41. Histograms of Fugro's full profile rut depths (individual) for all control sites in 2021

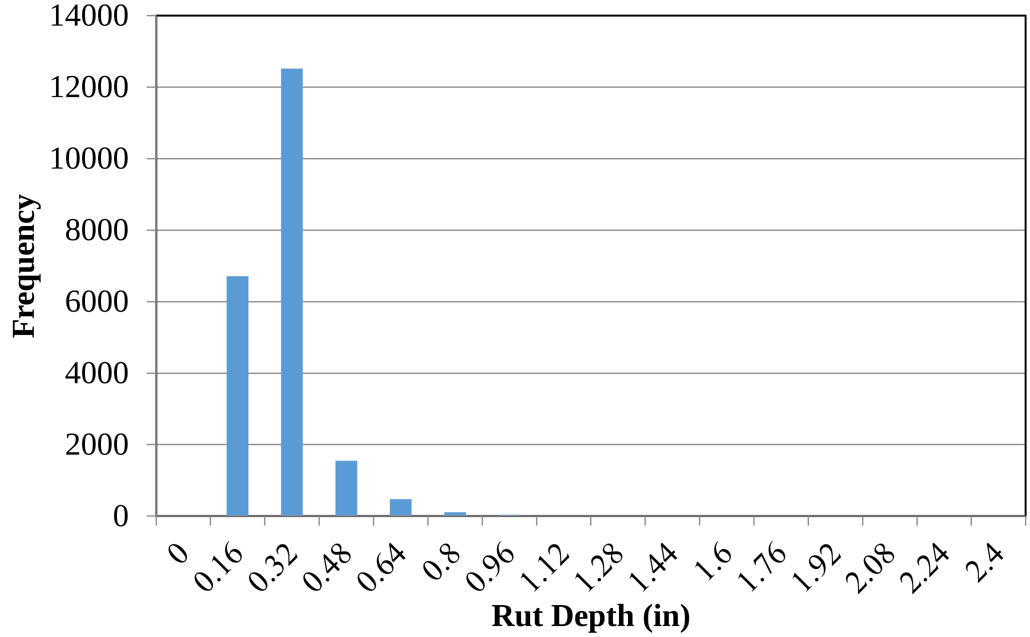

(a) LWP

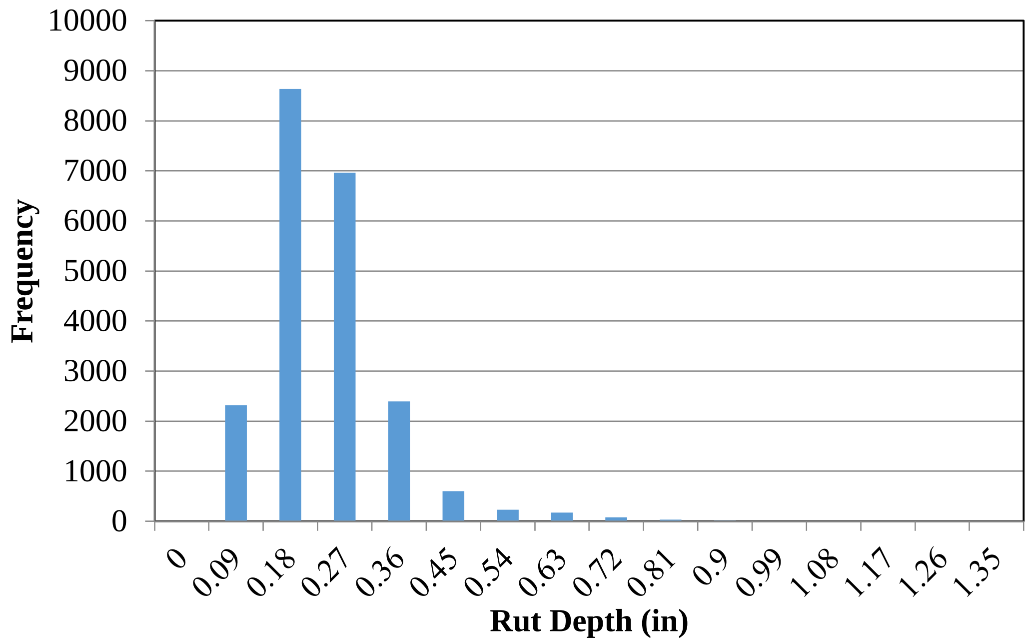

(b) RWP

Figure 42. Histograms of Fugro's 5-point rut depths (individual) for all control sites in 2021

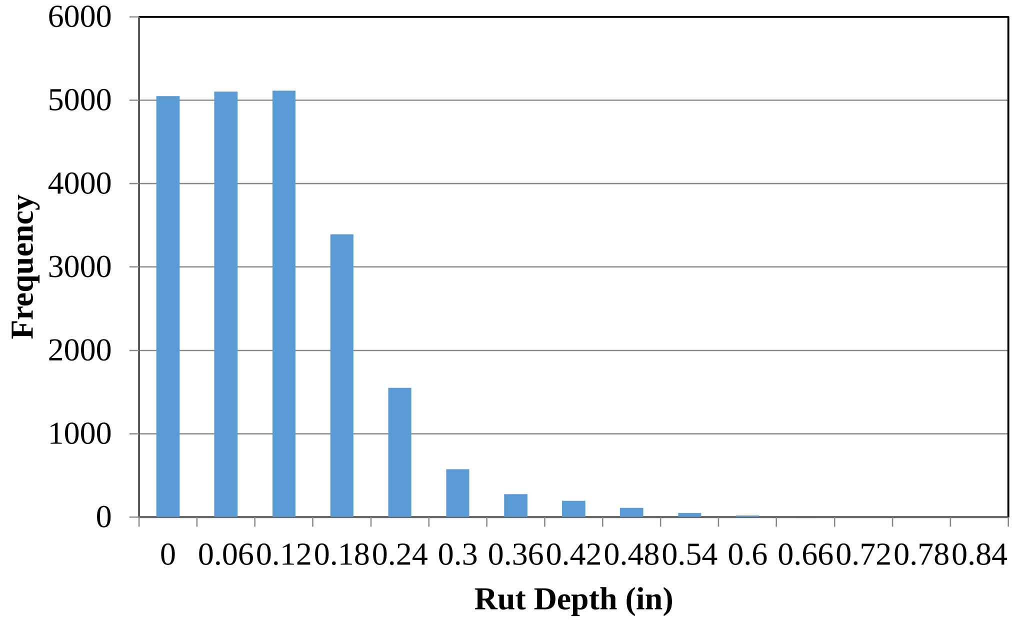

(a) LWP

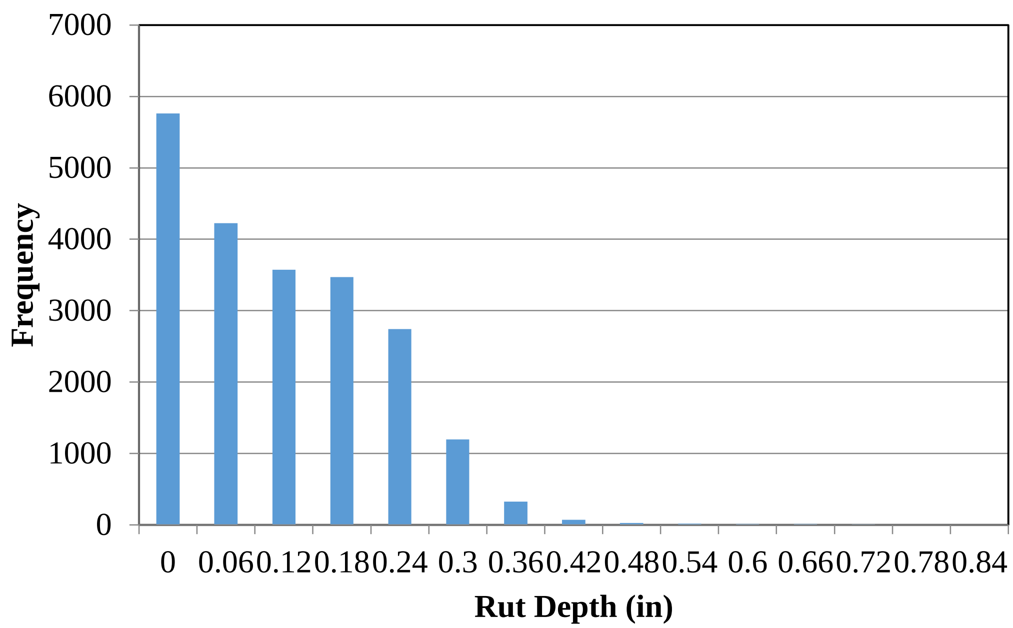

(b) RWP

Figure 43. Histograms of LTRC's 5-point rut depths (individual) for all control sites in 2021

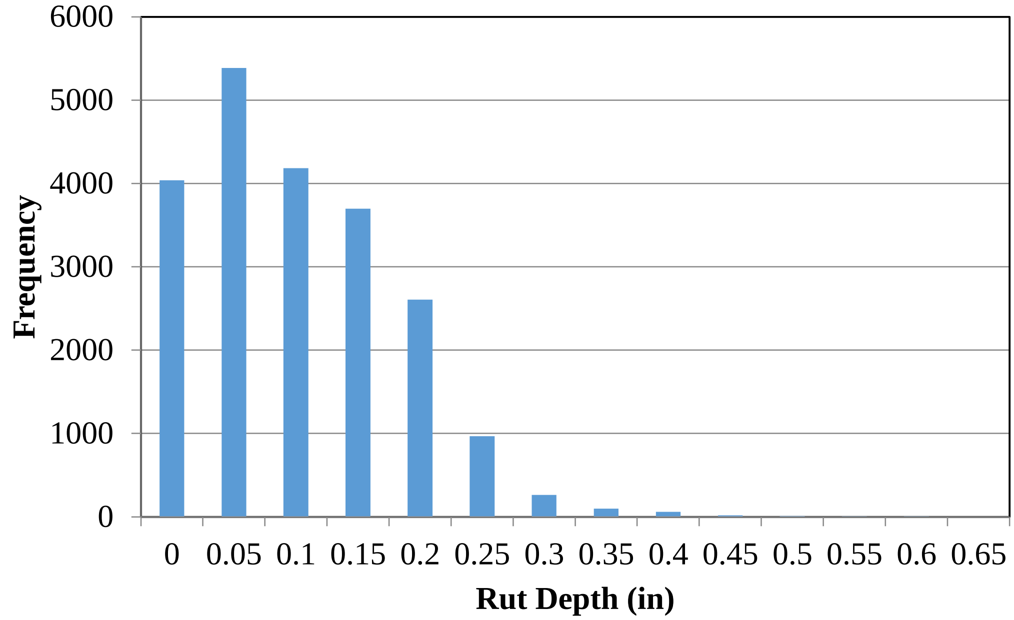

(a) LWP

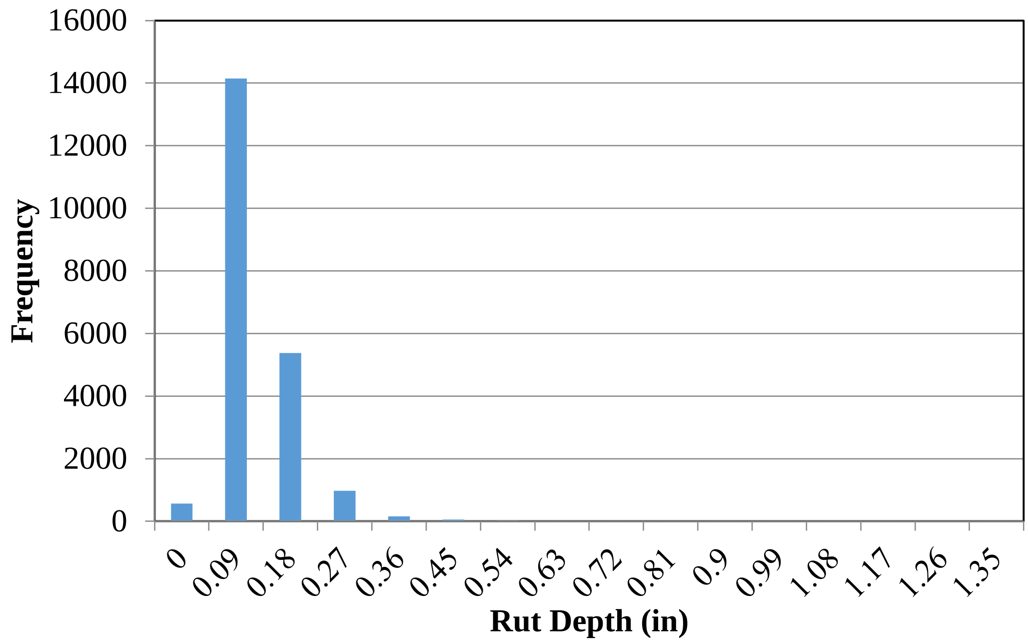

(b) RWP

Figure 44. Scatterplot of Fugro's full profile rut depth vs. Fugro's 5-point rut depth for CS03 in 2020

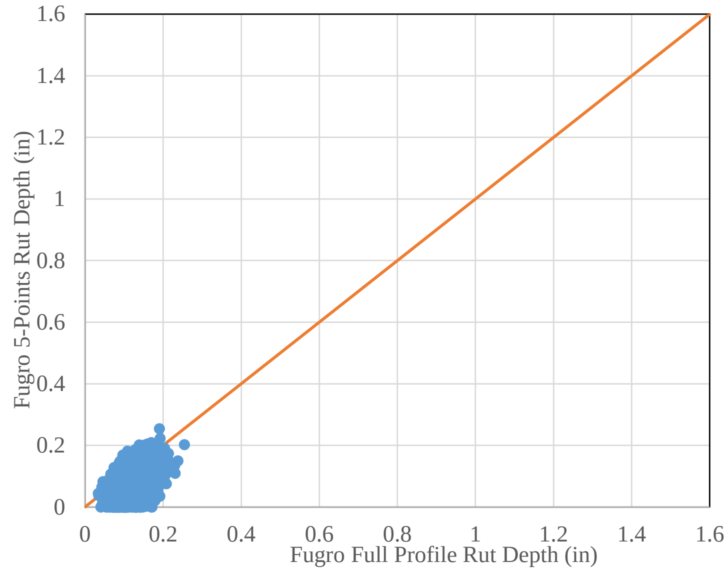

(a) LWP

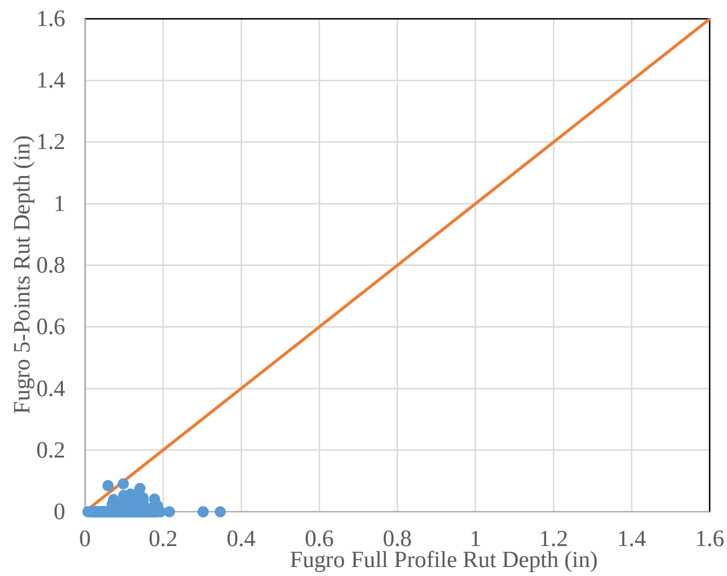

(b) RWP

Figure 45. Scatterplot of Fugro's full profile rut depth vs. Fugro's 5-point rut depth for CS06 in 2020

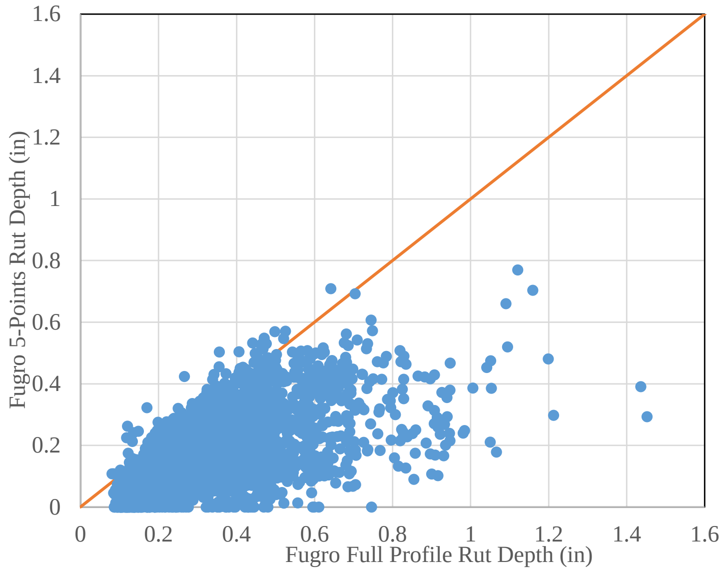

(a) LWP

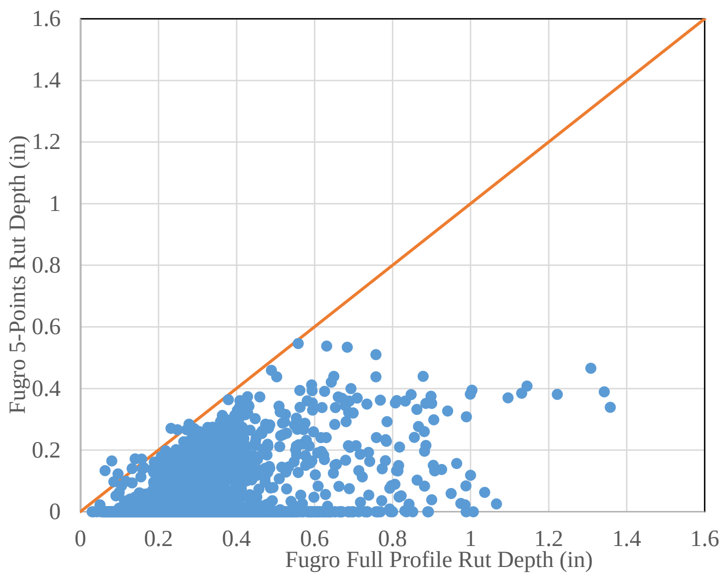

(b) RWP

Figure 46. Scatterplot of Fugro's full profile rut depth vs. Fugro's 5-point rut depth for CS07 in 2020

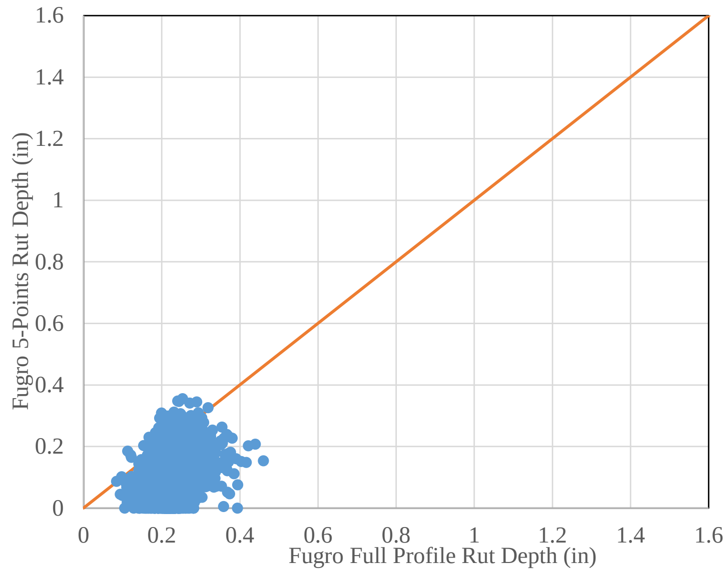

(a) LWP

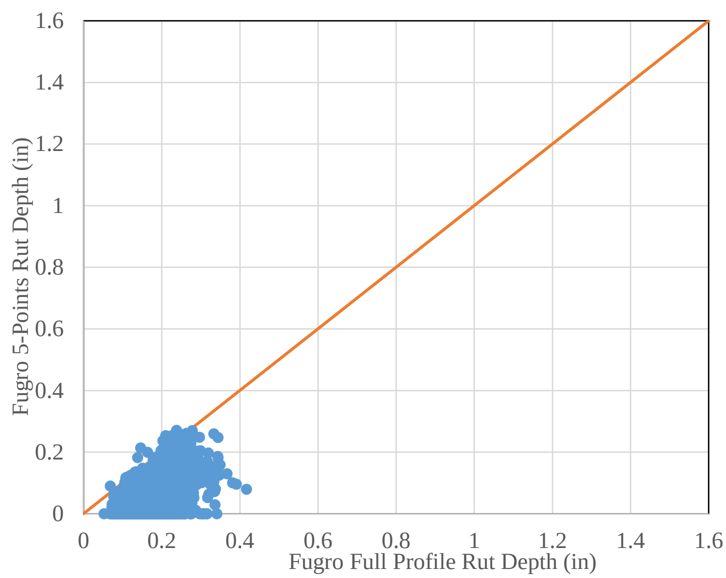

(b) RWP

Figure 47. Scatterplot of Fugro's full profile rut depth vs. Fugro's 5-point rut depth for CS08 in 2020

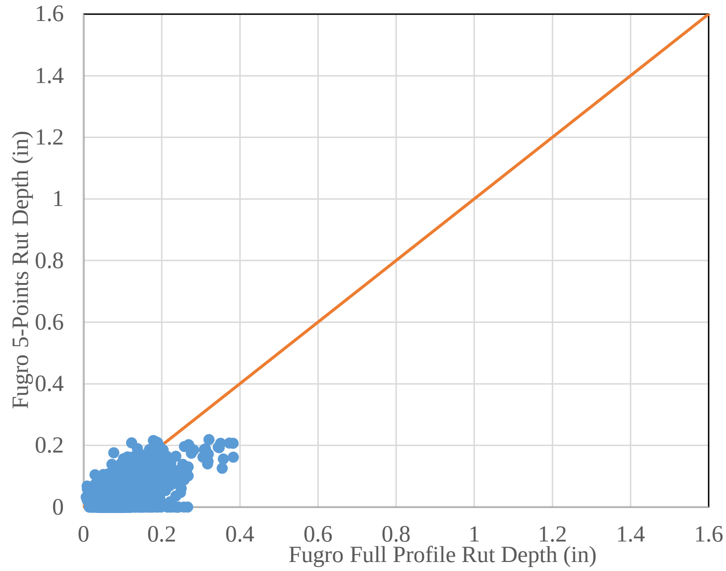

(a) LWP

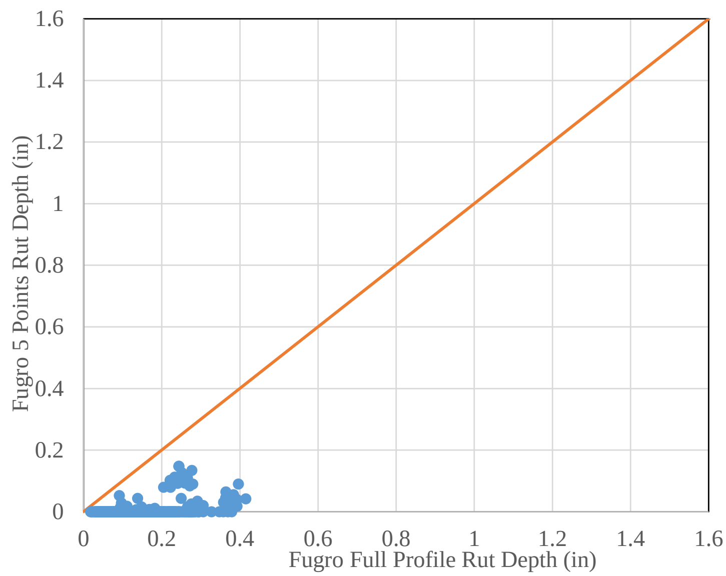

(b) RWP

Figure 48. Scatterplot of Fugro's full profile rut depth vs. Fugro's 5-point rut depth for CS09 in 2020

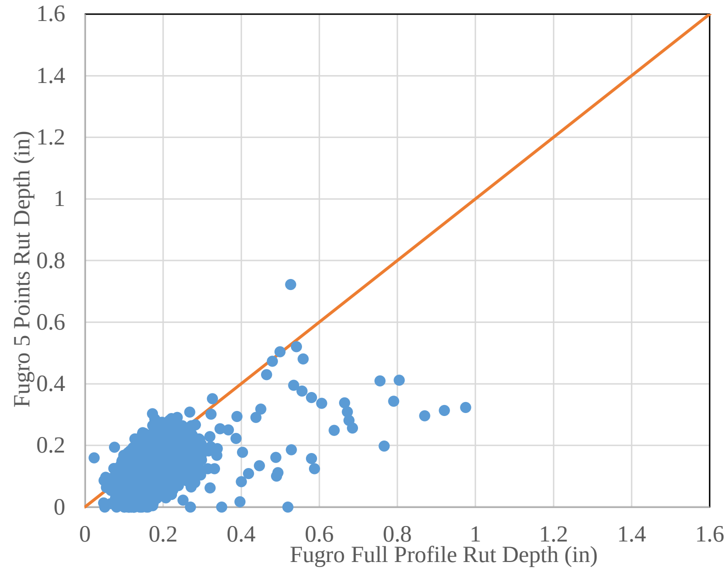

(a) LWP

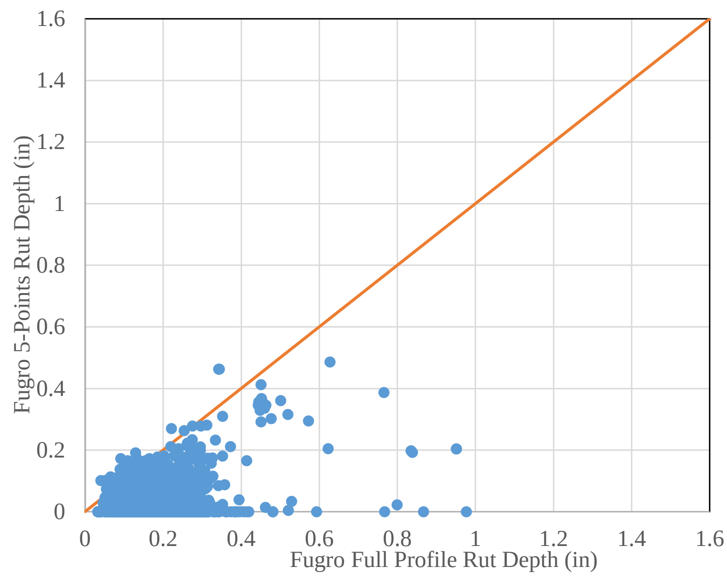

(b) RWP

Figure 49. Scatterplot of Fugro's full profile rut depth vs. Fugro's 5-point rut depth for CS10 in 2020

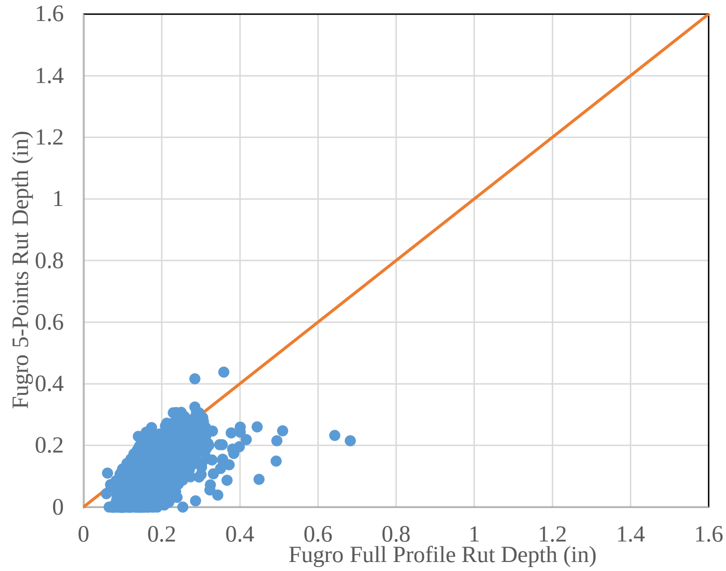

(a) LWP

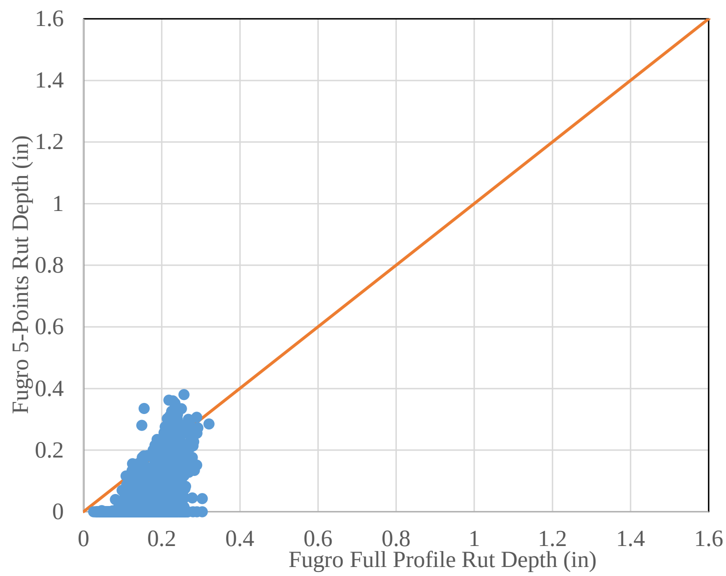

(b) RWP

Figure 50. Scatterplot of Fugro's full profile rut depth vs. Fugro's 5-point rut depth for CS12 in 2020

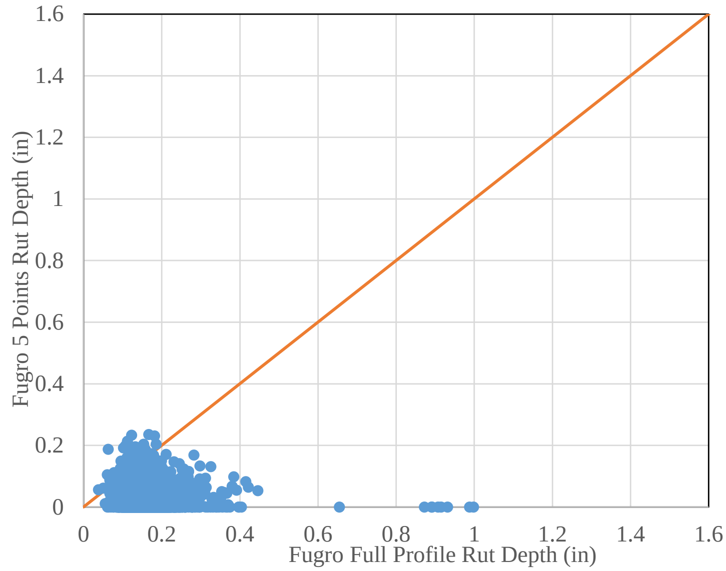

(a) LWP

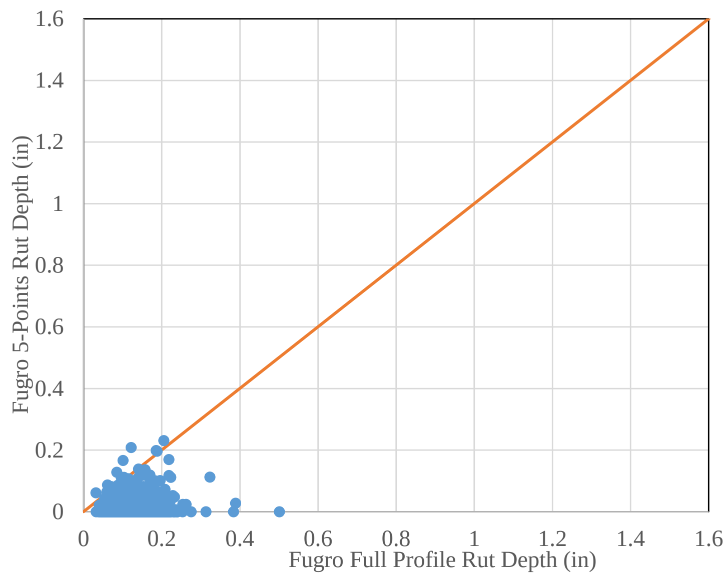

(b) RWP

Figure 51. Scatterplot of Fugro's full profile rut depth vs. Fugro's 5-point rut depth for CS13 in 2020

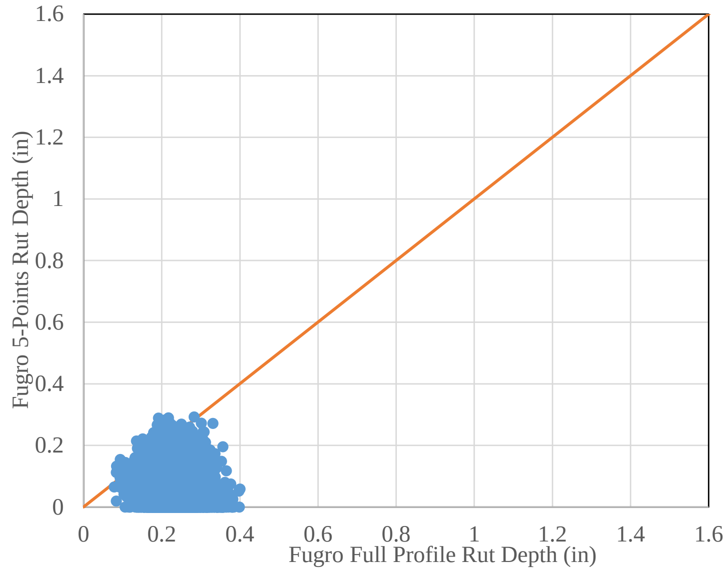

(a) LWP

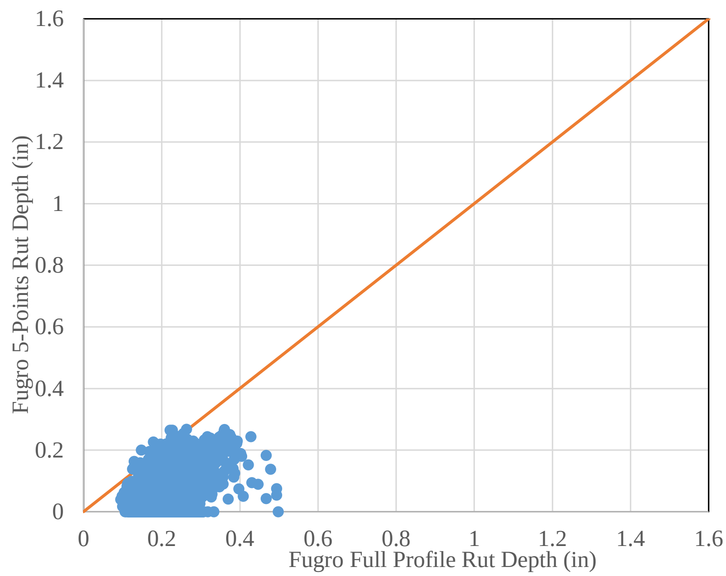

(b) RWP

Figure 52. Scatterplot of Fugro's full profile rut depth vs. Fugro's 5-point rut depth for CS03 in 2021

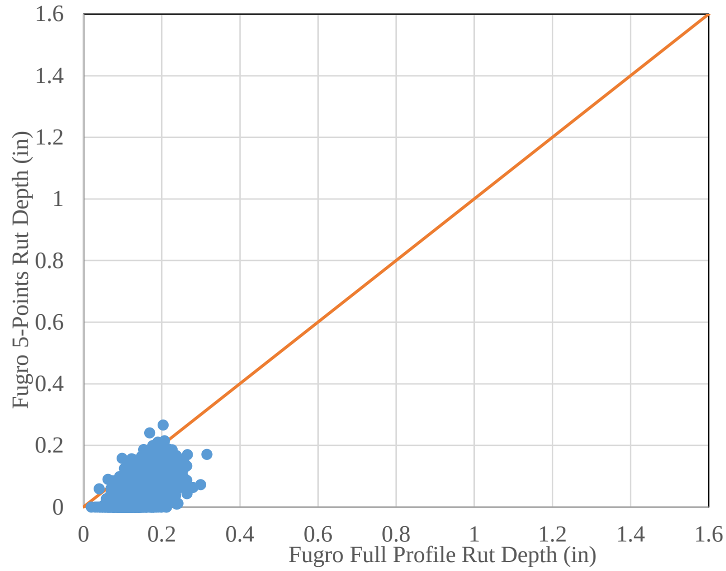

(a) LWP

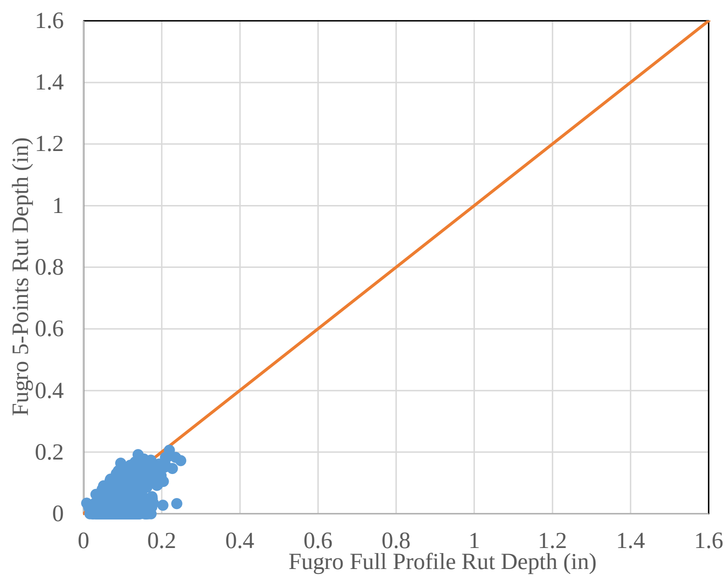

(b) RWP

Figure 53. Scatterplot of Fugro's full profile rut depth vs. Fugro's 5-point rut depth for CS06 in 2021

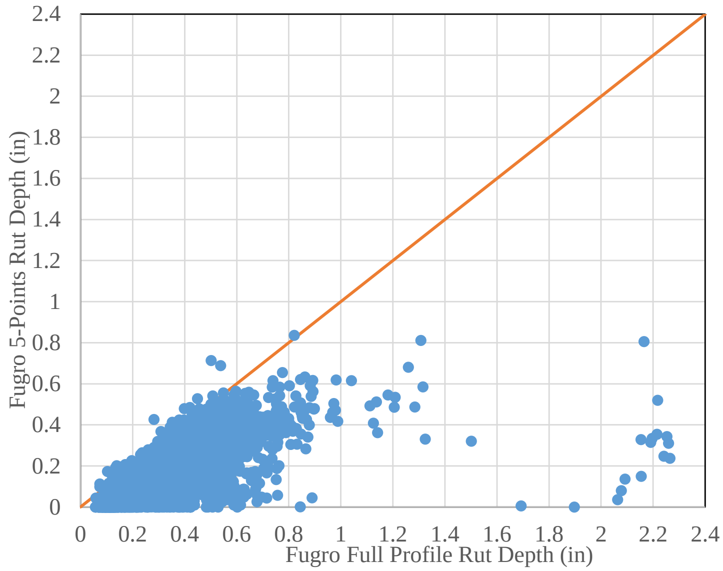

(a) LWP

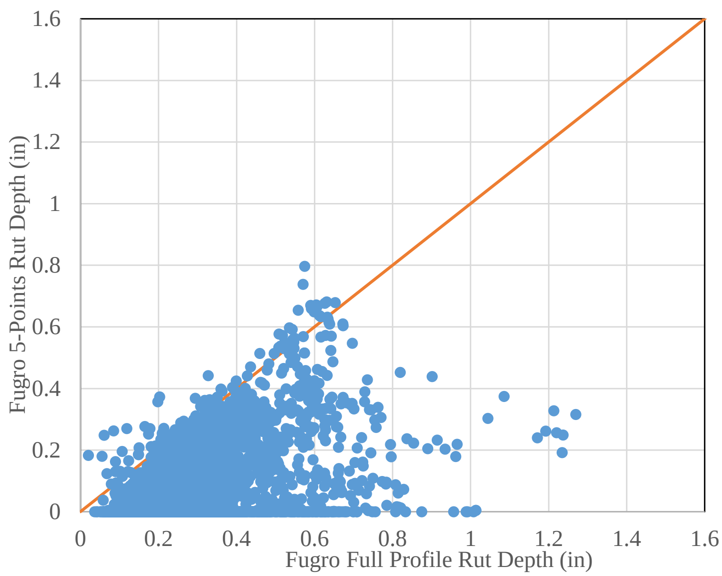

(b) RWP

Figure 54. Scatterplot of Fugro's full profile rut depth vs. Fugro's 5-point rut depth for CS07 in 2021

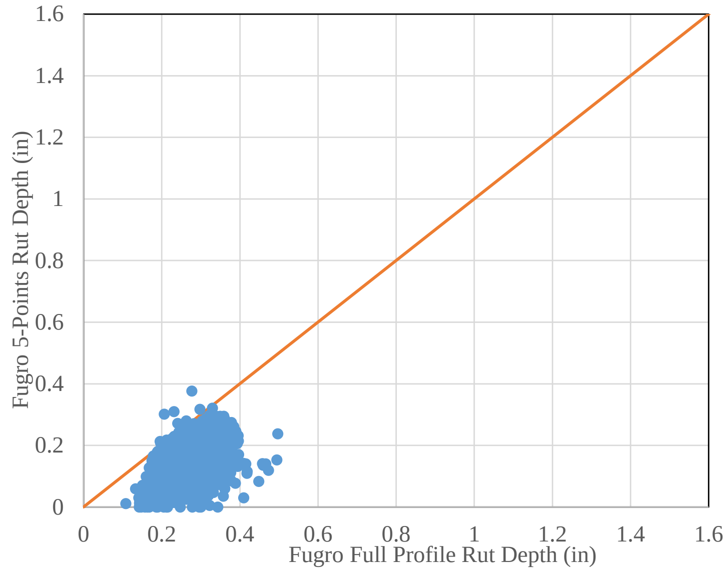

(a) LWP

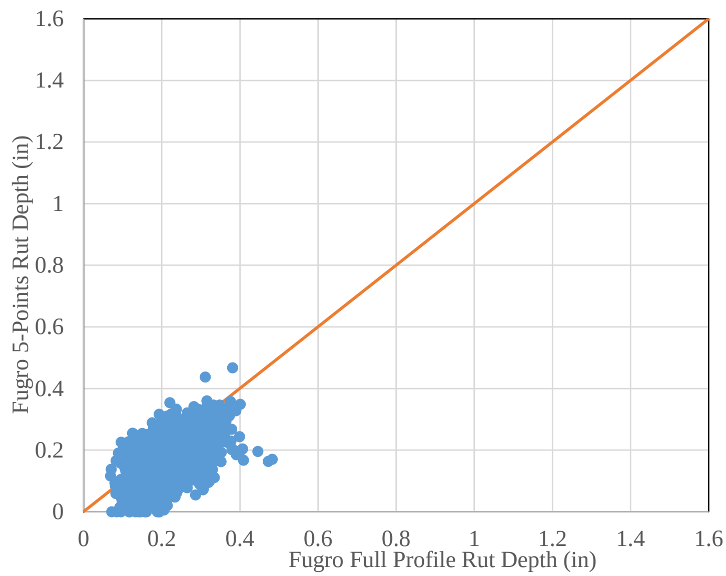

(b) RWP

Figure 55. Scatterplot of Fugro's full profile rut depth vs. Fugro's 5-point rut depth for CS08 in 2021

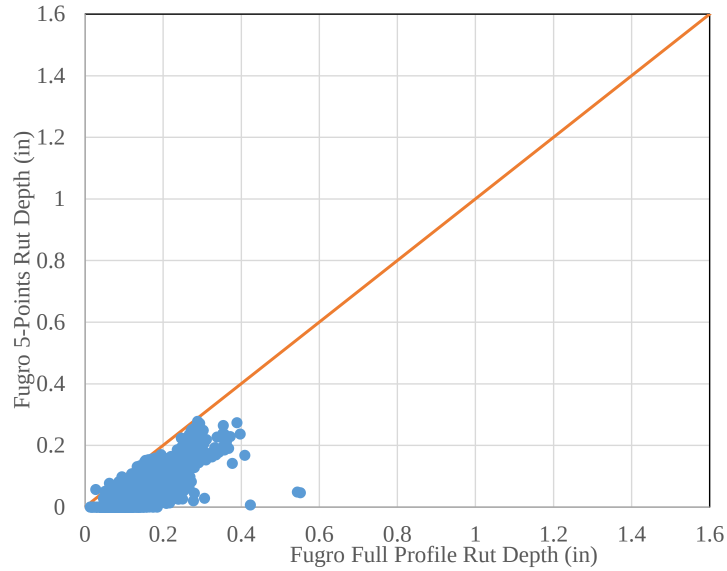

(a) LWP

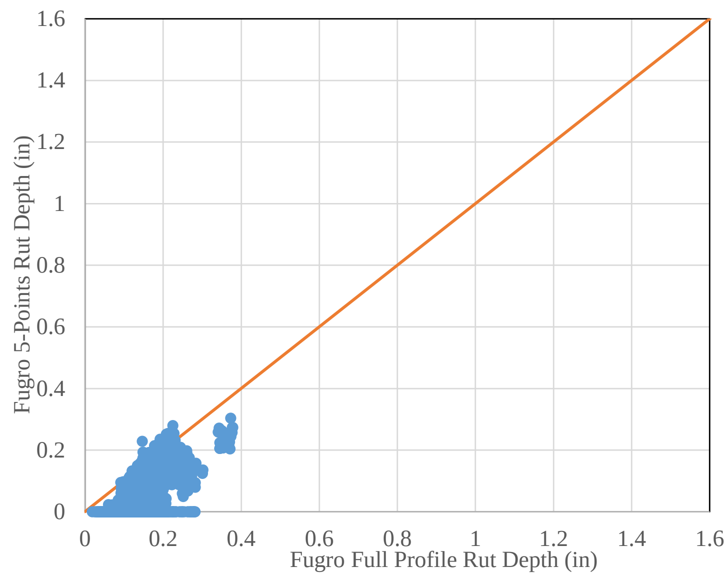

(b) RWP

Figure 56. Scatterplot of Fugro's full profile rut depth vs. Fugro's 5-point rut depth for CS09 in 2021

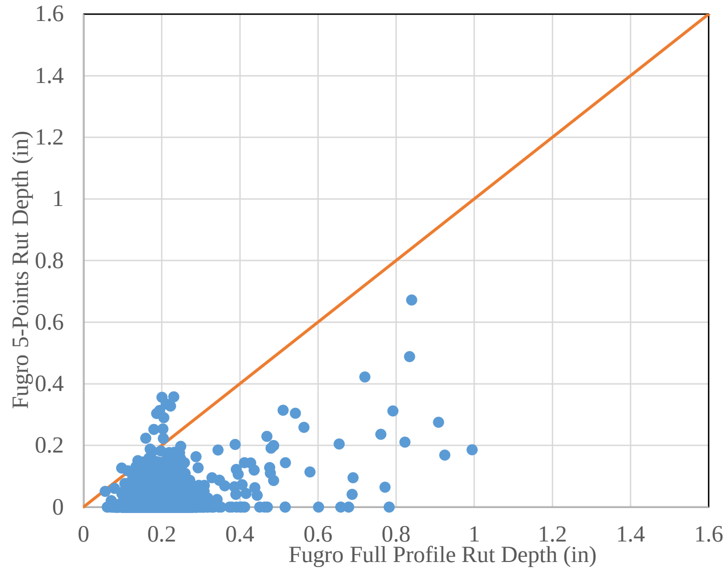

(a) LWP

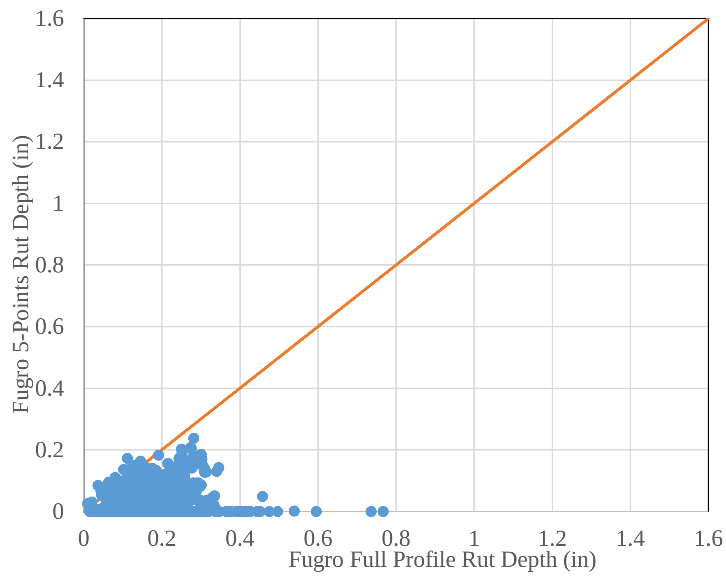

(b) RWP

Figure 57. Scatterplot of Fugro's full profile rut depth vs. Fugro's 5-Point rut depth for CS10 in 2021

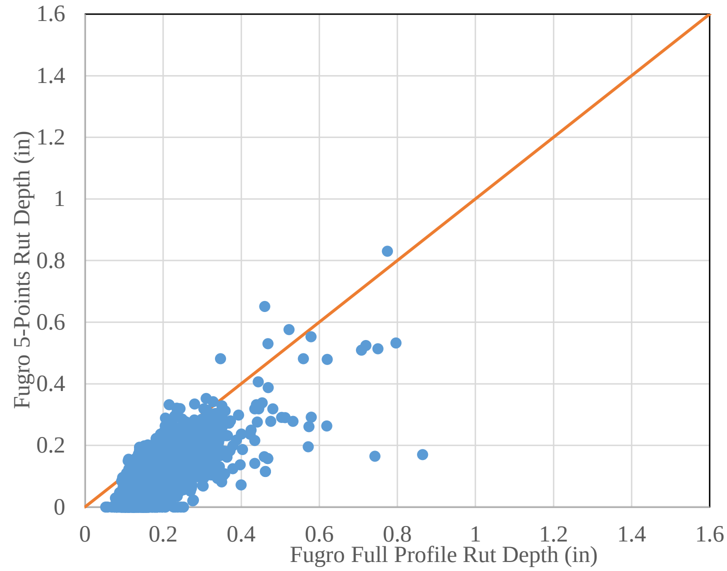

(a) LWP

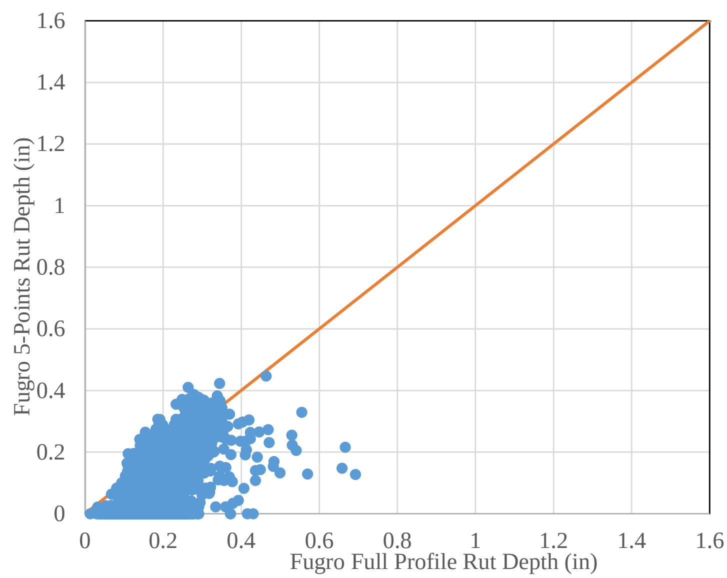

(b) RWP

Figure 58. Scatterplot of Fugro's full profile rut depth vs. Fugro's 5-point rut depth for CS12 in 2021

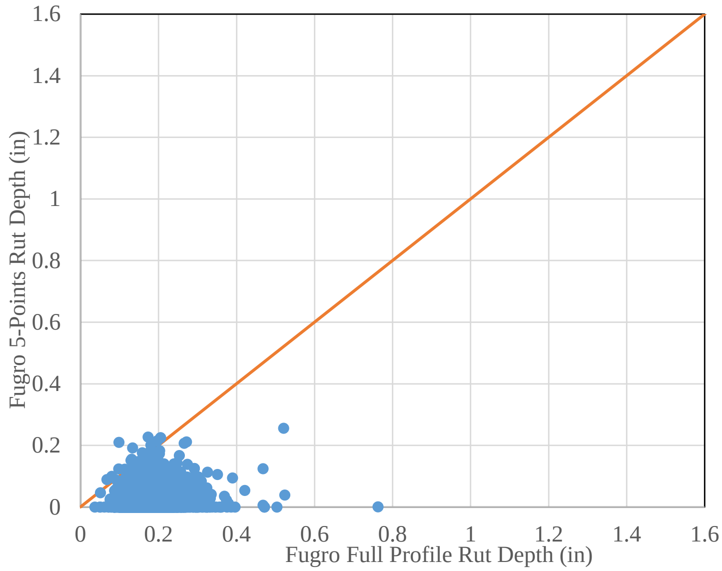

(a) LWP

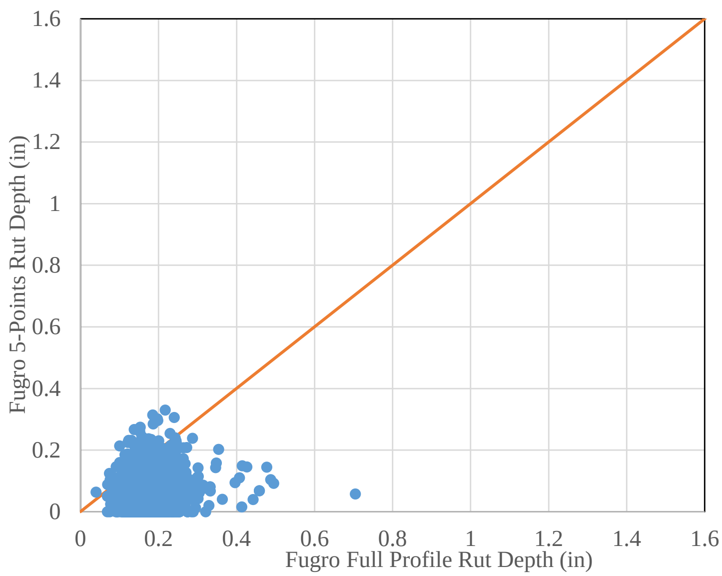

(b) RWP

Figure 59. Scatterplot of Fugro's full profile rut depth vs. Fugro's 5-point rut depth for CS13 in 2021

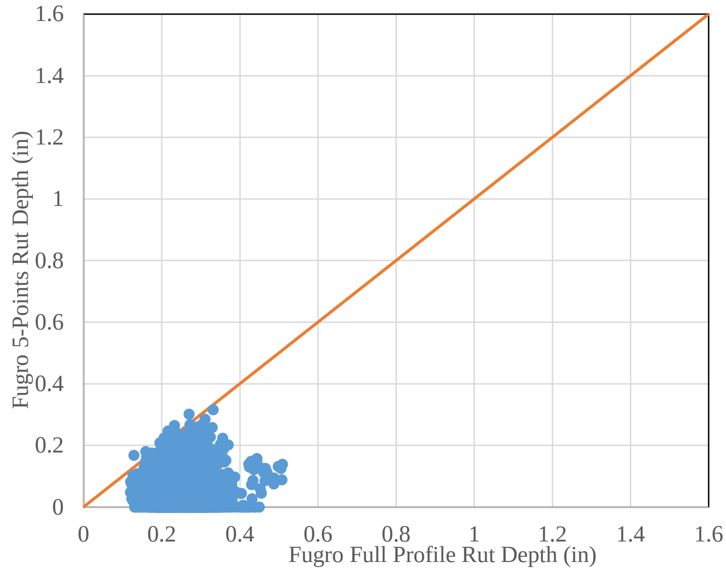

(a) LWP

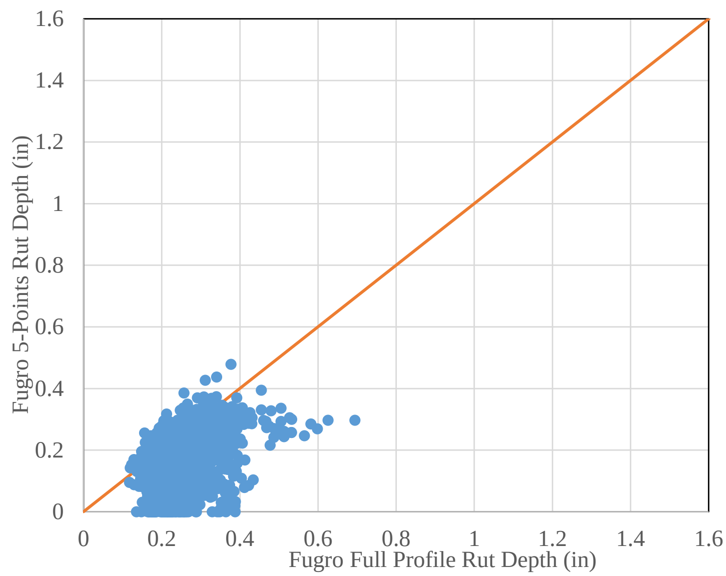

(b) RWP

Figure 60. Measured profiles of rut depth for CS03 in 2020

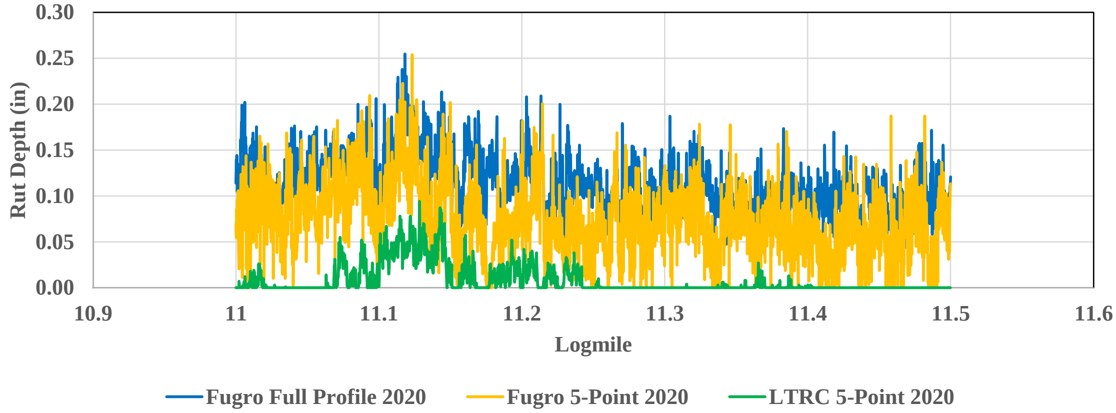

(a) LWP

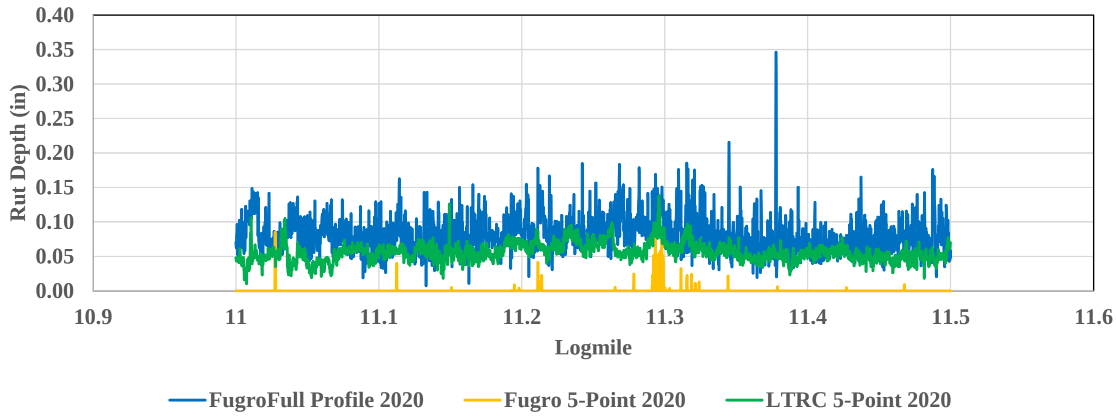

(b) RWP

Figure 61. Measured profiles of rut depth for CS06 in 2020

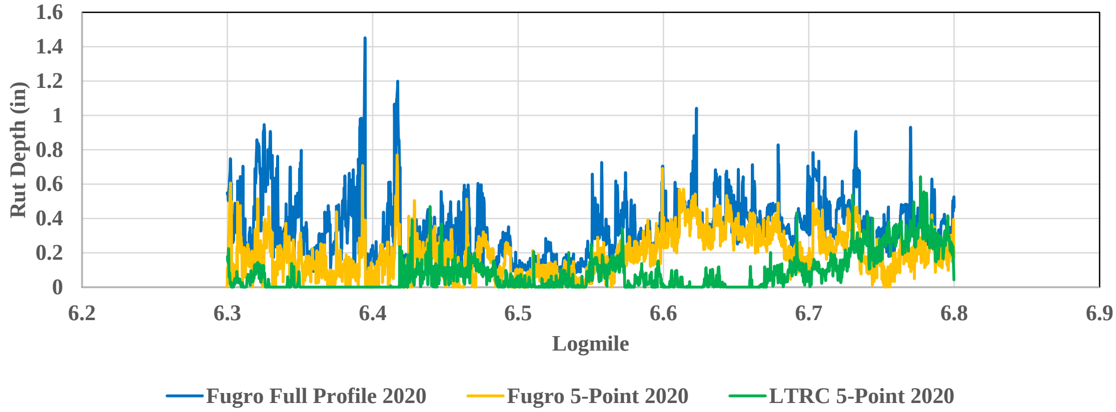

(a) LWP

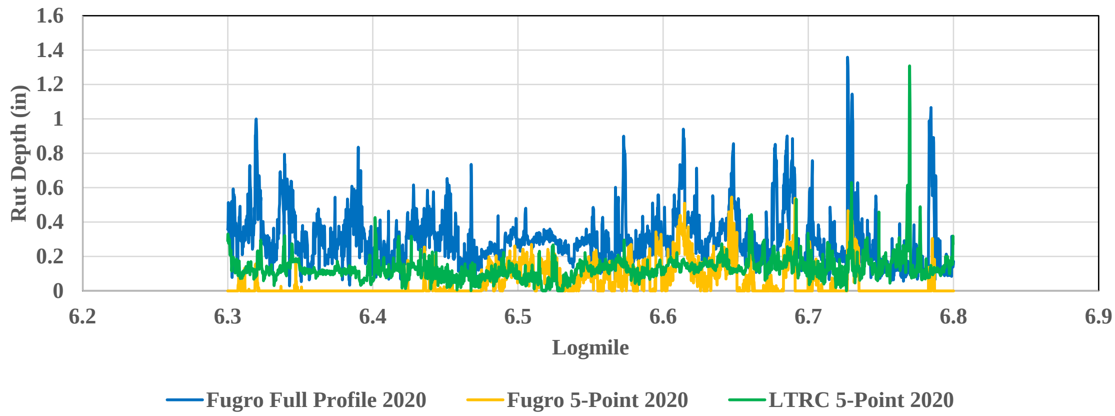

(b) RWP

Figure 62. Measured profiles of rut depth for CS07 in 2020

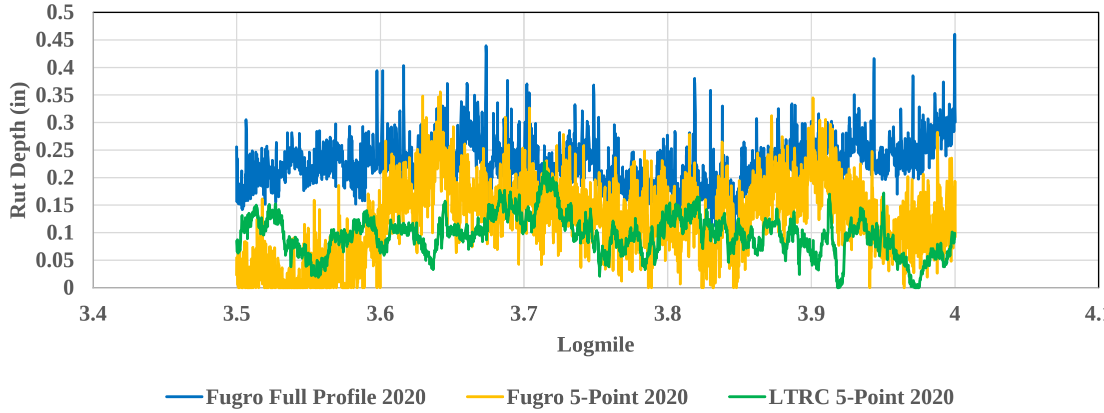

(a) LWP

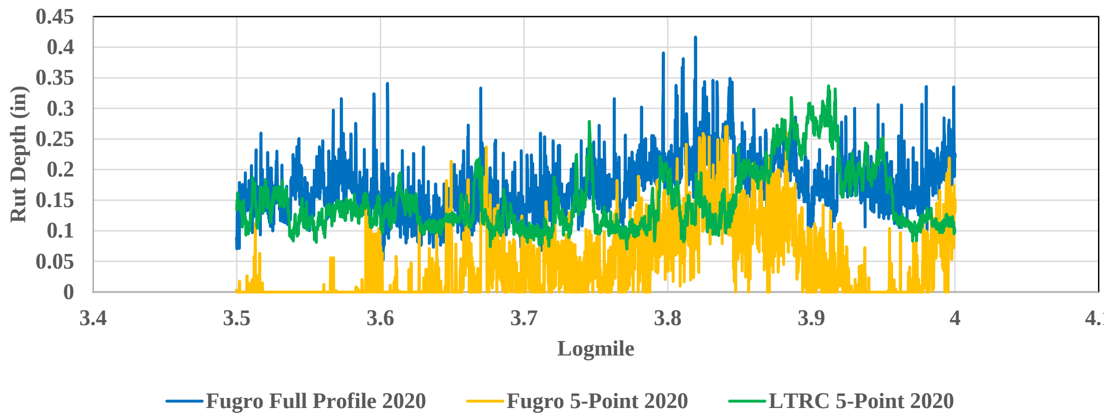

(b) RWP

Figure 63. Measured profiles of rut depth for CS08 in 2020

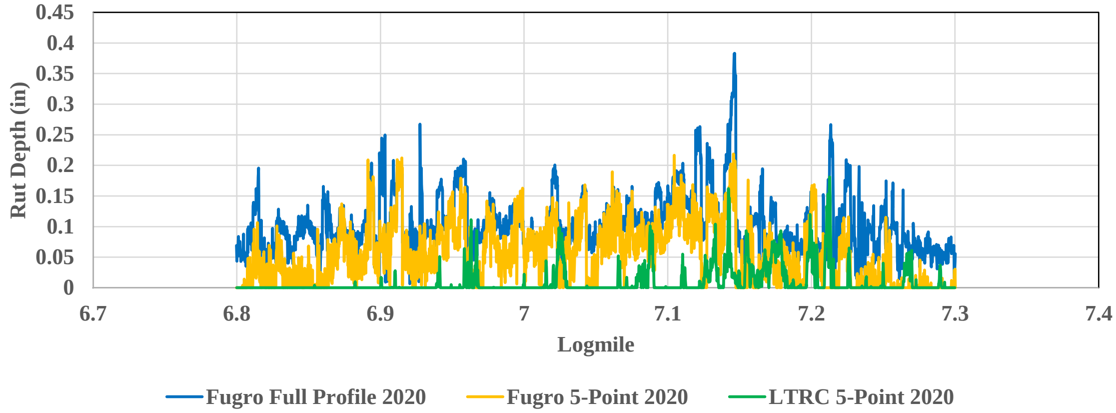

(a) LWP

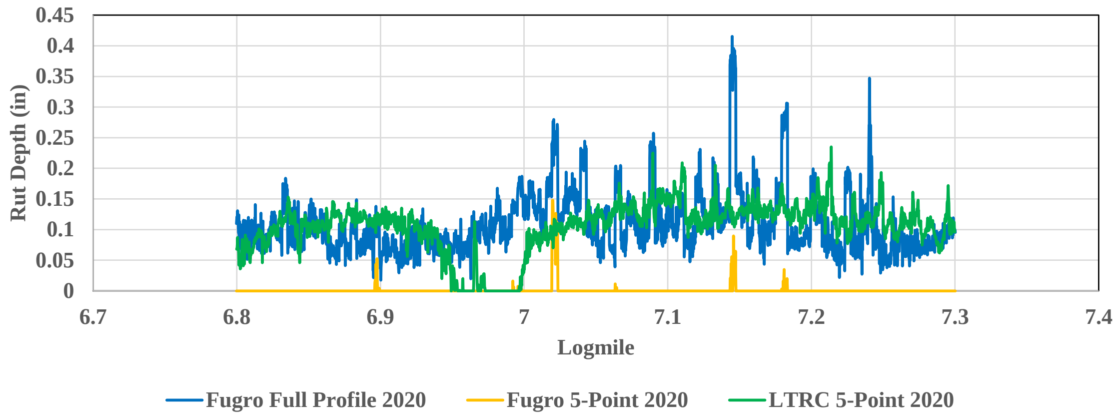

(b) RWP

Figure 64. Measured profiles of rut depth for CS09 in 2020

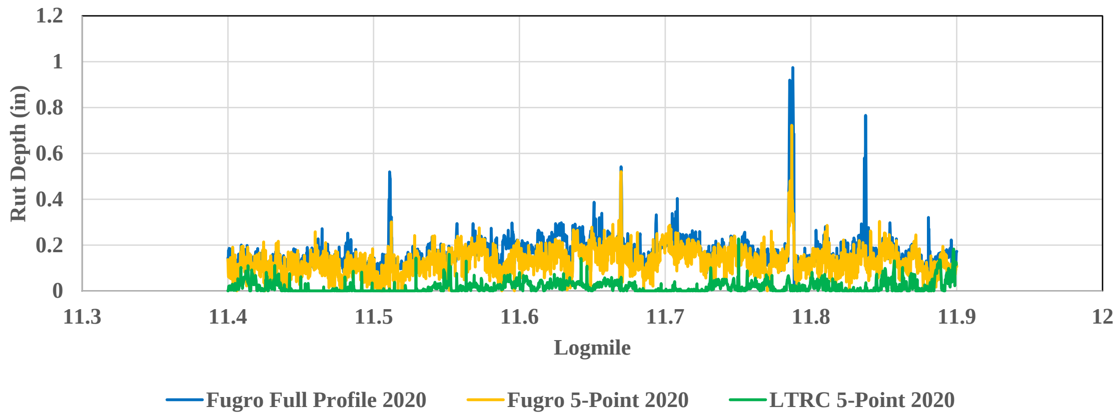

(a) LWP

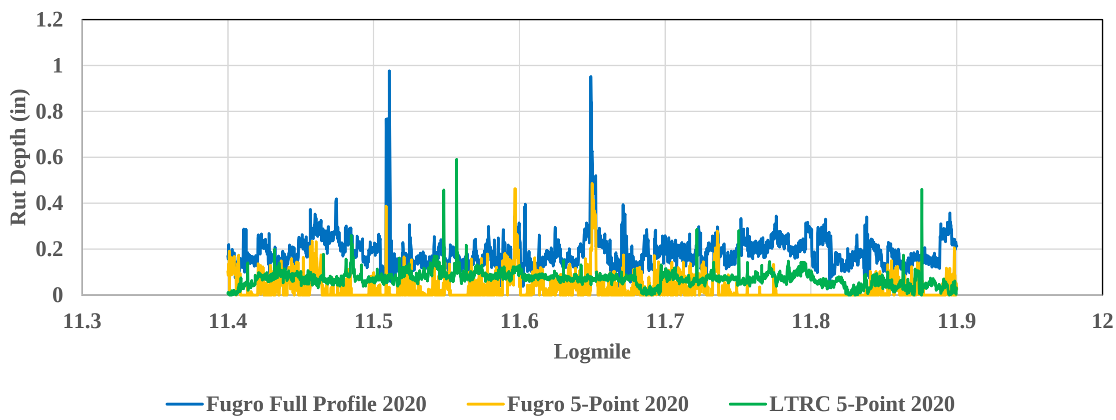

(b) RWP

Figure 65. Measured profiles of rut depth for CS10 in 2020

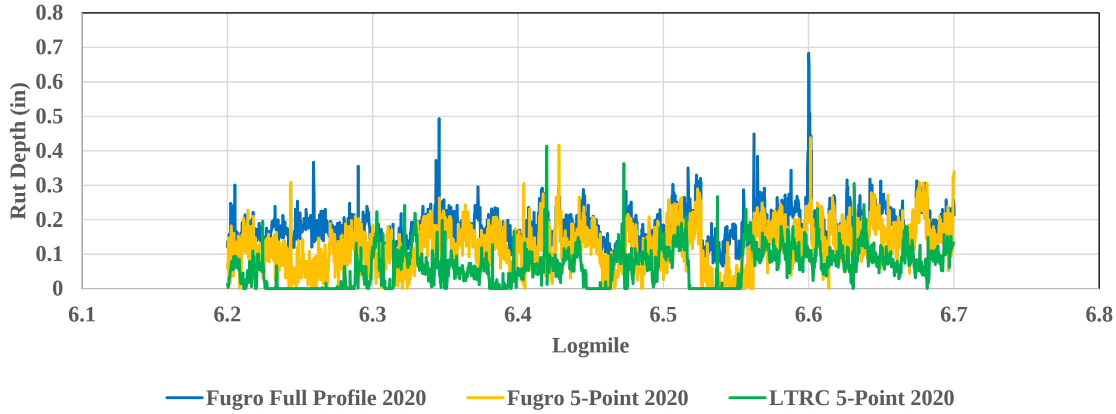

(a) LWP

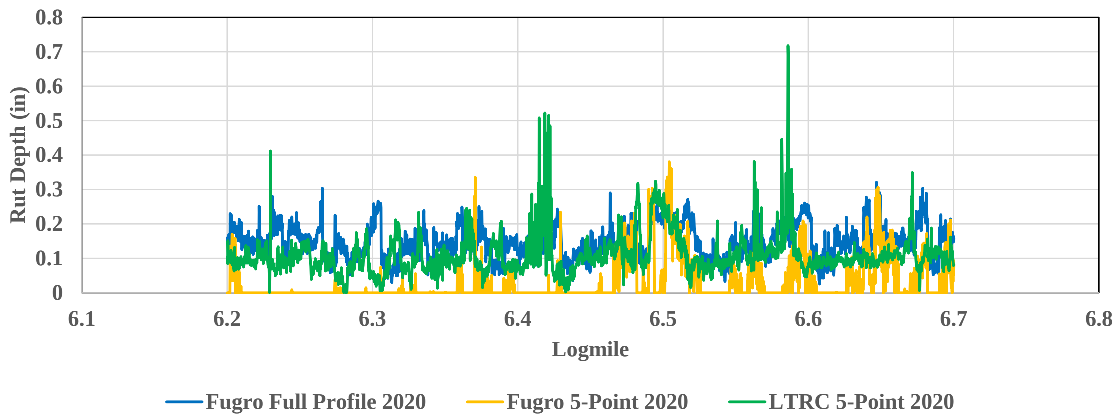

(b) RWP

Figure 66. Measured profiles of rut depth for CS12 in 2020

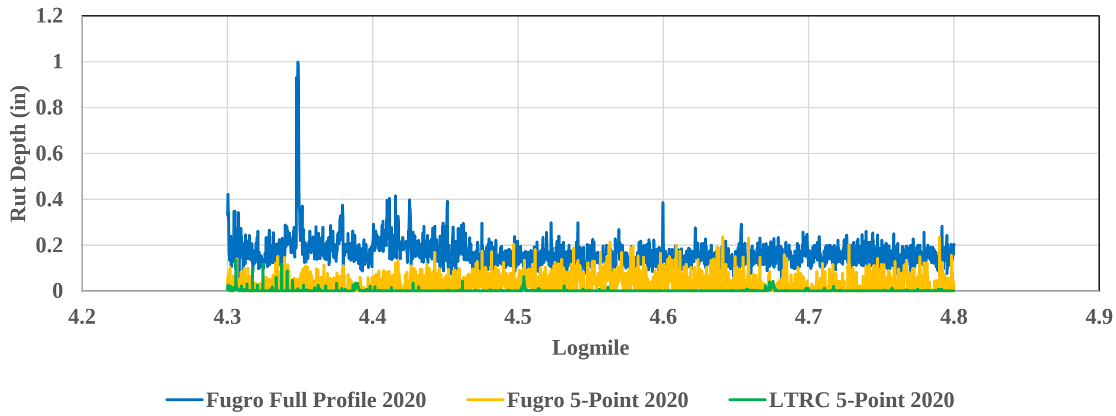

(a) LWP

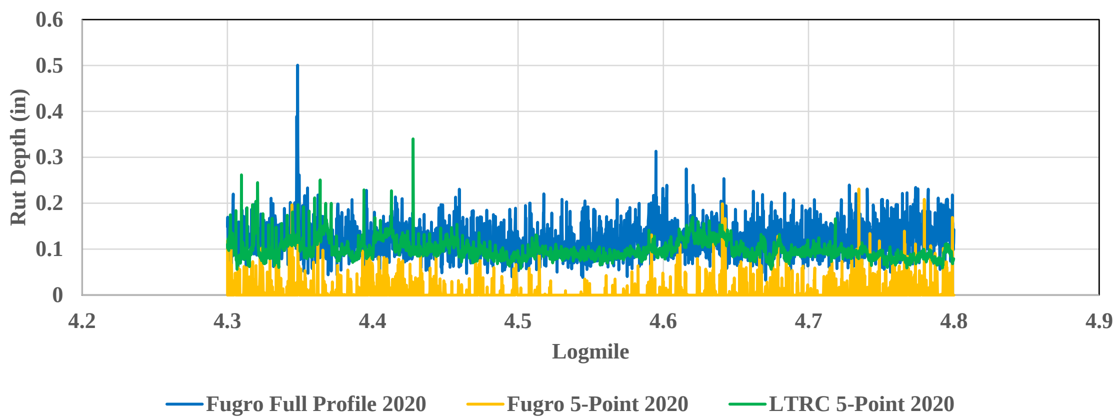

(b) RWP

Figure 67. Measured profiles of rut depth for CS13 in 2020

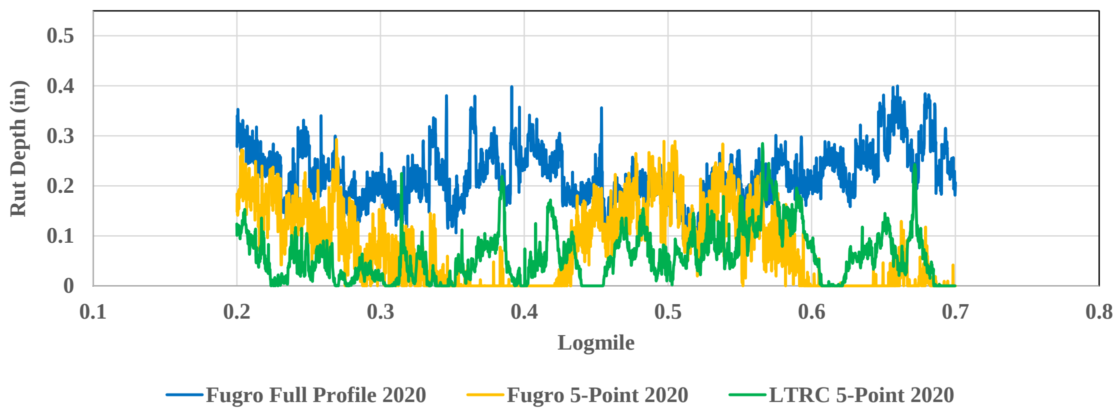

(a) LWP

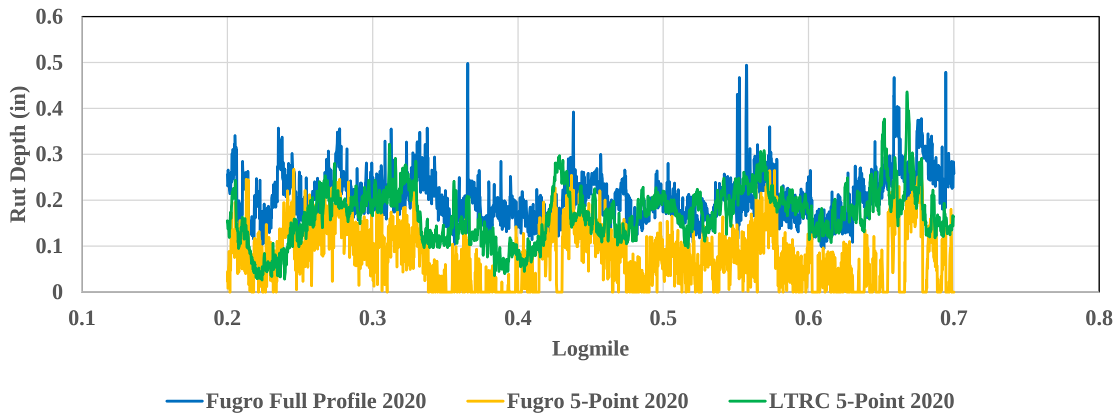

(b) RWP

Figure 68. Measured profiles of rut depth for CS03 in 2021

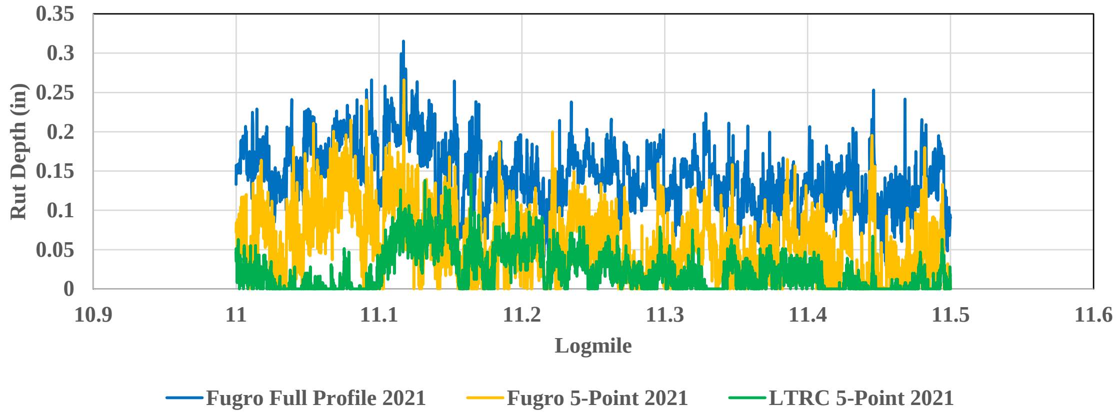

(a) LWP

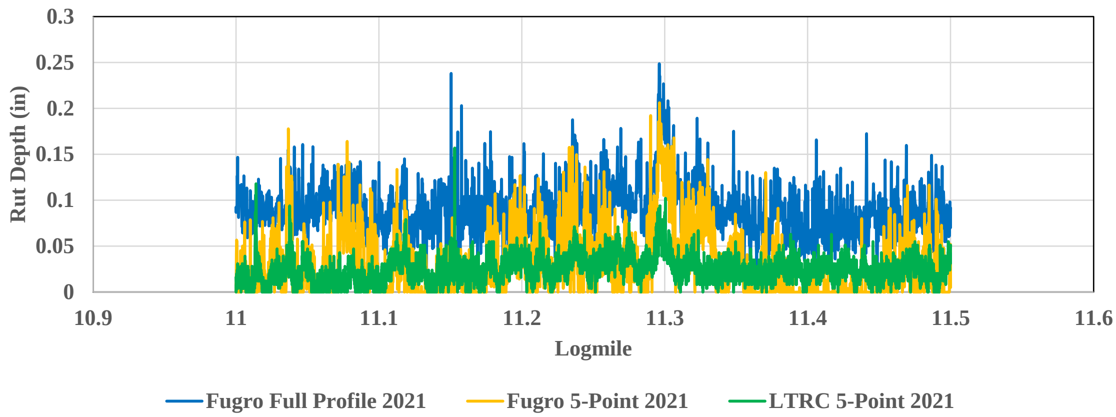

(b) RWP

Figure 69. Measured profiles of rut depth for CS06 in 2021

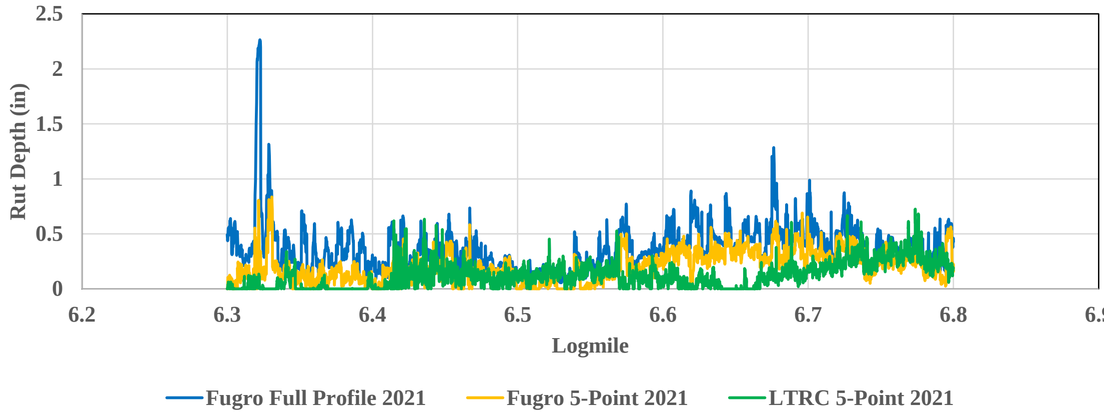

(a) LWP

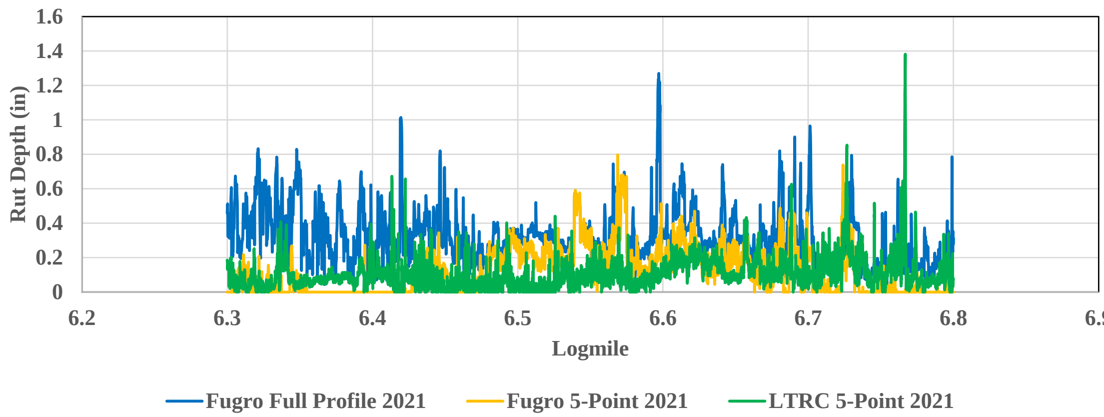

(b) RWP

Figure 70. Measured profiles of rut depth for CS07 in 2021

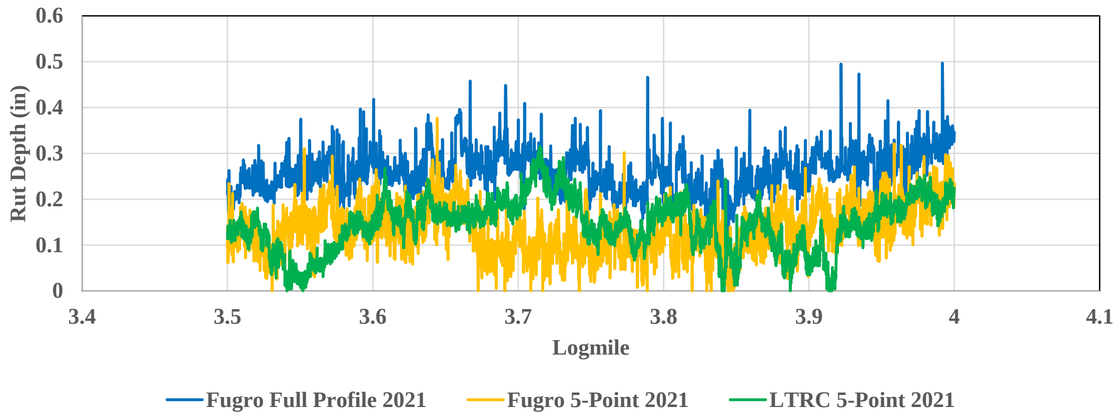

(a) LWP

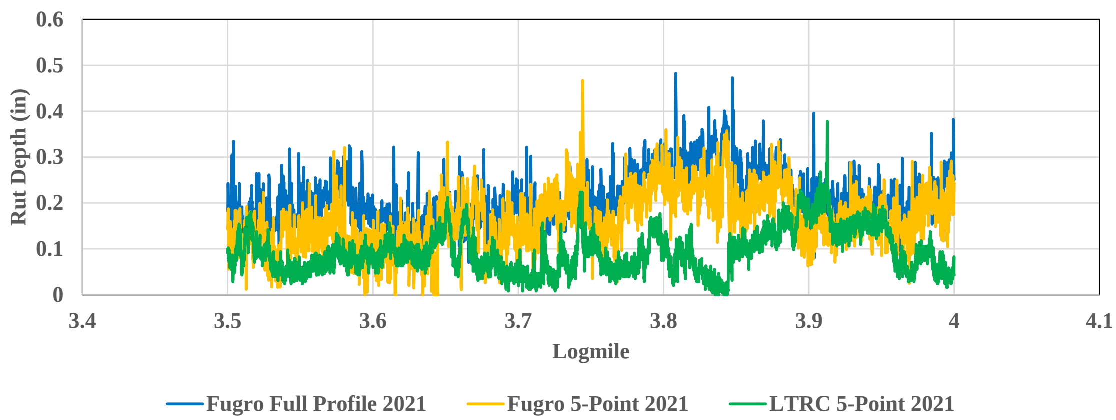

(b) RWP

Figure 71. Measured profiles of rut depth for CS08 in 2021

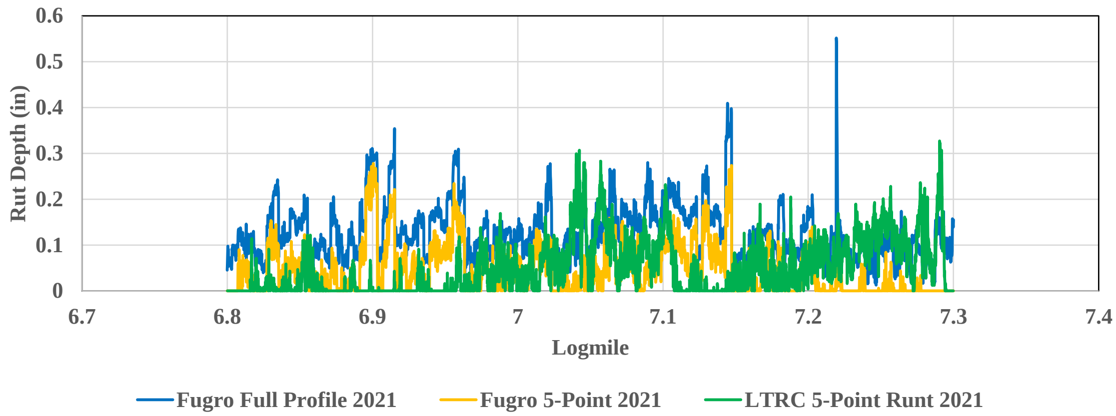

(a) LWP

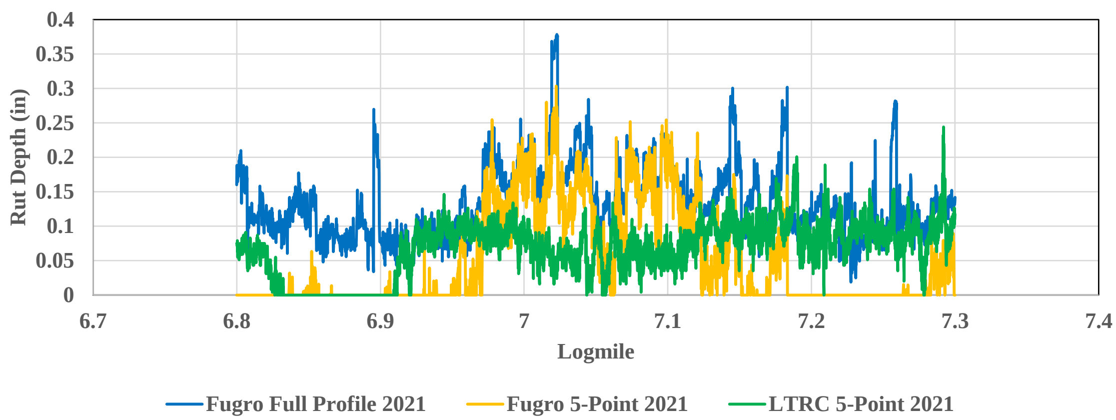

(b) RWP

Figure 72. Measured profiles of rut depth for CS09 in 2021

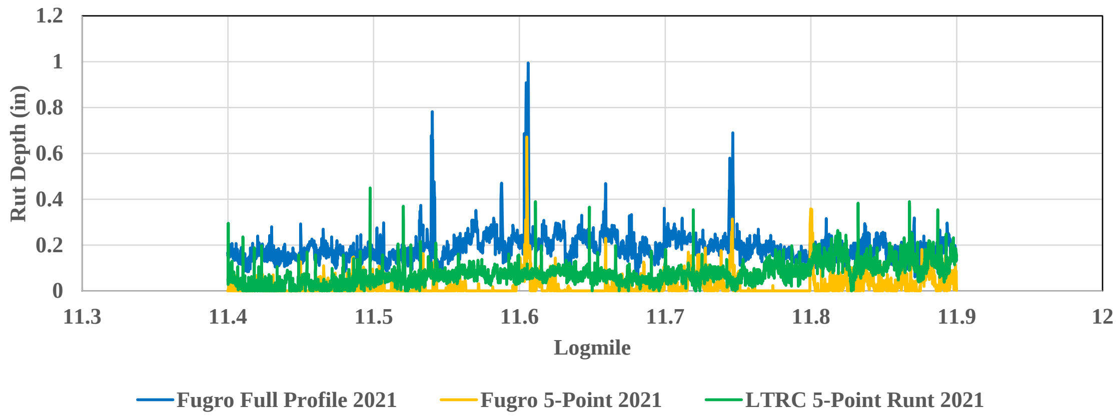

(a) LWP

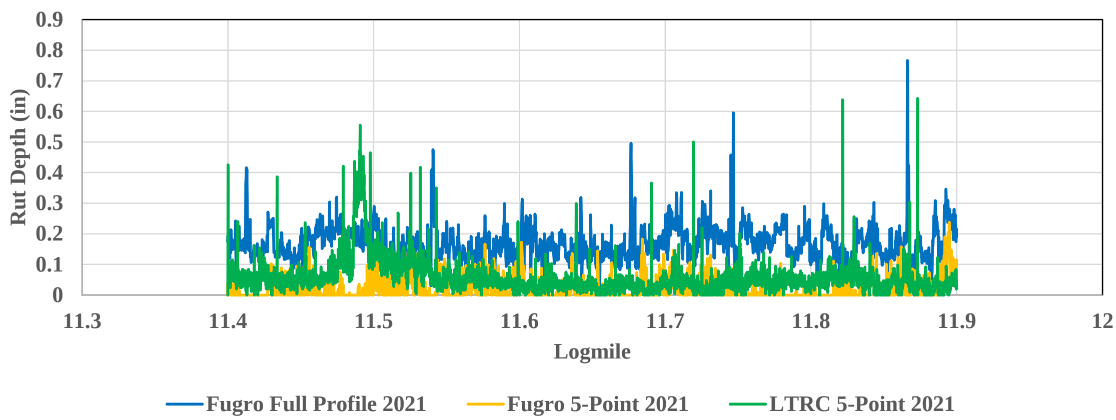

(b) RWP

Figure 73. Measured profiles of rut depth for CS10 in 2020

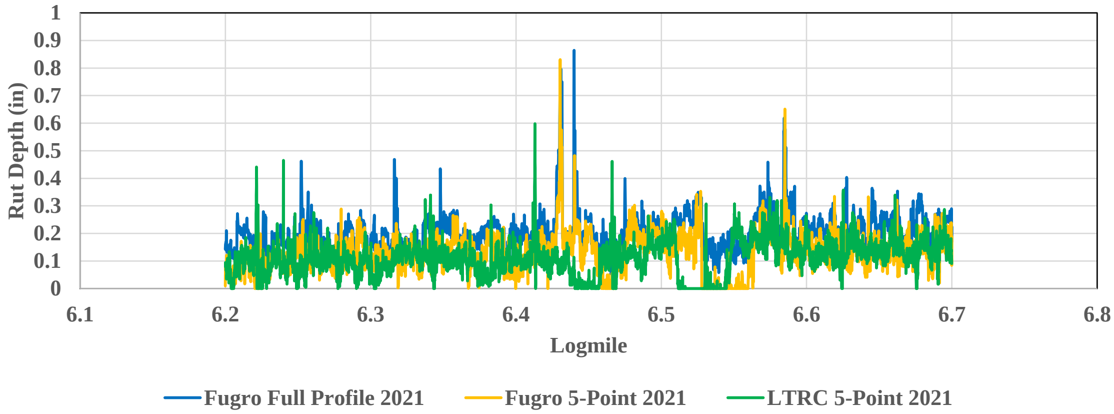

(a) LWP

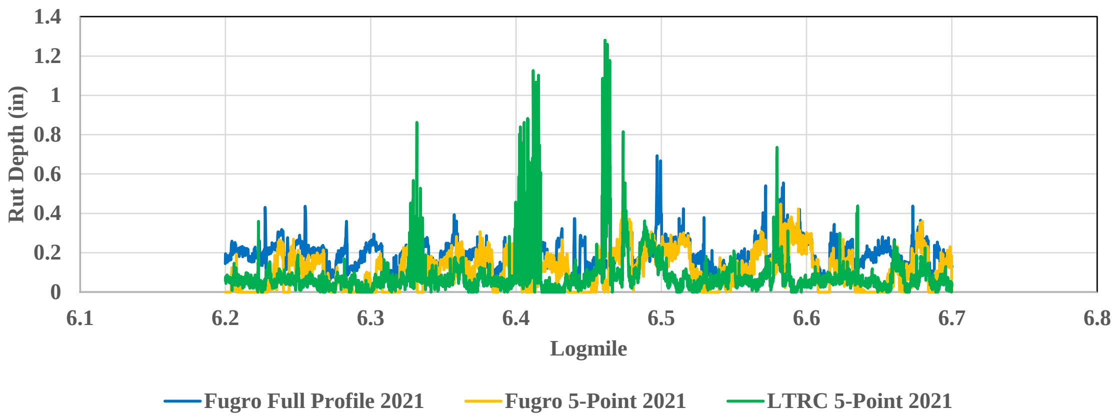

(b) RWP

Figure 74. Measured profiles of rut depth for CS12 in 2021

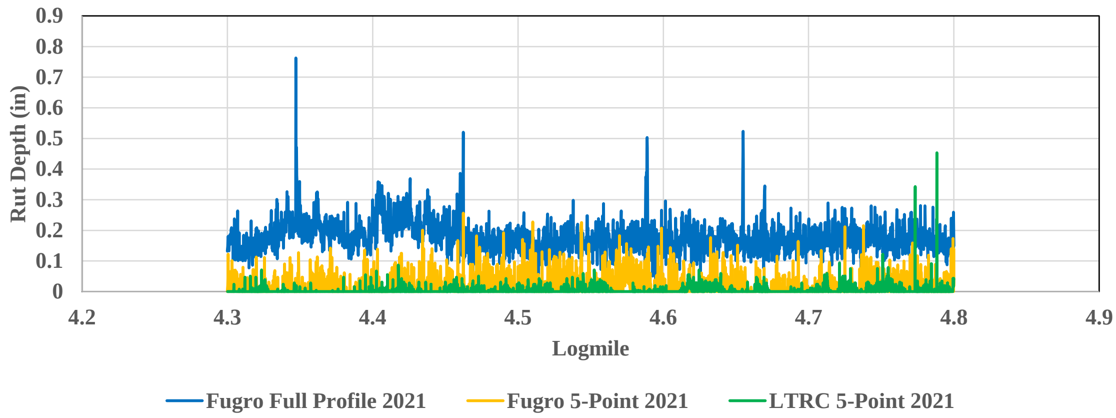

(a) LWP

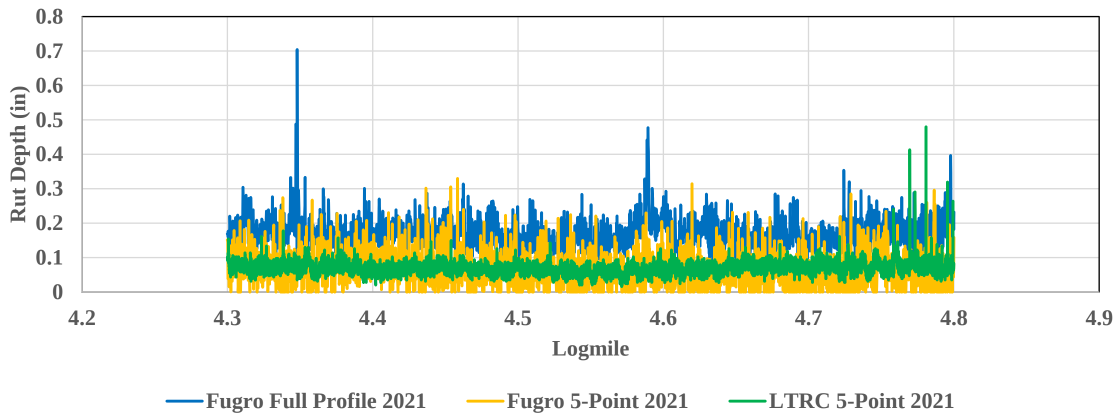

(b) RWP

Figure 75. Measured profiles of rut depth for CS13 in 2021

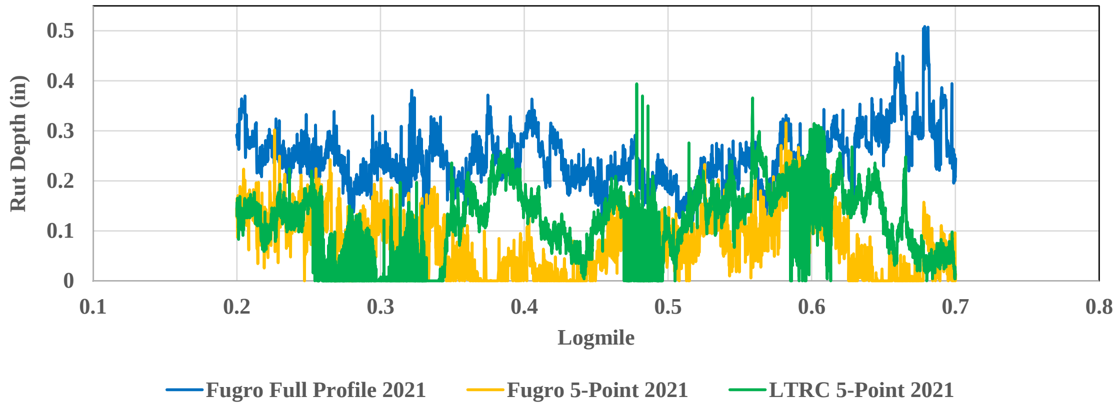

(a) LWP

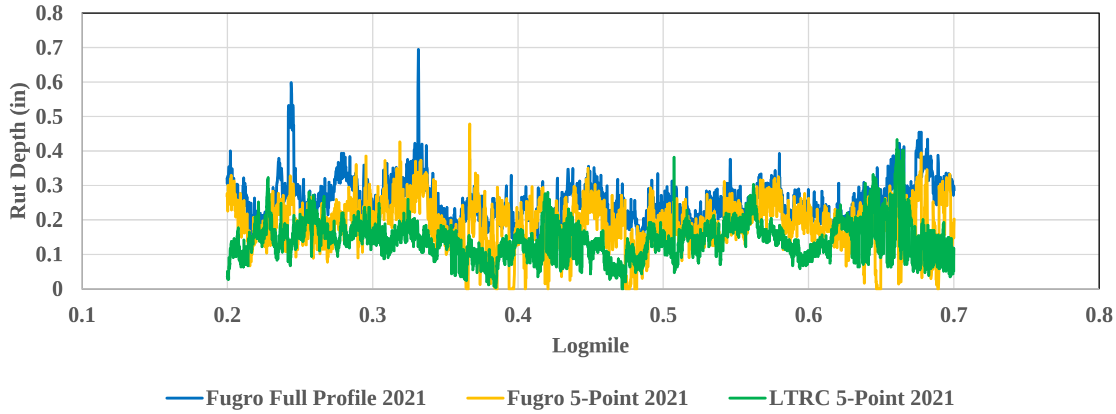

(b) RWP

Figure 76. Histograms of Fugro's full profile rut depths (0.004-mile average) for all control sites in 2020

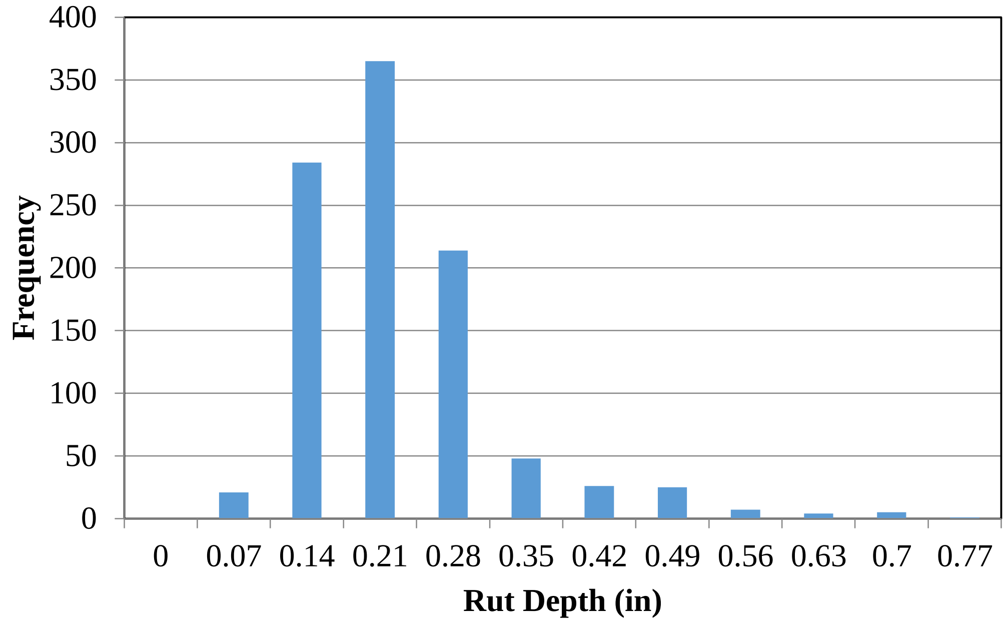

(a) LWP

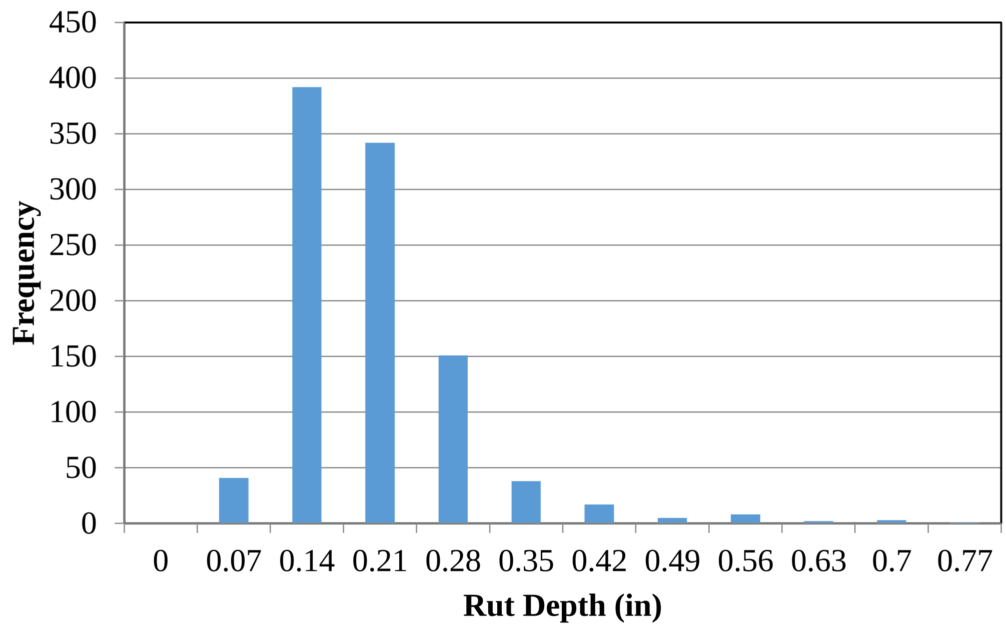

(b) RWP

Figure 77. Histograms of Fugro's 5-point rut depths (0.004-mile average) for all control Sites in 2020

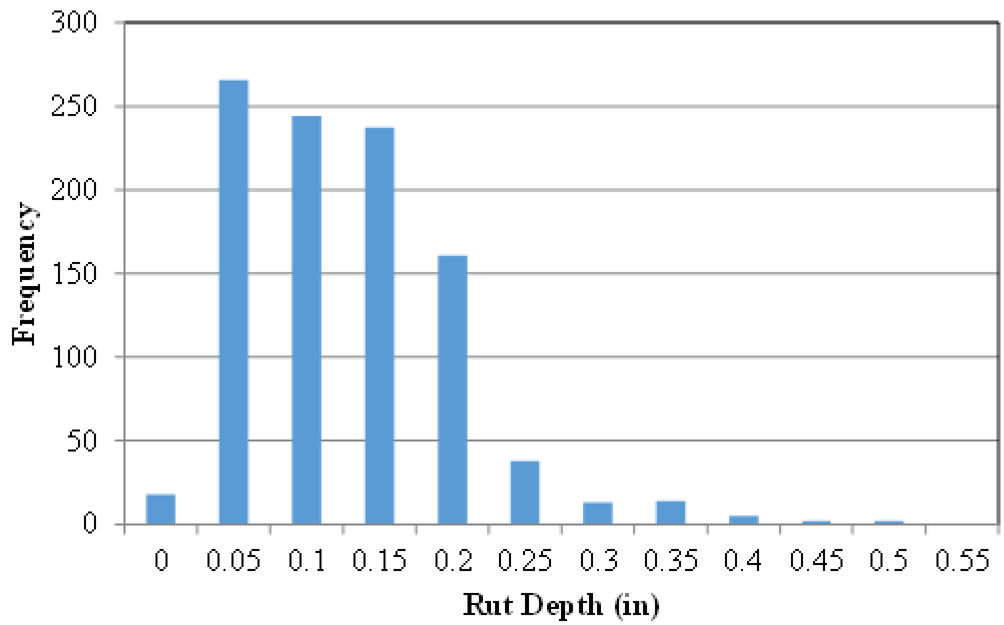

(a) LWP

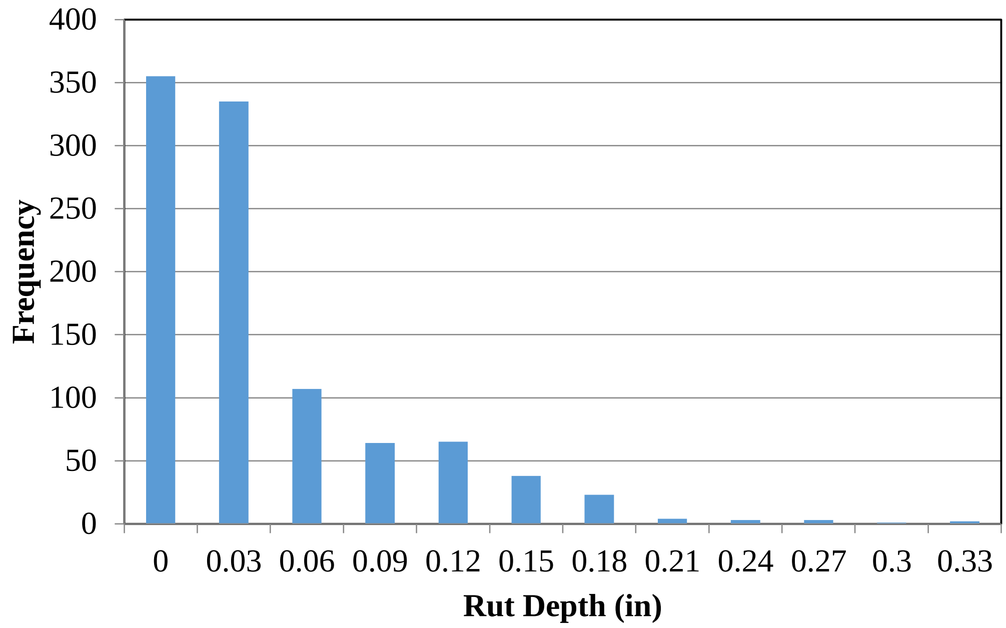

(b) RWP

Figure 78. Histograms of LTRC's 5-point rut depths (0.004-mile average) for all control sites in 2020

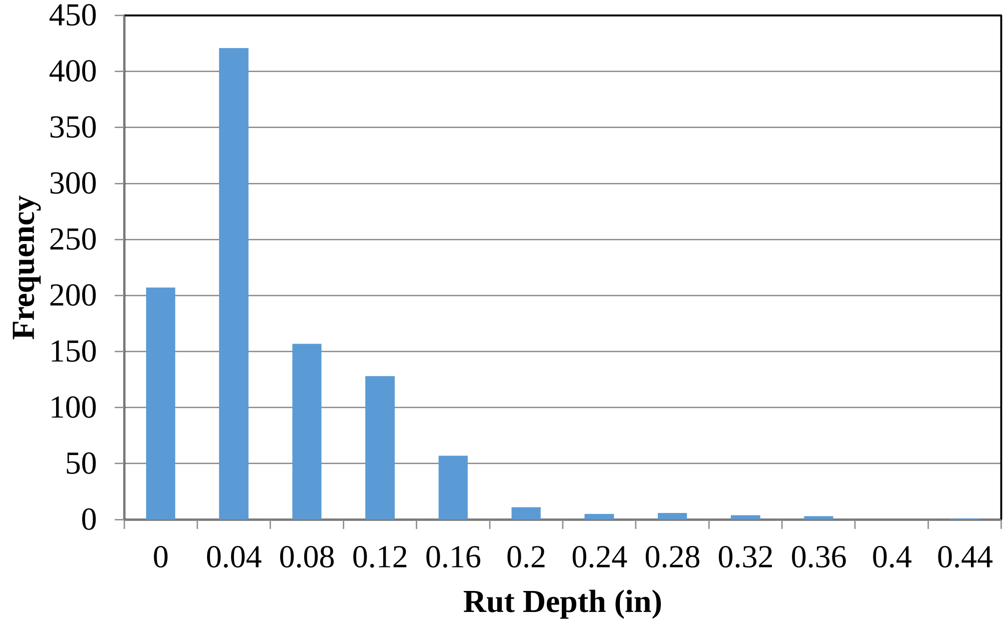

(a) LWP

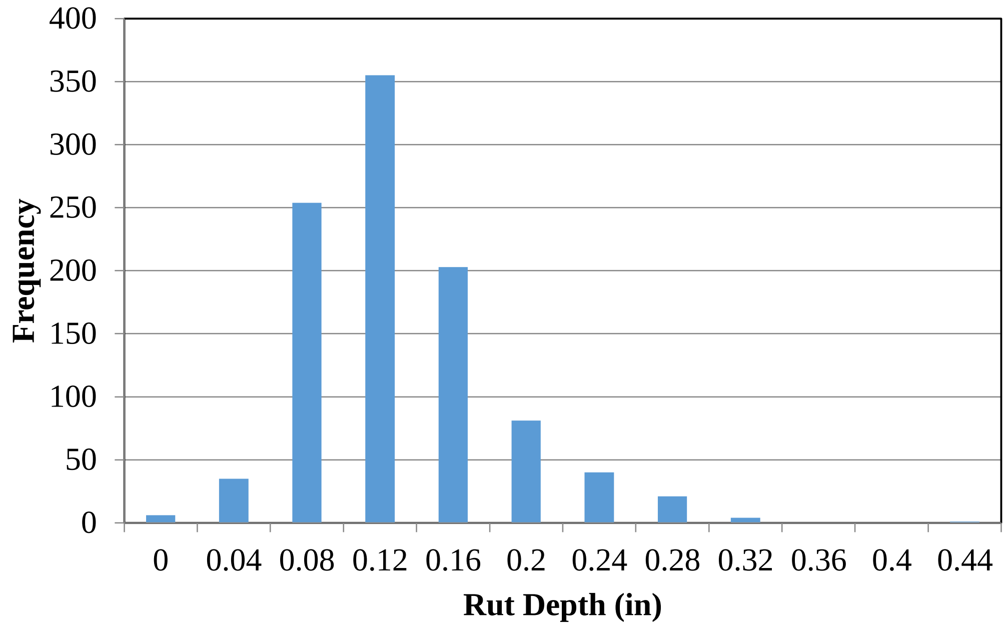

(b) RWP

Figure 79. Histograms of Fugro's full profile rut depths (0.004-mile average) for all control sites in 2021

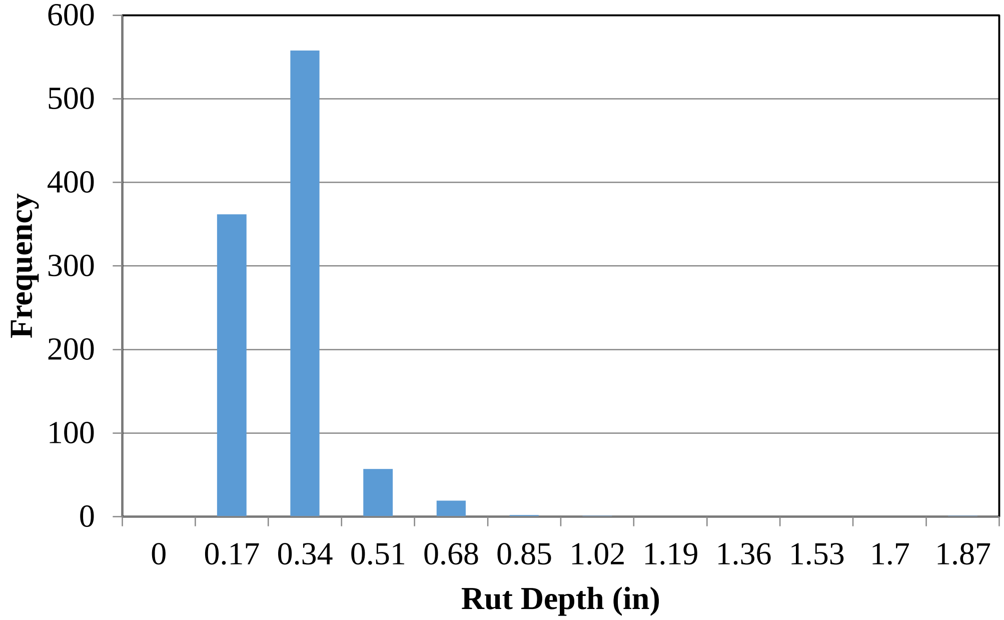

(a) LWP

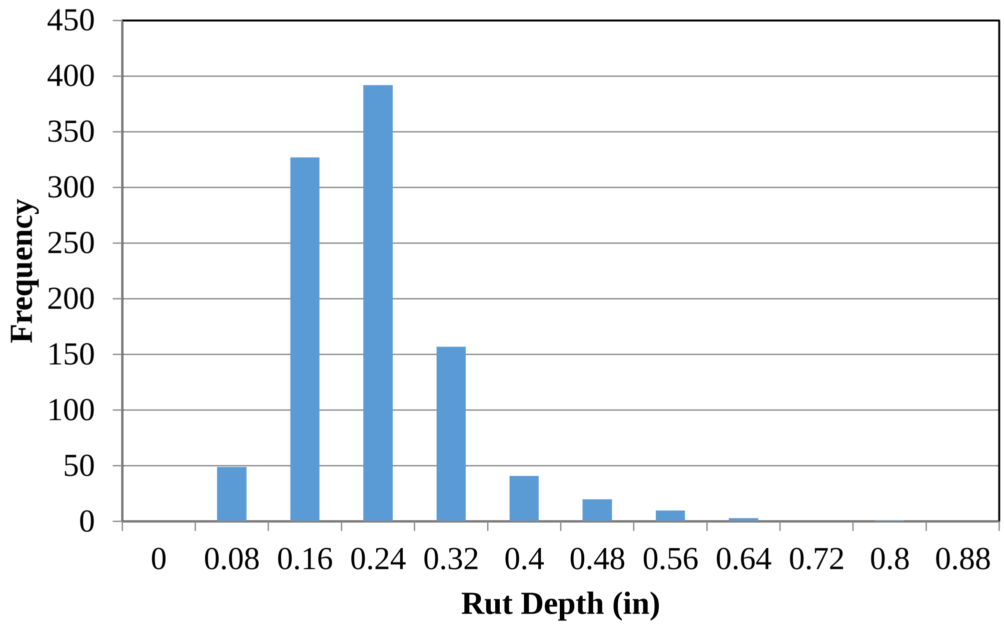

(b) RWP

Figure 80. Histograms of Fugro's 5-point rut depths (0.004-mile average) for all control sites in 2021

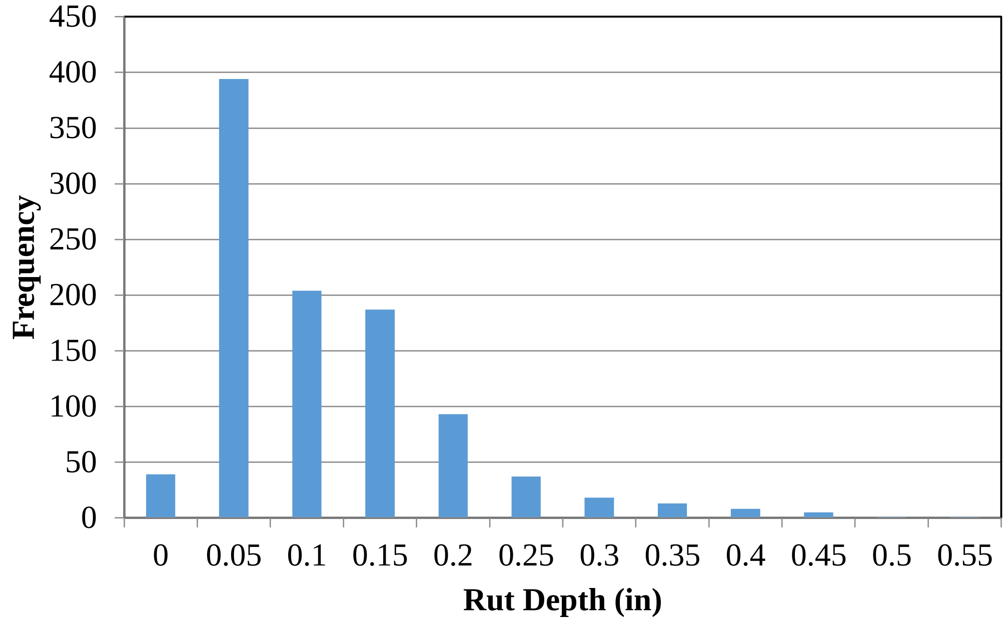

(a) LWP

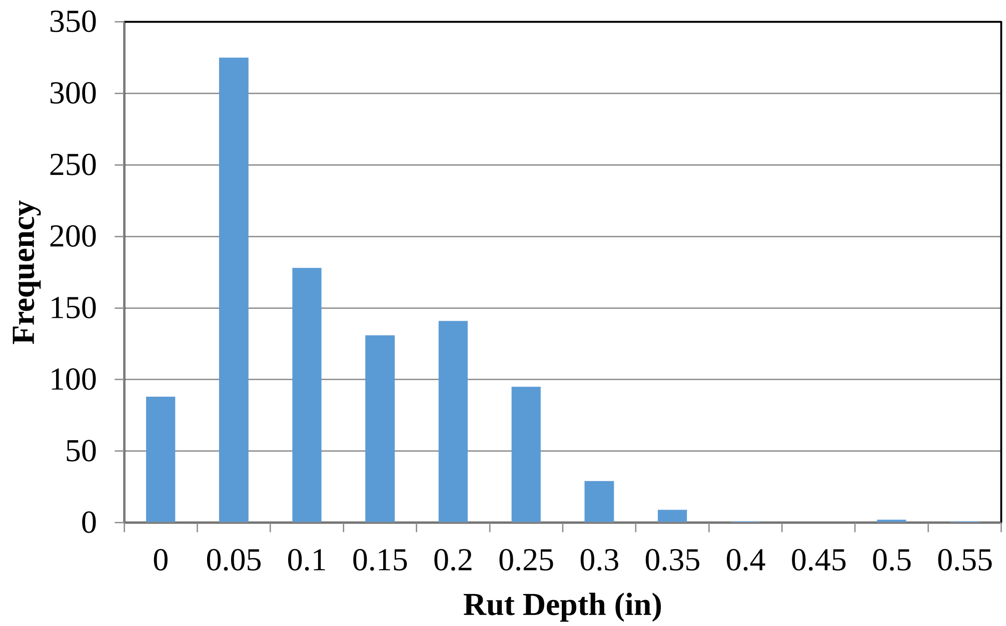

(b) RWP

Figure 81. Histograms of LTRC's 5-point rut depths (0.004-mile average) for all control sites in 2021

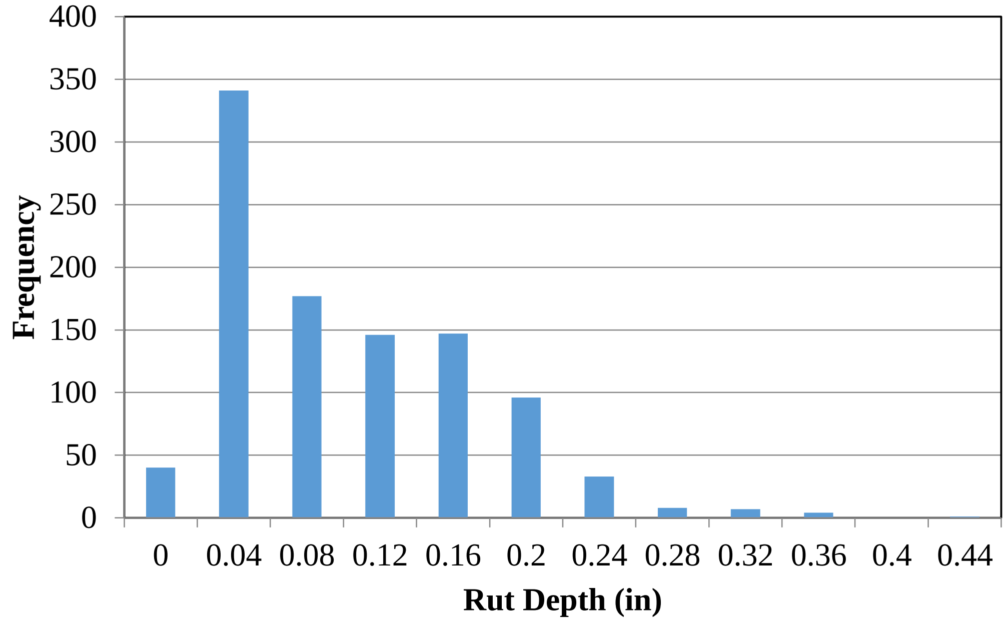

(a) LWP

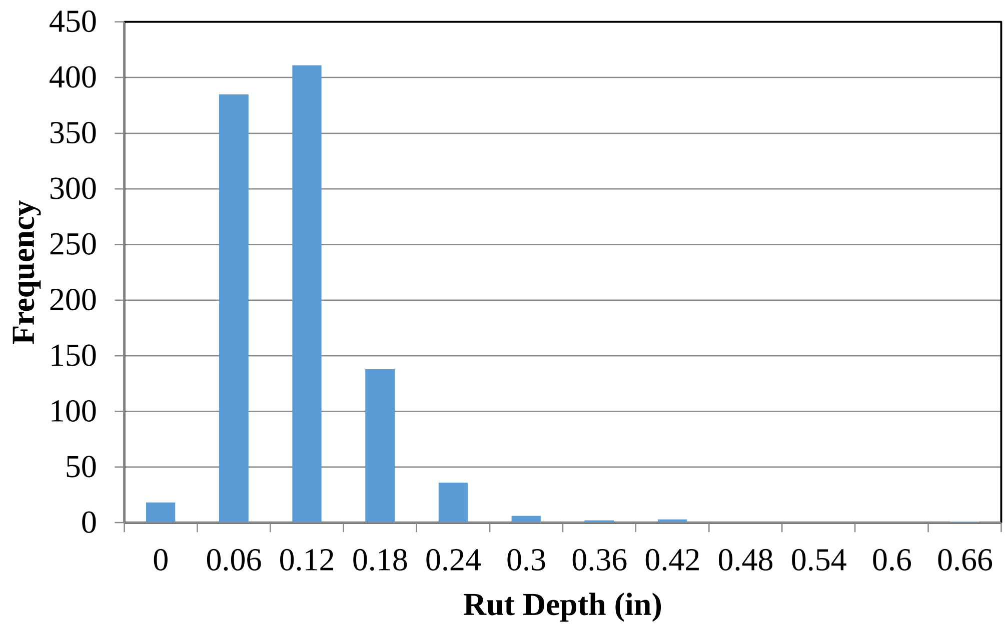

(b) RWP

Figure 82. Histograms of Fugro's full profile rut depths (0.1-mile average) for all control sites in 2020

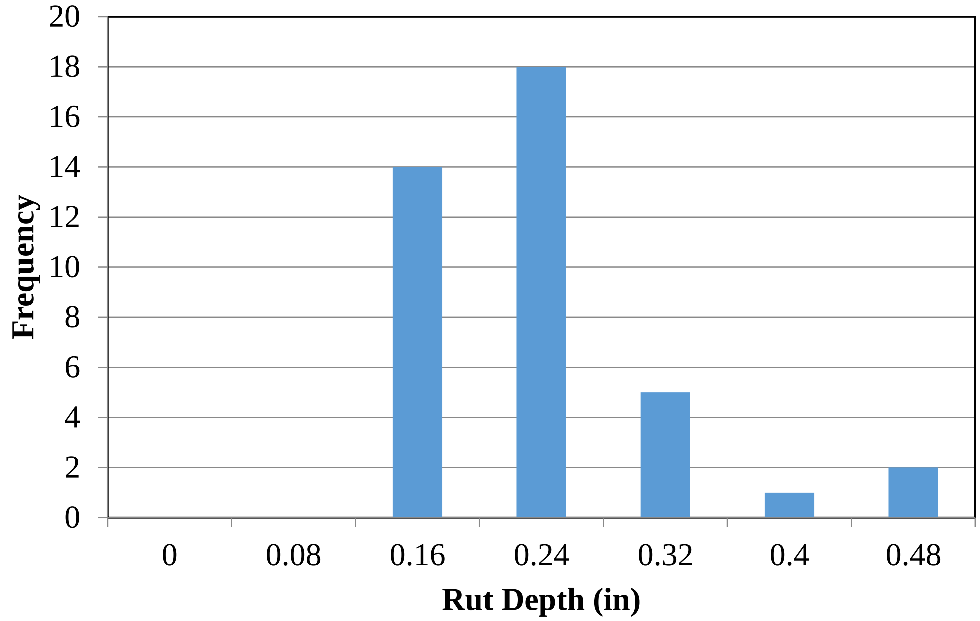

(a) LWP

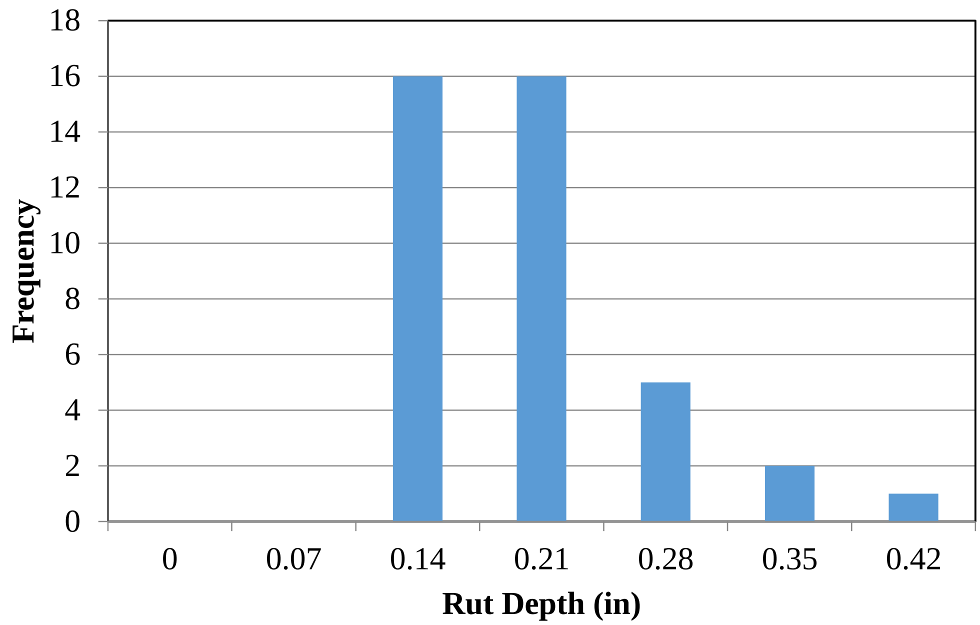

(b) RWP

Figure 83. Histograms of Fugro's 5-point rut depths (0.1-mile average) for all control sites in 2020

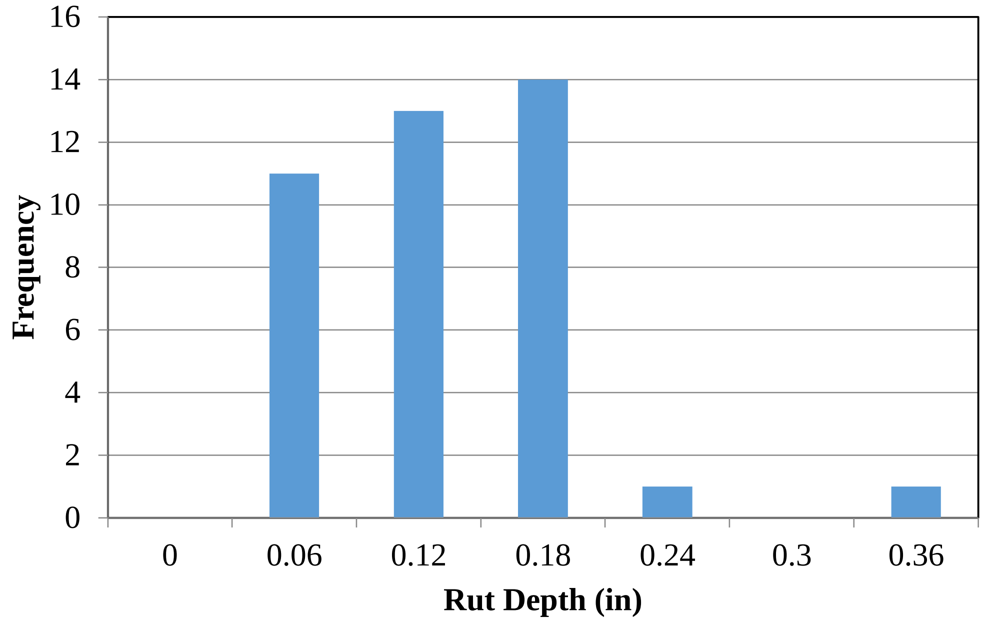

(a) LWP

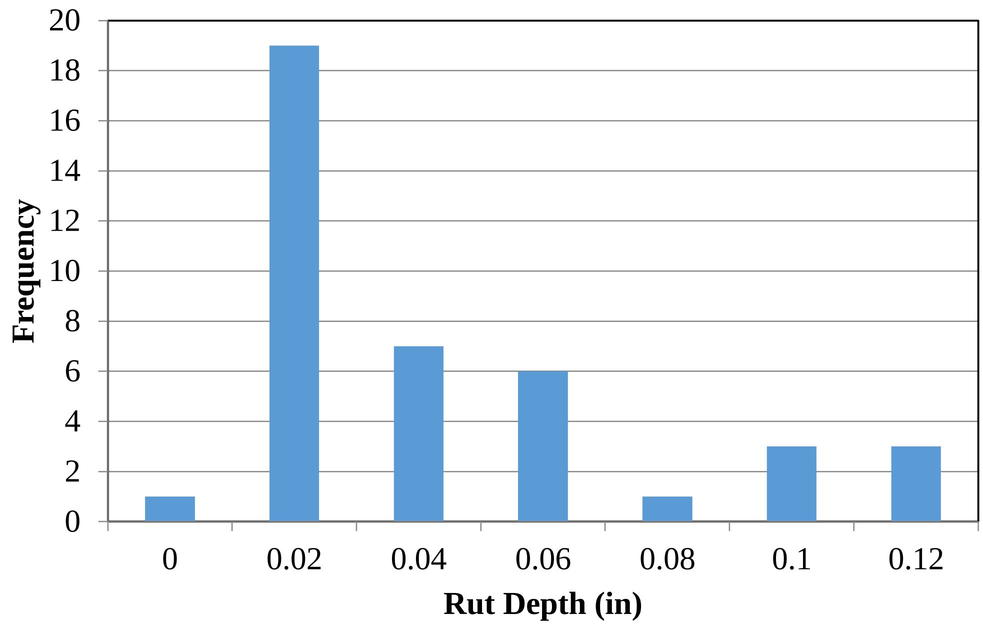

(b) RWP

Figure 84. Histograms of LTRC's 5-point rut depths (0.1-mile average) for all control sites in 2020

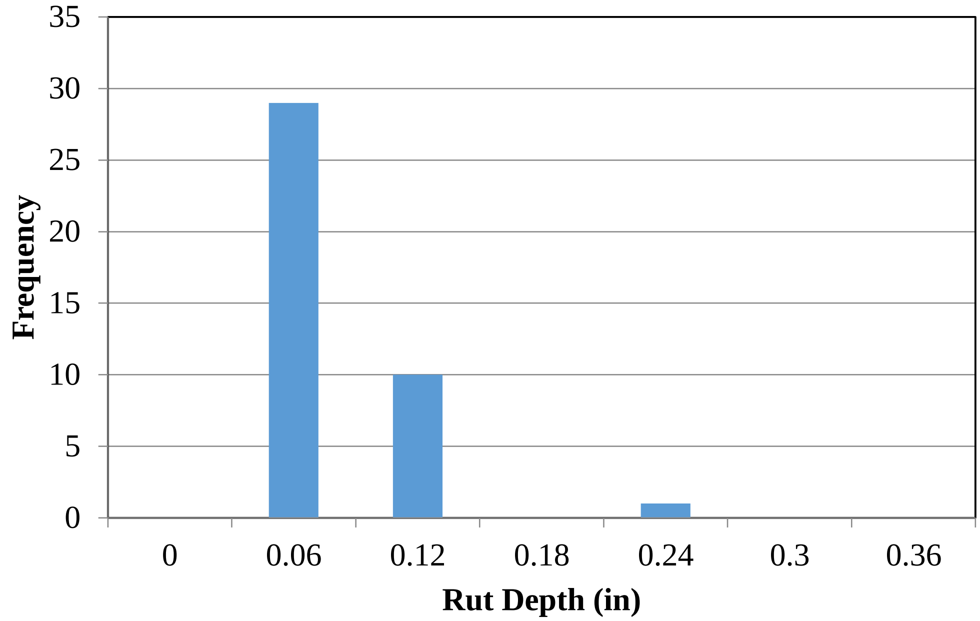

(a) LWP

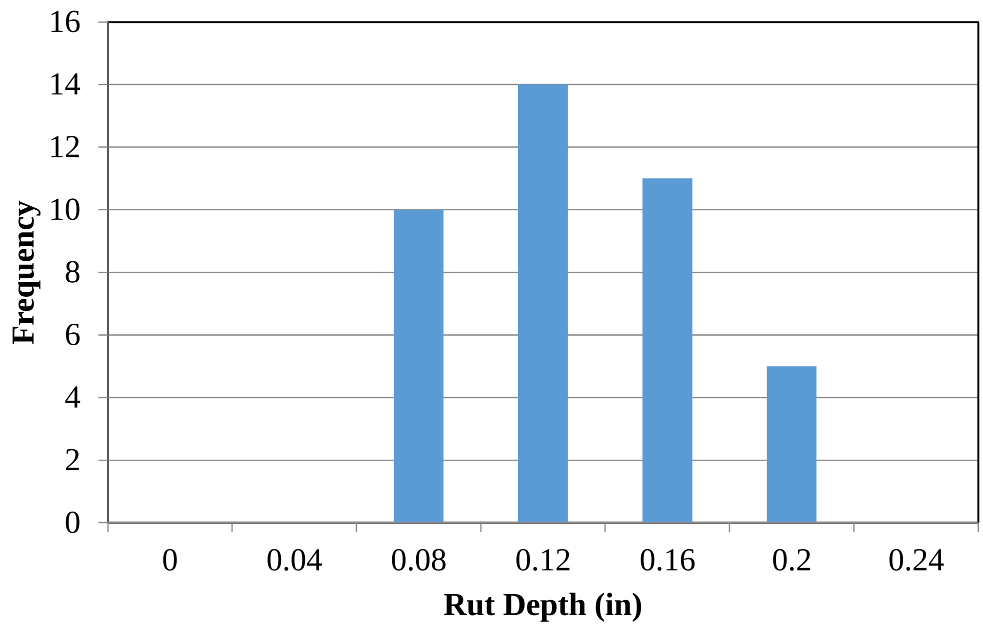

(b) RWP

Figure 85. Histograms of Fugro's full profile rut depths (0.1-mile average) for all control sites in 2021

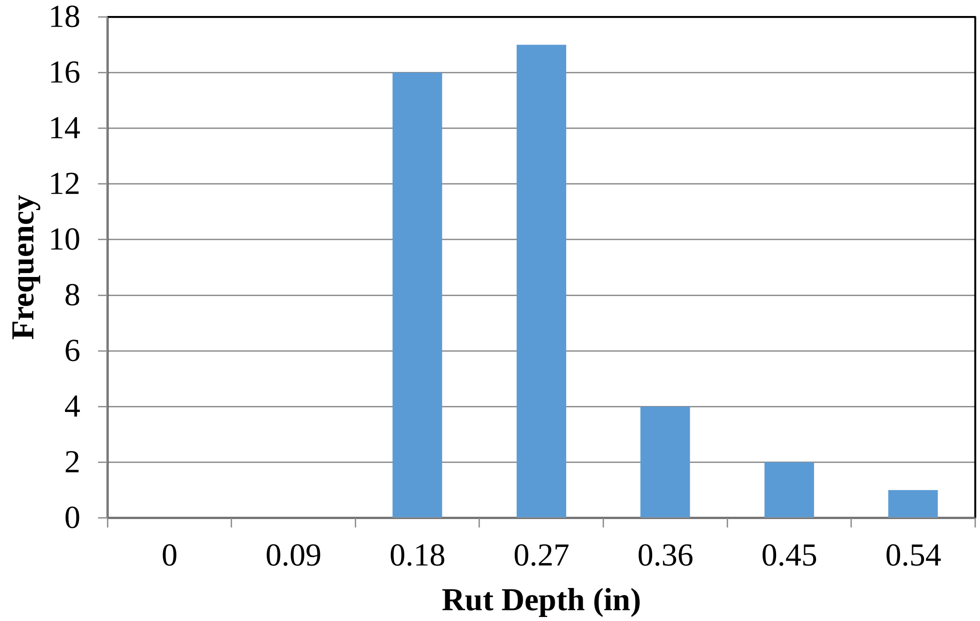

(a) LWP

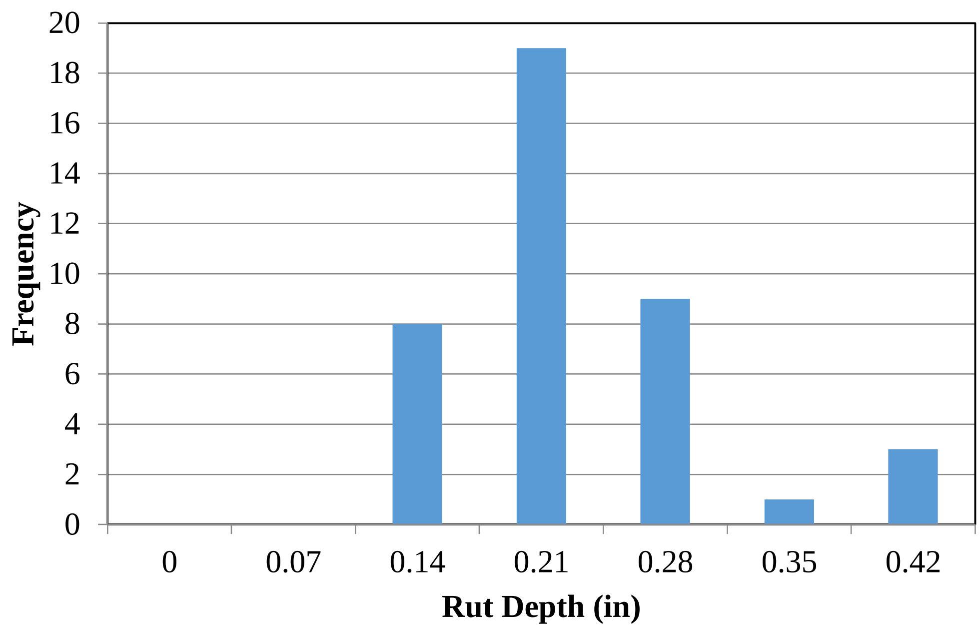

(b) RWP

Figure 86. Histograms of Fugro's 5-point rut depths (0.1-mile average) for all control sites in 2021

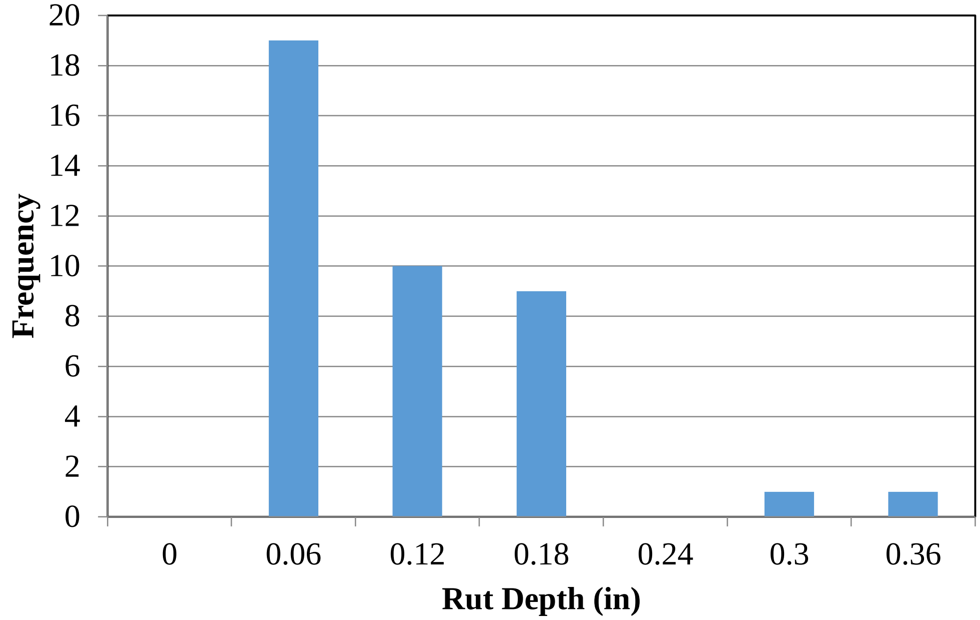

(a) LWP

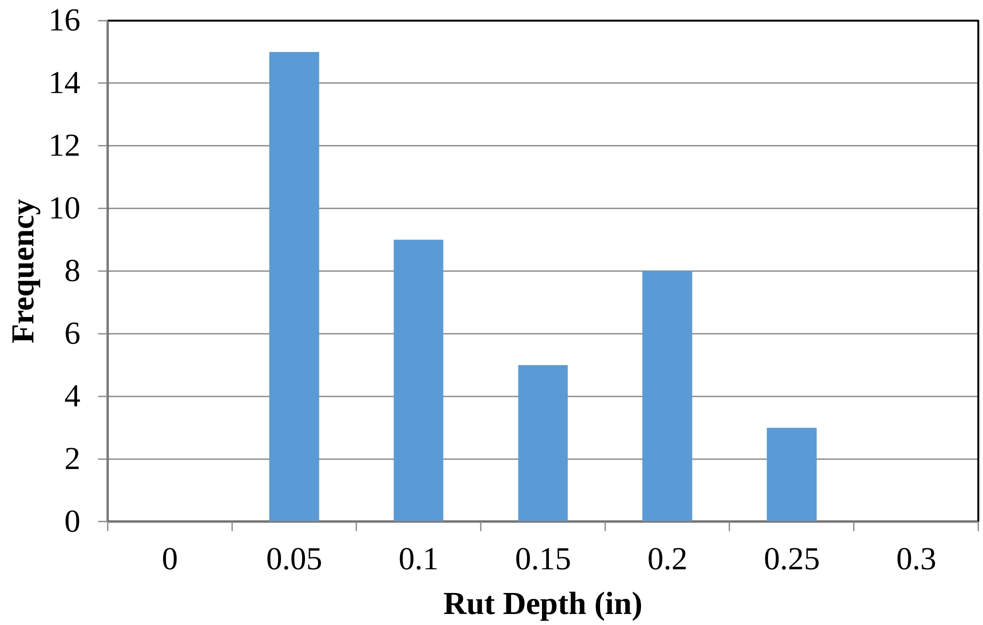

(b) RWP

Figure 87. Histograms of LTRC's 5-point rut depths (0.1-mile average) for all control sites in 2021

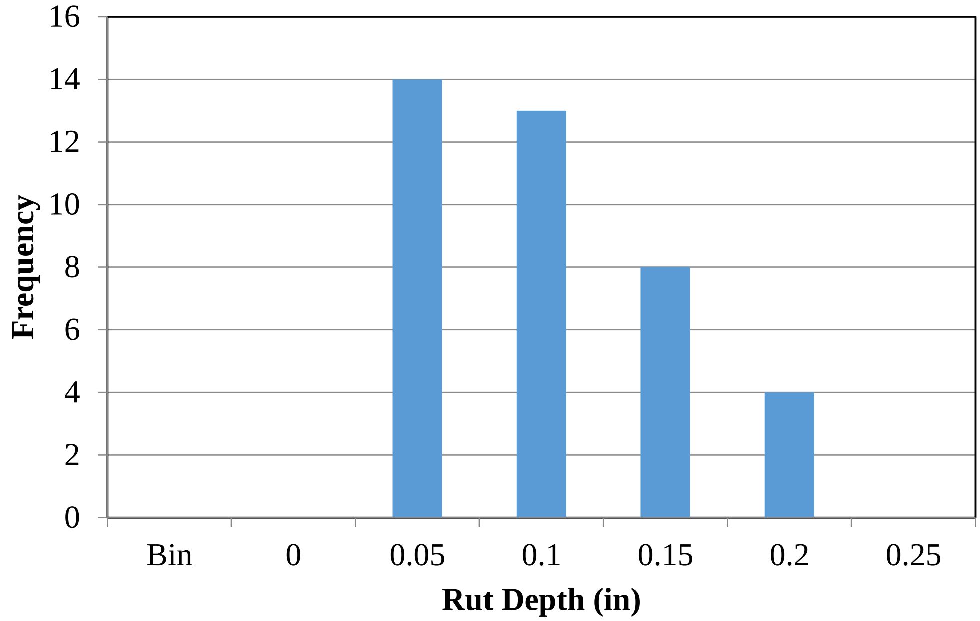

(a) LWP

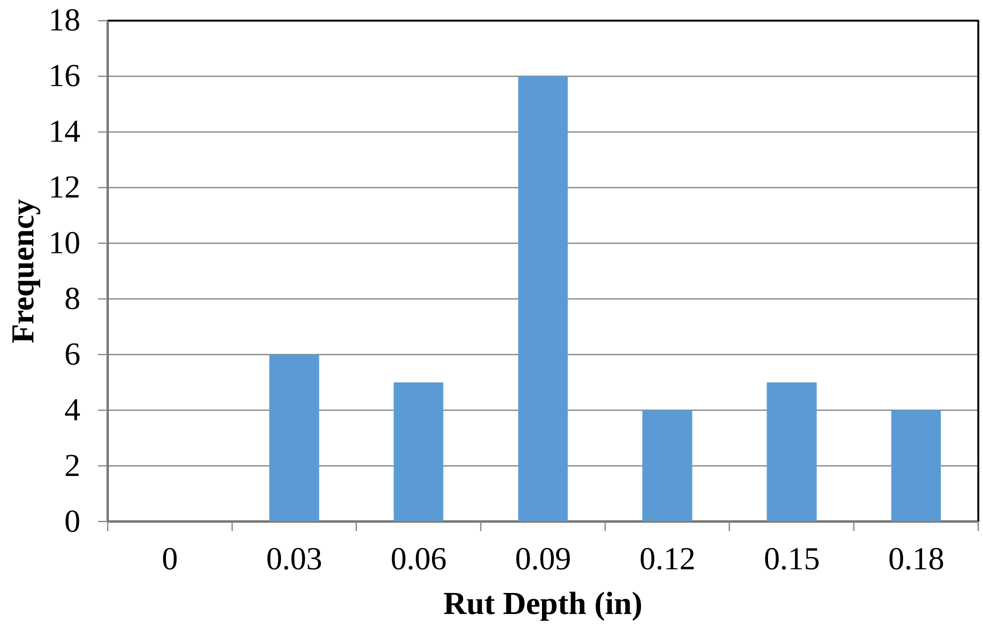

(b) RWP

Figure 88. Histograms of Fugro's full profile rut depths (0.004-mile average) for all selected sites

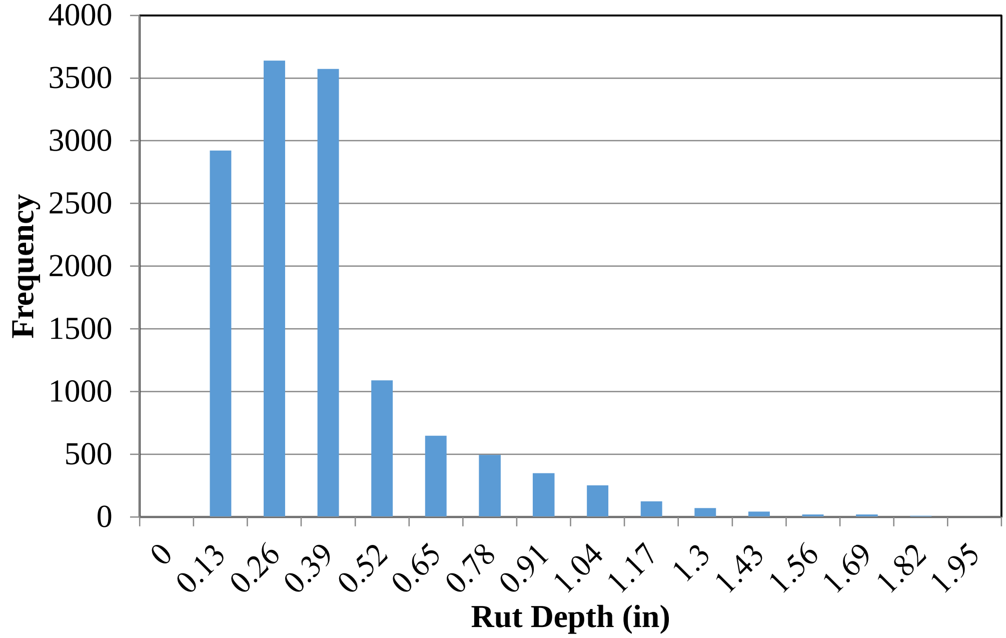

(a) LWP

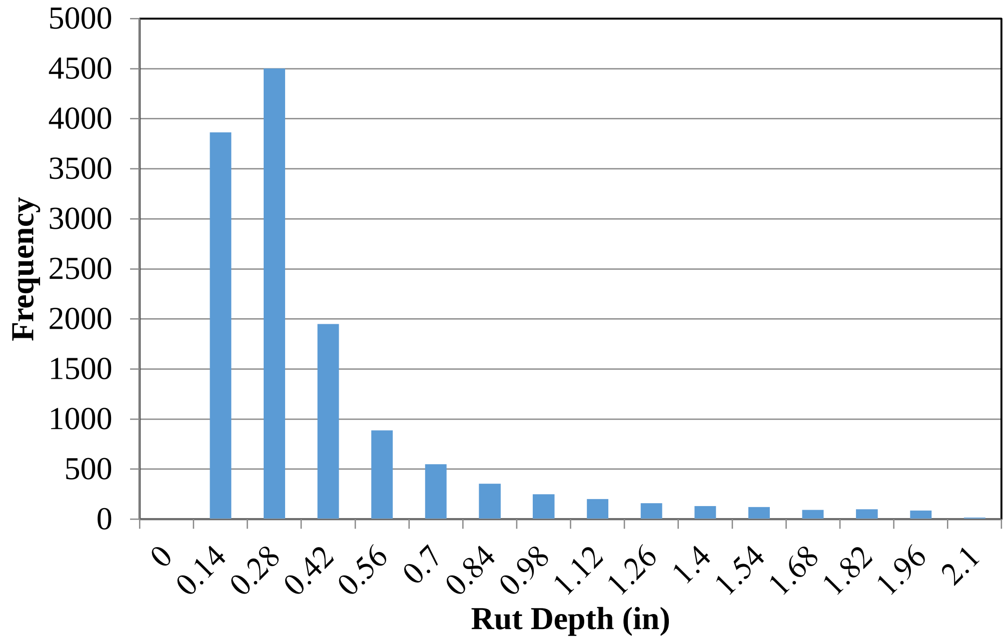

(b) RWP

Figure 89. Histograms of LTRC's 5-point rut depths (0.004-mile average) for all selected sites

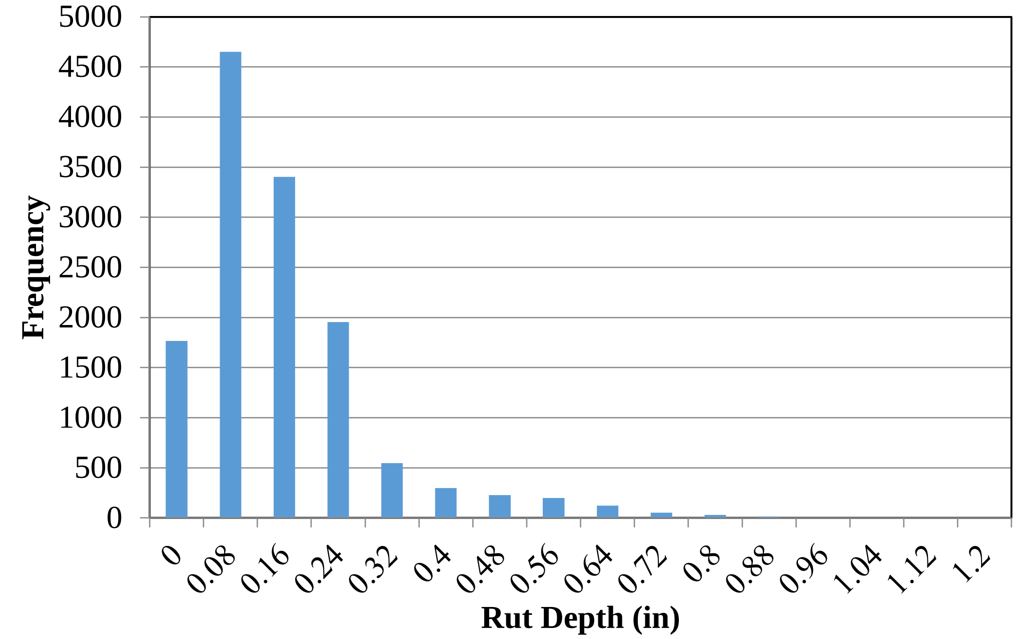

(a) LWP

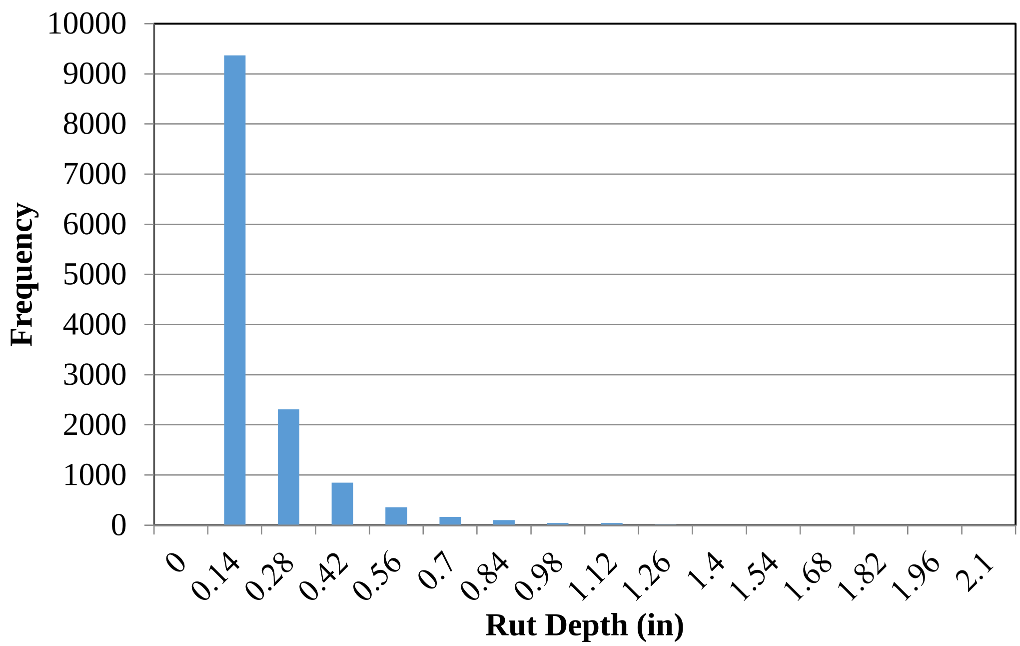

(b) RWP

Figure 90. Scatterplot of Fugro's full profile rut depth vs. LTRC's 5-point rut depth for CS826-10

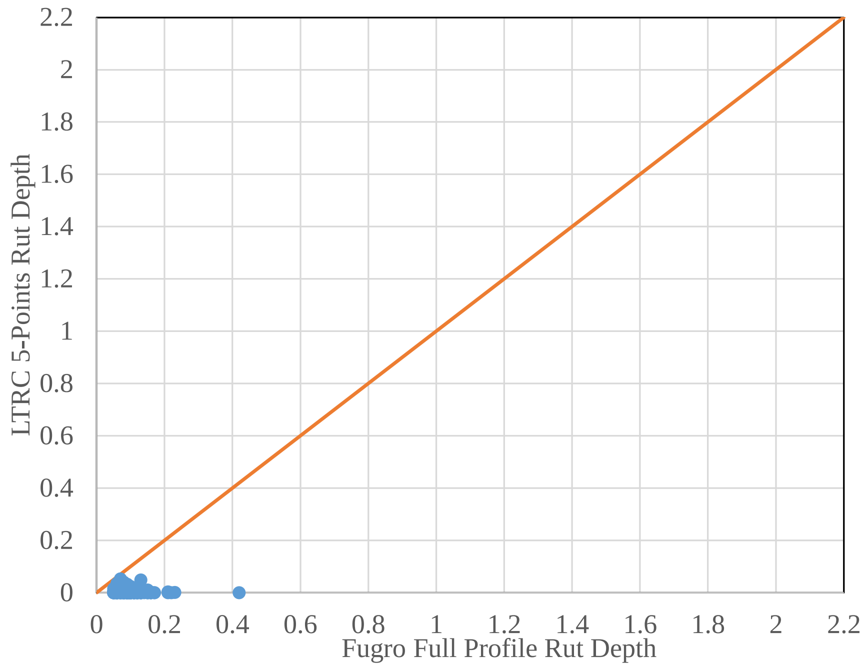

(a) LWP

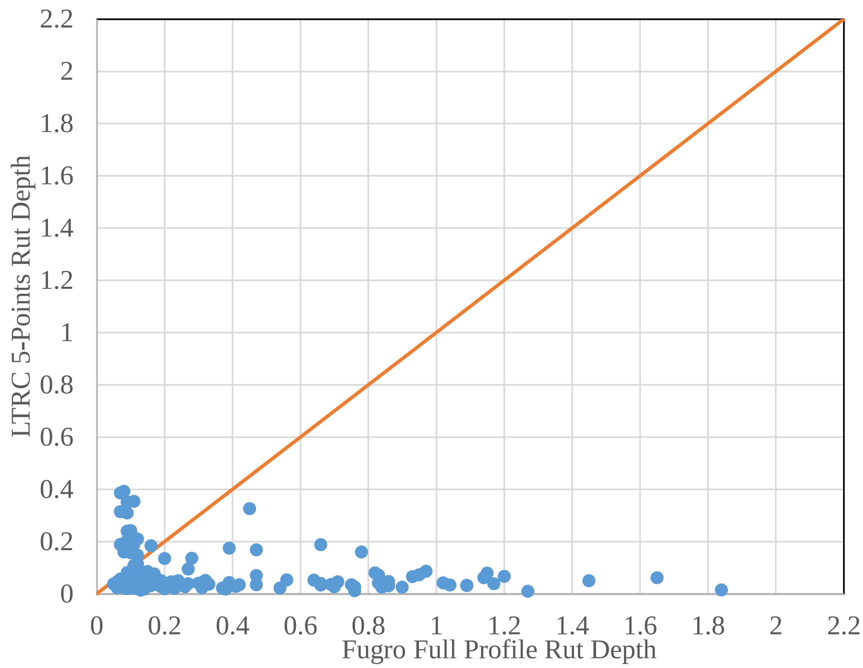

(b) RWP

Figure 91. Scatterplot of Fugro's full profile rut depth vs. LTRC's 5-point rut depth for CS824-23

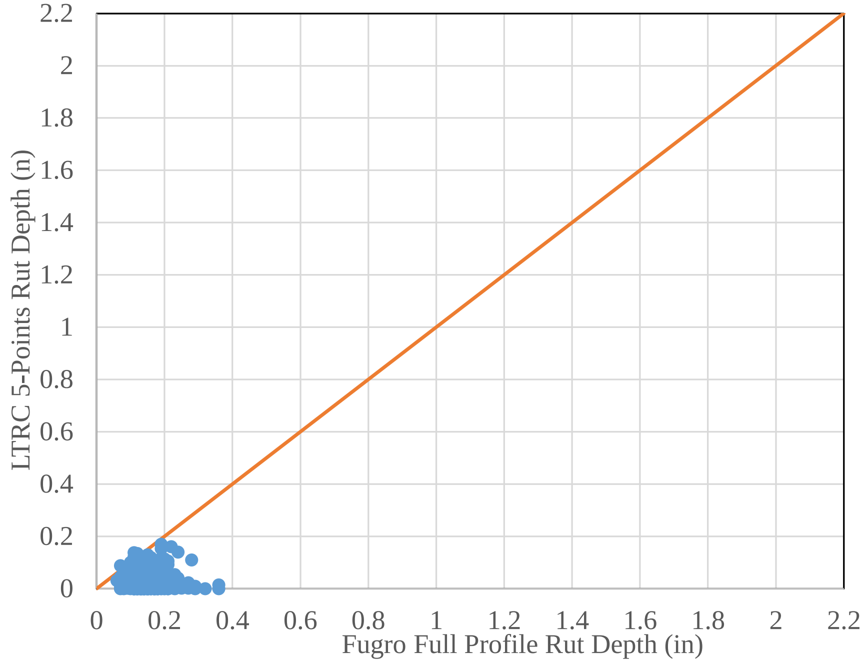

(a) LWP

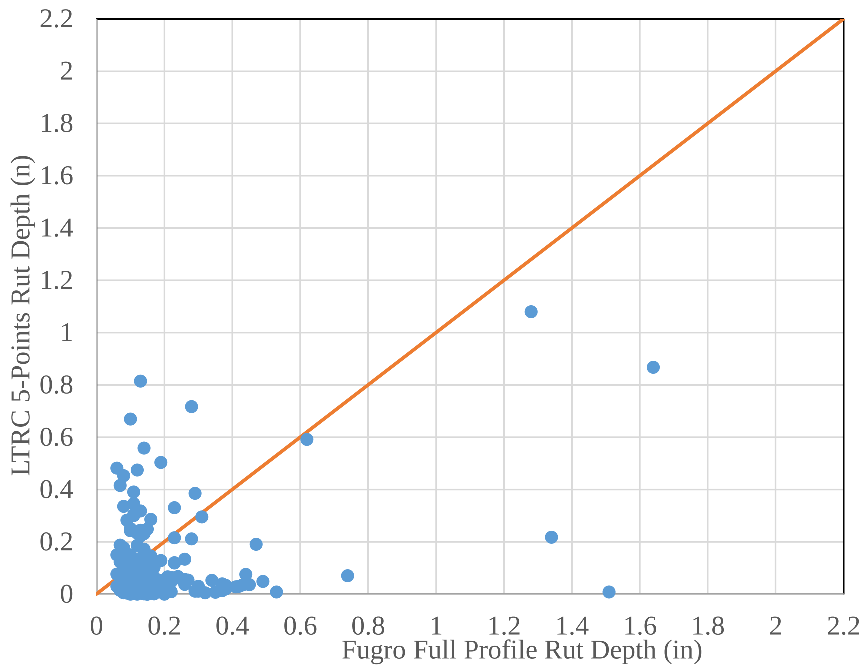

(b) RWP

Figure 92. Scatterplot of Fugro's full profile rut depth vs. LTRC's 5-point rut depth for CS226-01

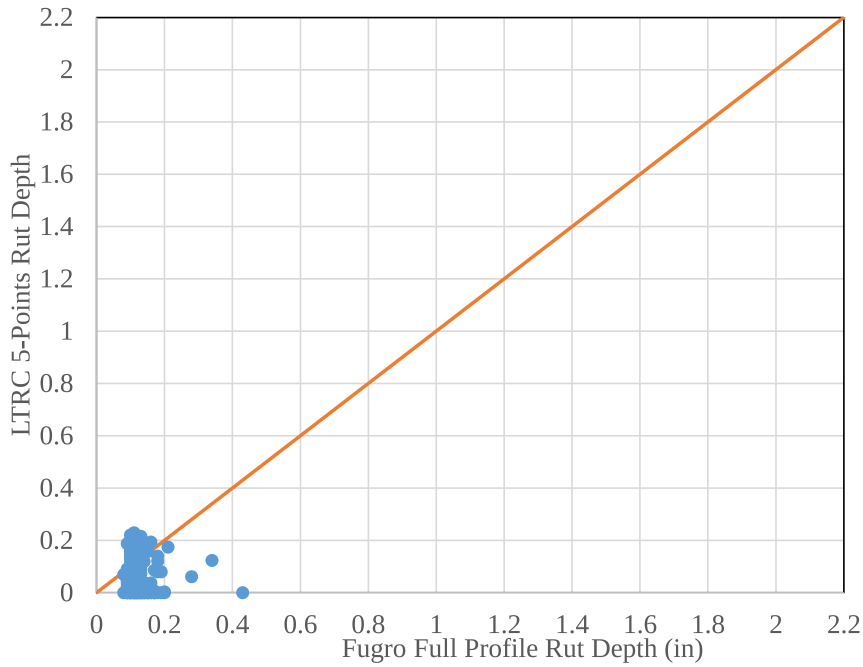

(a) LWP

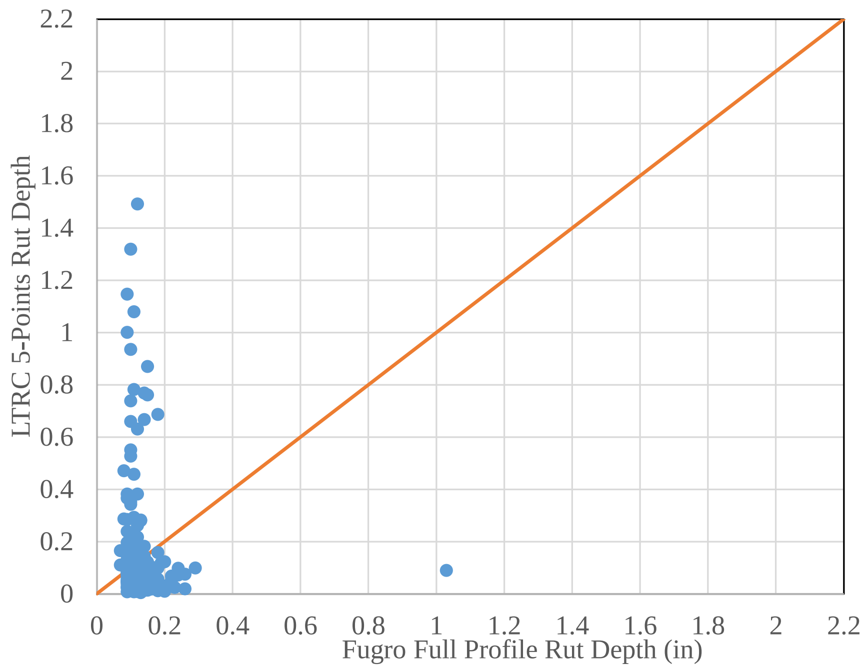

(b) RWP

Figure 93. Scatterplot of Fugro's full profile rut depth vs. LTRC's 5-point rut depth for CS013-05 (logmile: 5.68-6.34)

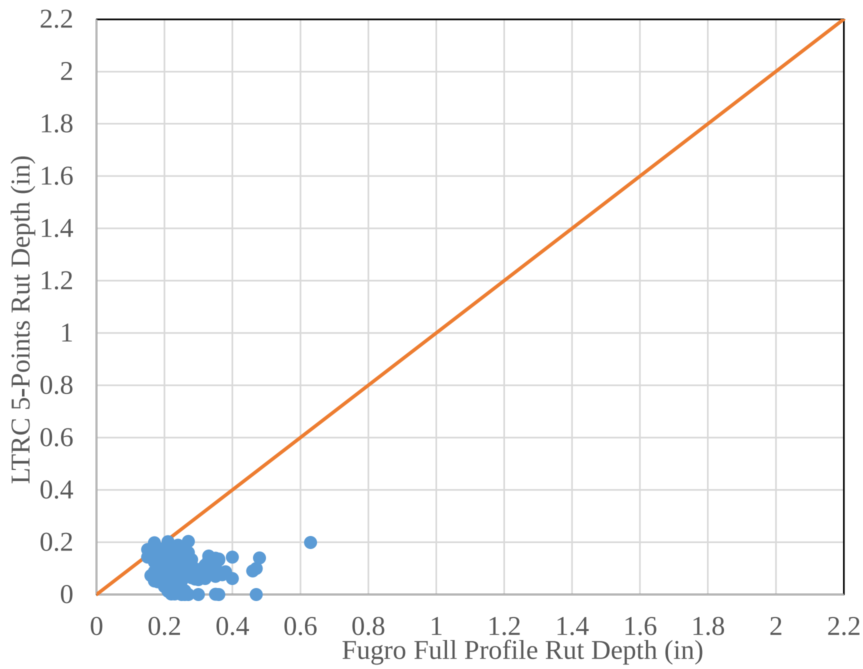

(a) LWP

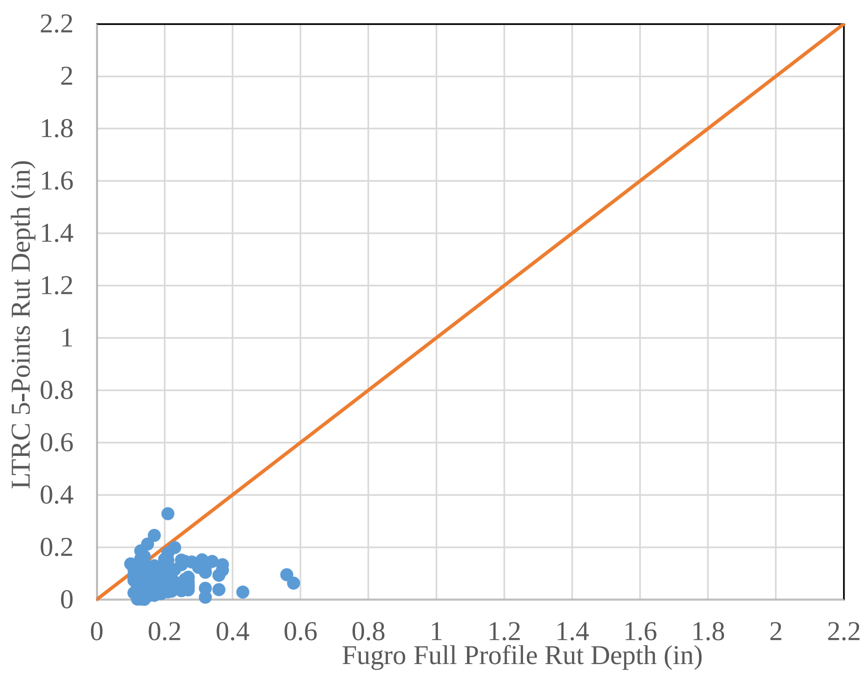

(b) RWP

Figure 94. Scatterplot of Fugro's full profile rut depth vs. LTRC's 5-point rut depth for CS452-90

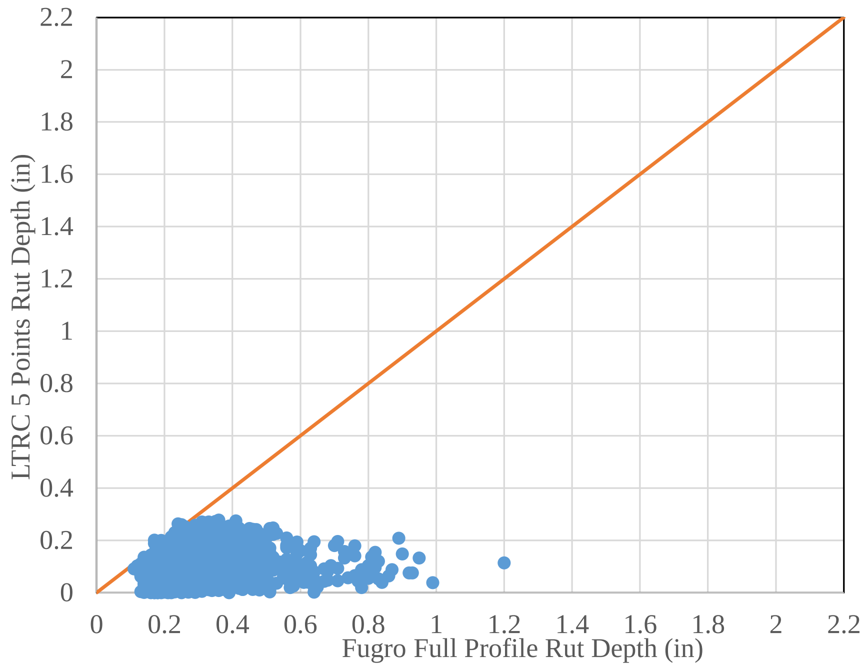

(a) LWP

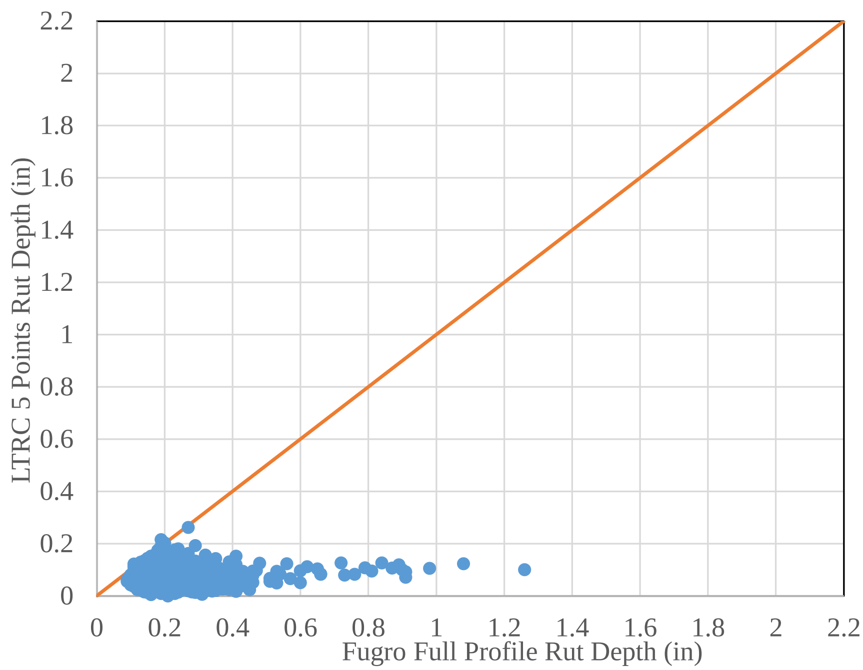

(b) RWP

Figure 95. Scatterplot of Fugro's full profile rut depth vs. LTRC's 5-point rut depth for CS852-30

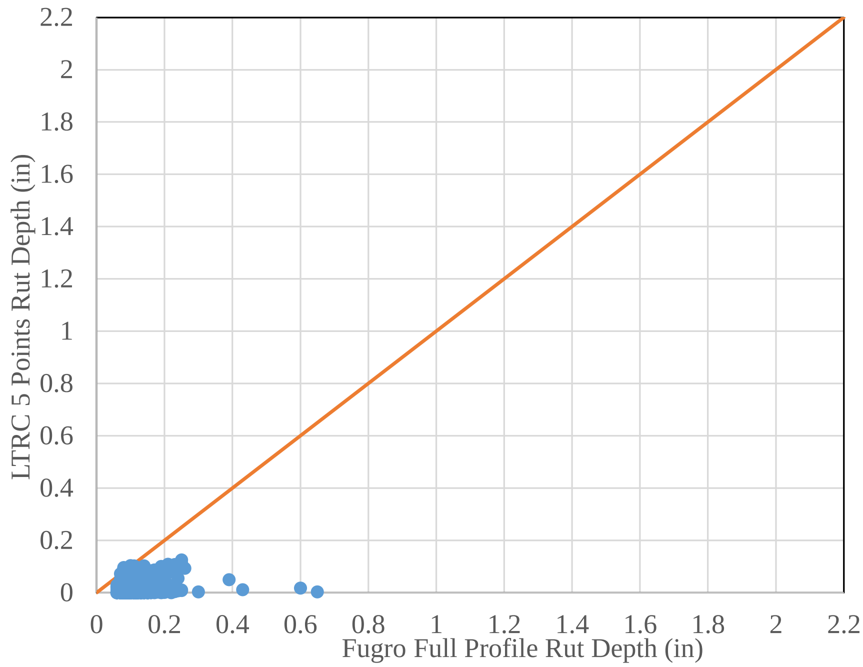

(a) LWP

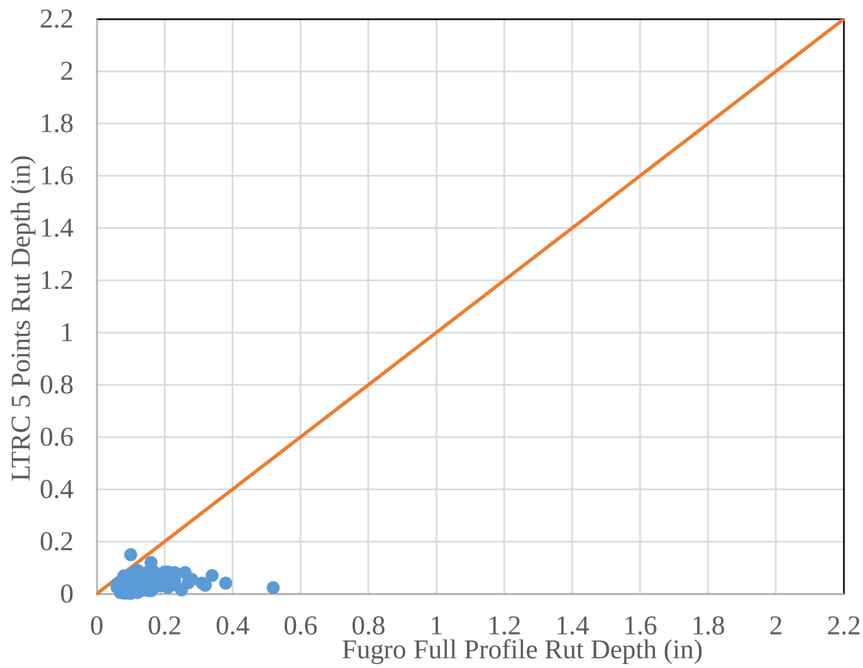

(b) RWP

Figure 96. Scatterplot of Fugro's full profile rut depth vs. LTRC's 5-point rut depth for CS803-04

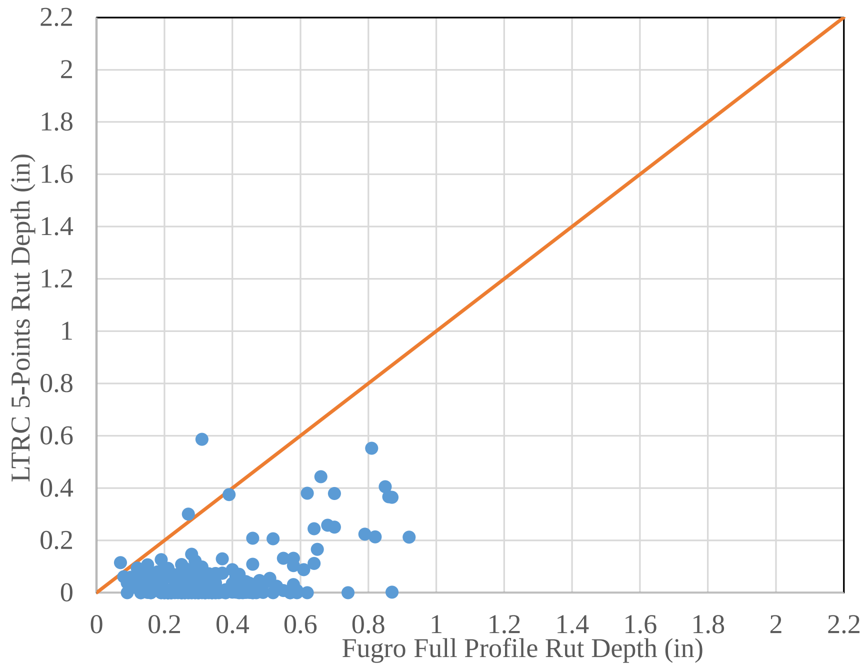

(a) LWP

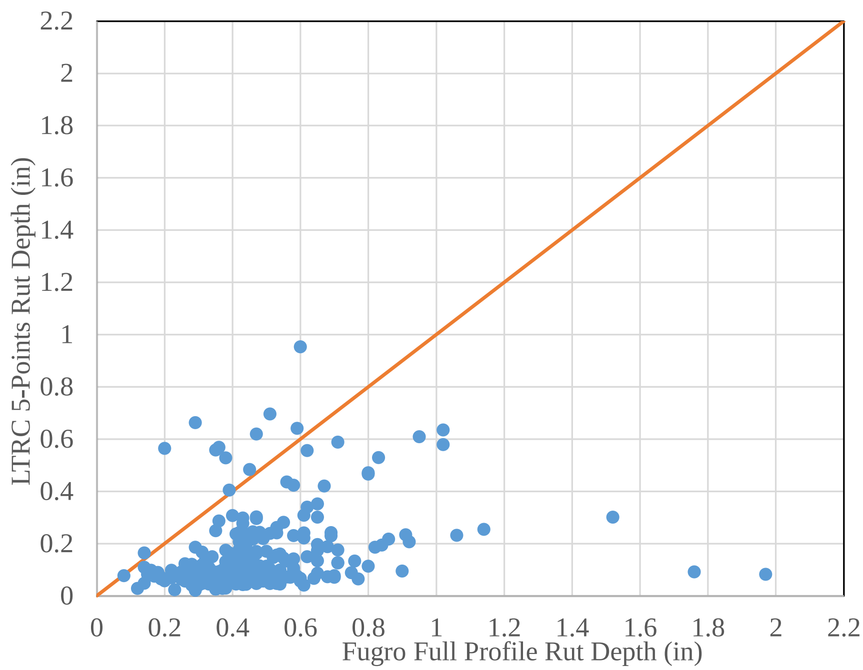

(b) RWP

Figure 97. Scatterplot of Fugro's full profile rut depth vs. LTRC's 5-point rut depth for CS269-02

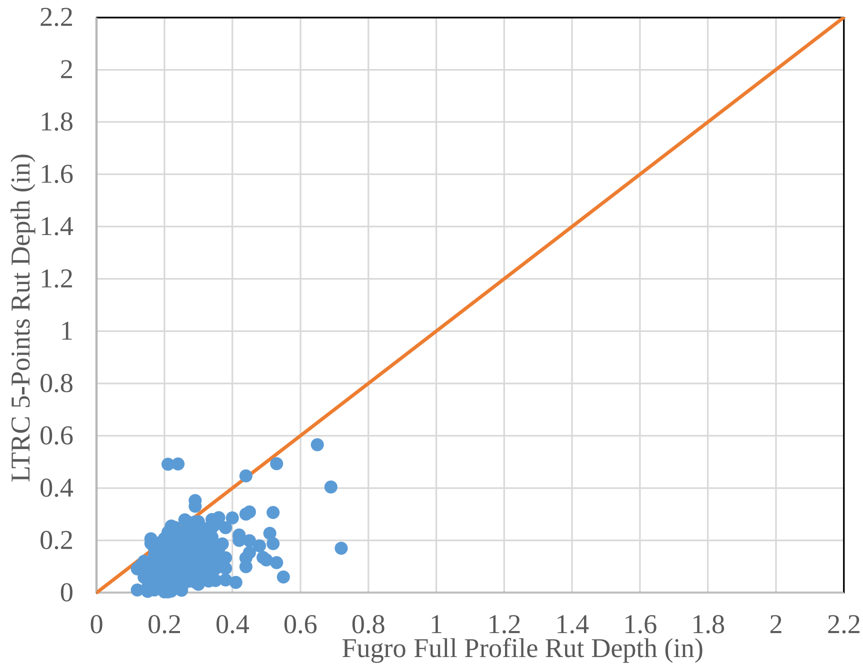

(a) LWP

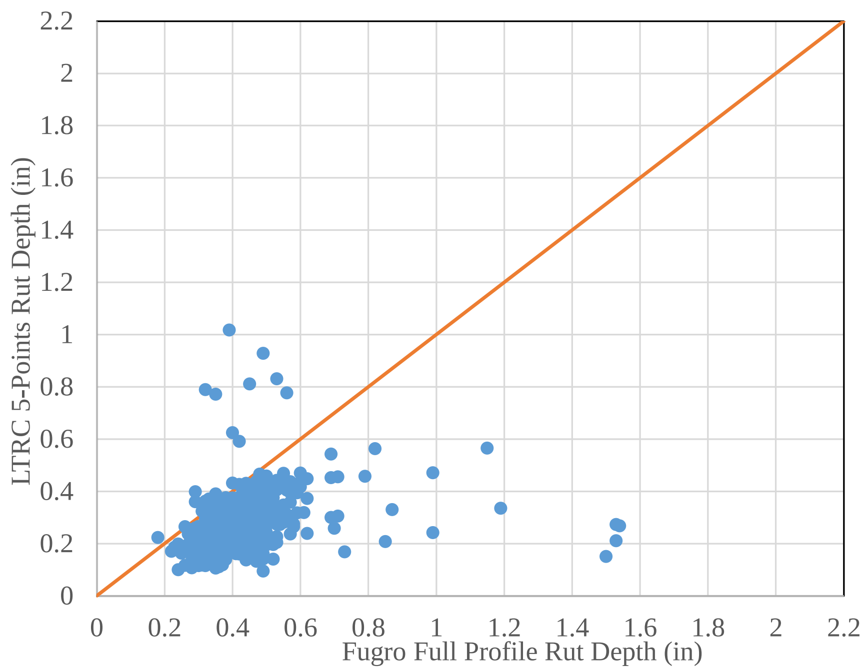

(b) RWP

Figure 98. Scatterplot of Fugro's full profile rut depth vs. LTRC's 5-point rut depth for CS061-04

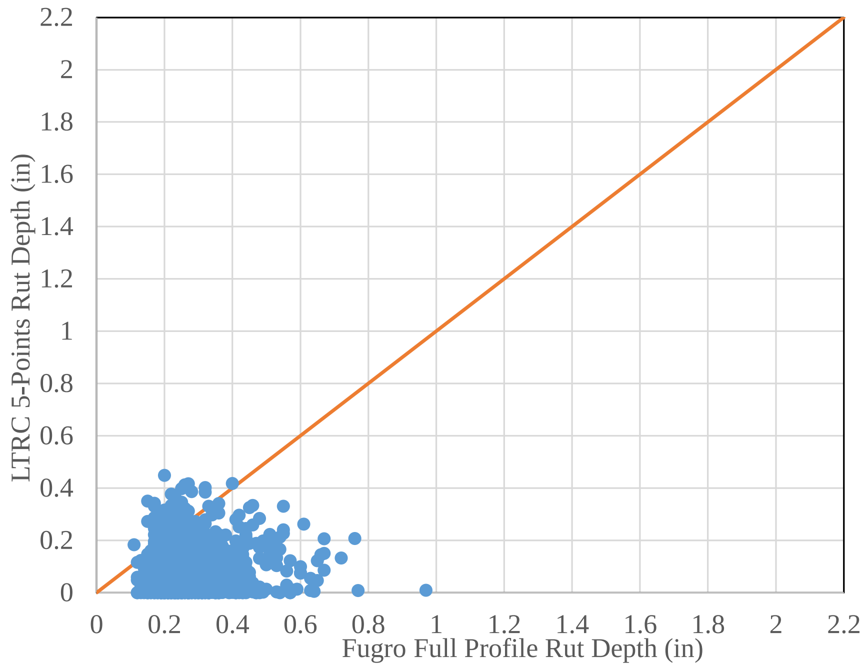

(a) LWP

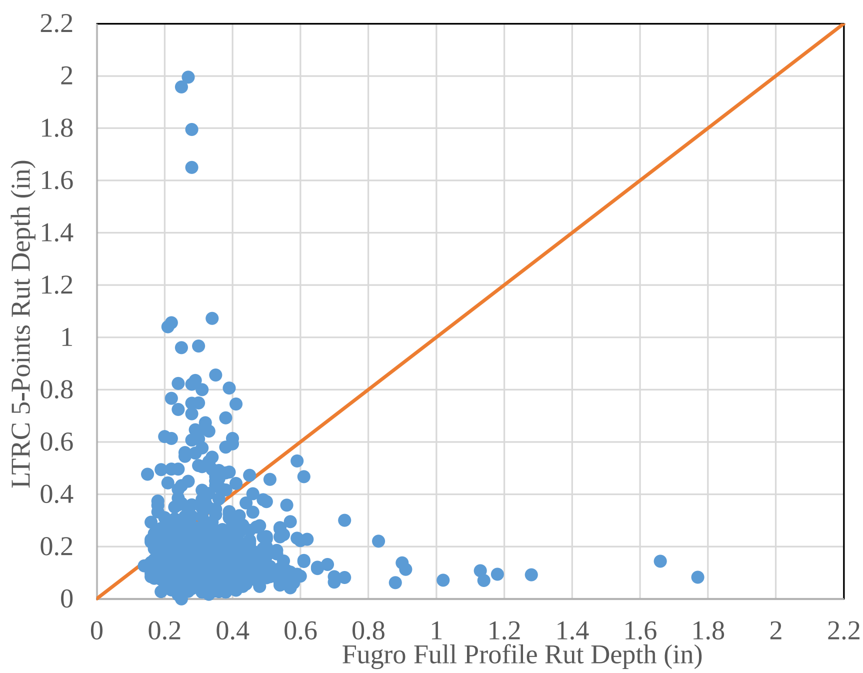

(b) RWP

Figure 99. Scatterplot of Fugro's full profile rut depth vs. LTRC's 5-point rut depth for CS257-04

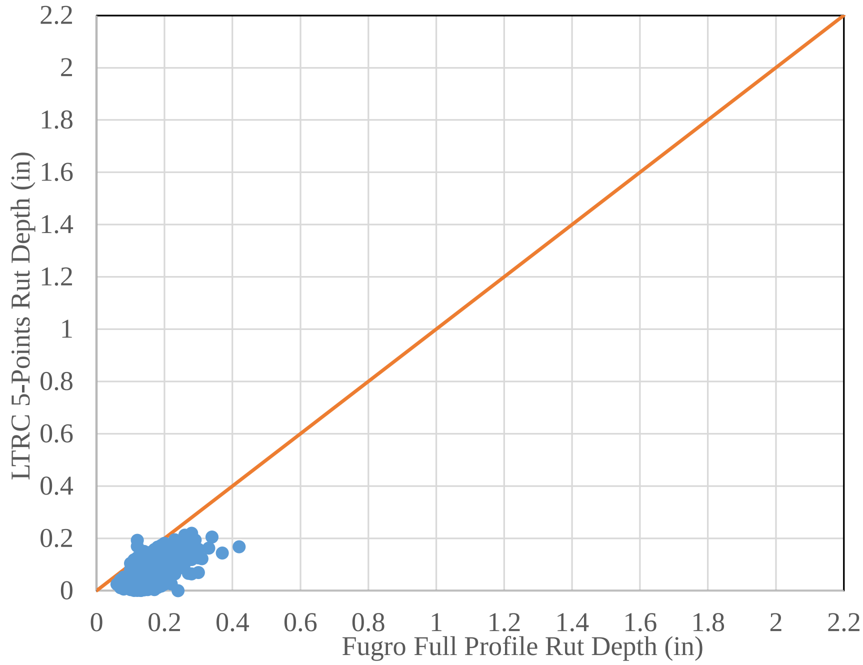

(a) LWP

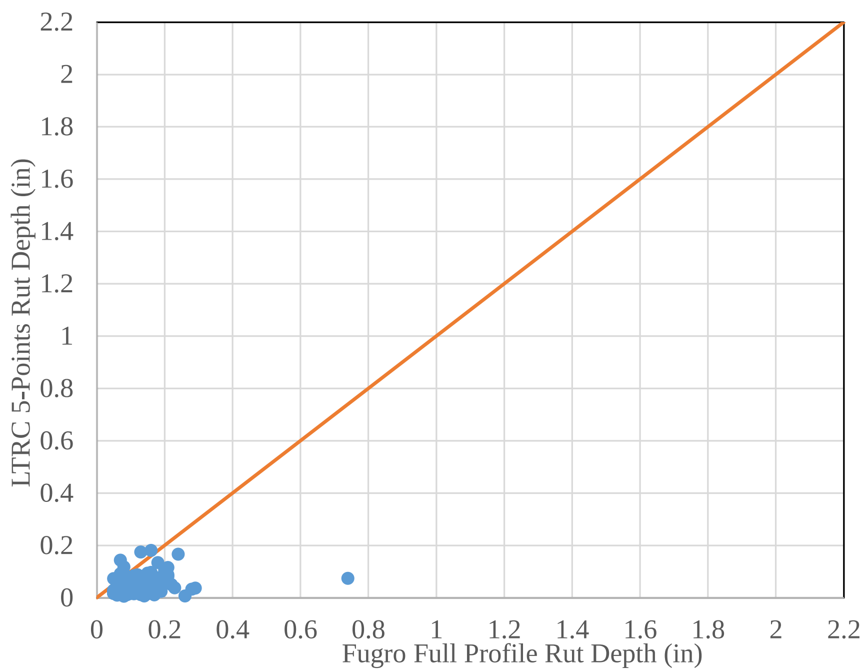

(b) RWP

Figure 100. Scatterplot of Fugro's full profile rut depth vs. LTRC's 5-point rut depth for CS282-01

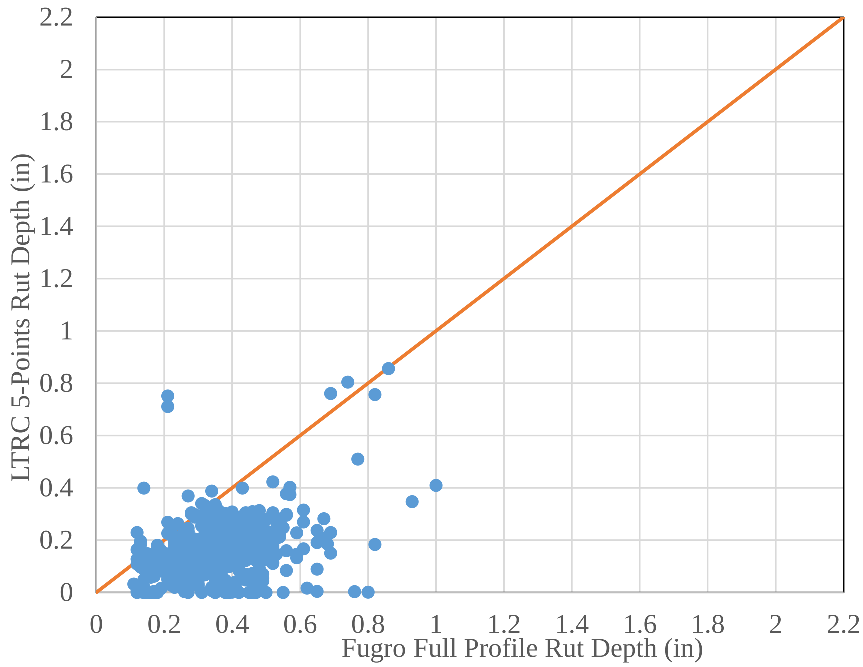

(a) LWP

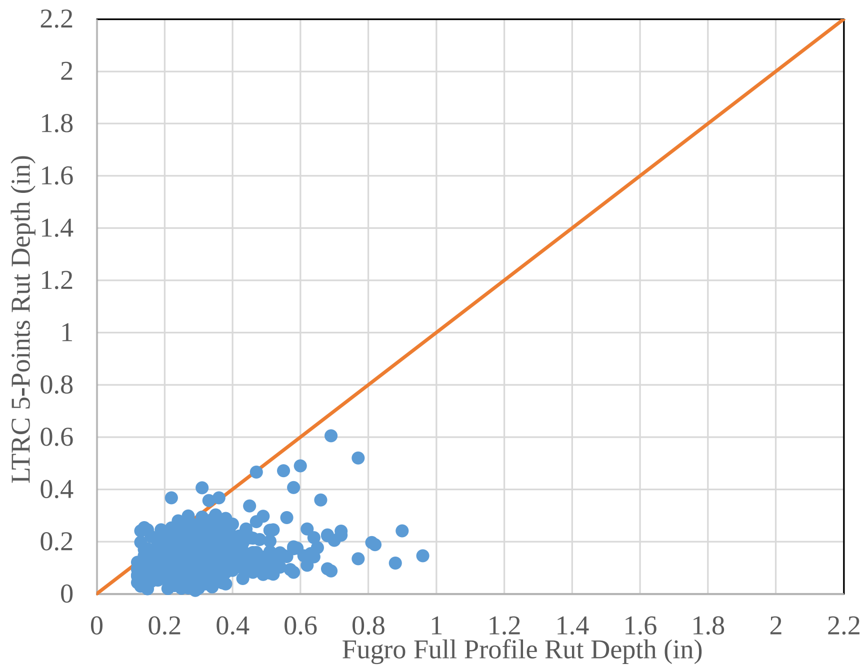

(b) RWP

Figure 101. Scatterplot of Fugro's full profile rut depth vs. LTRC's 5-point rut depth for CS013-05 (logmile:1.23-5.68)

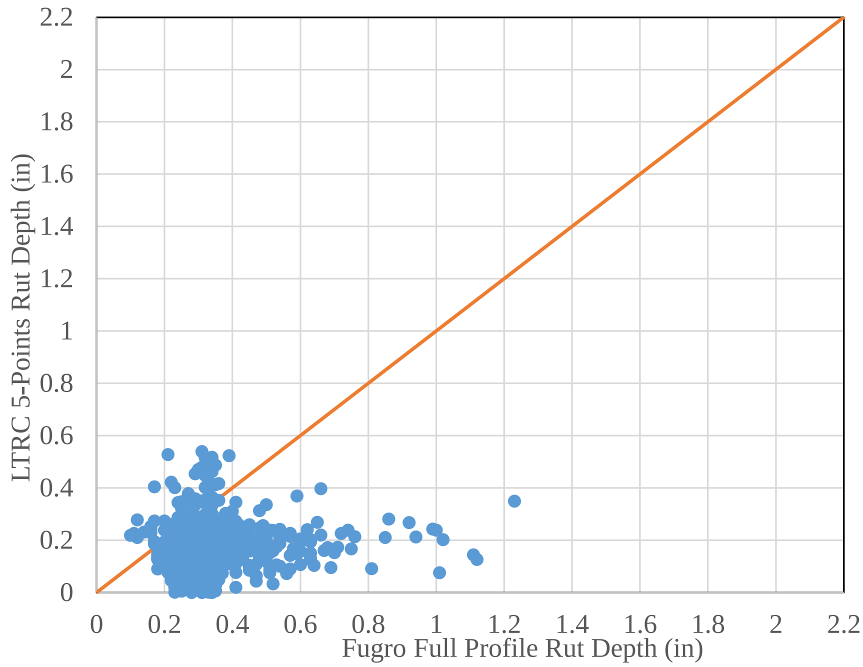

(a) LWP

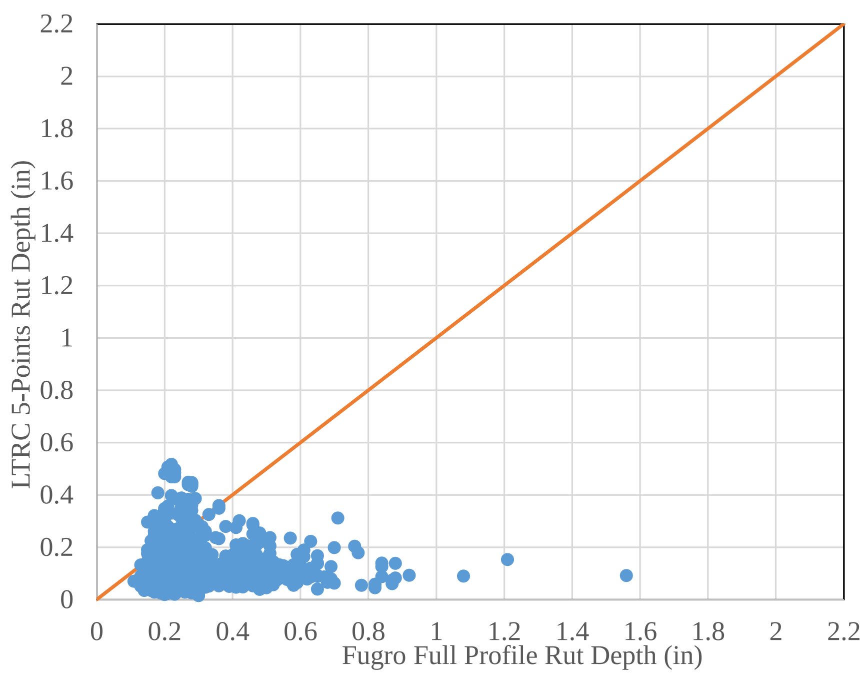

(b) RWP

Figure 102. Scatterplot of Fugro's full profile rut depth vs. LTRC's 5-point rut depth for CS803-25

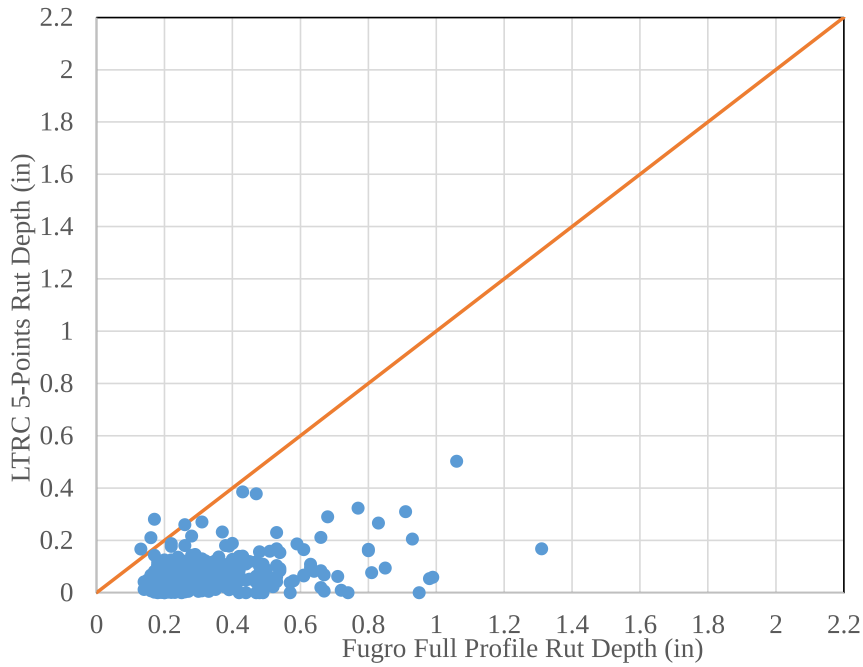

(a) LWP

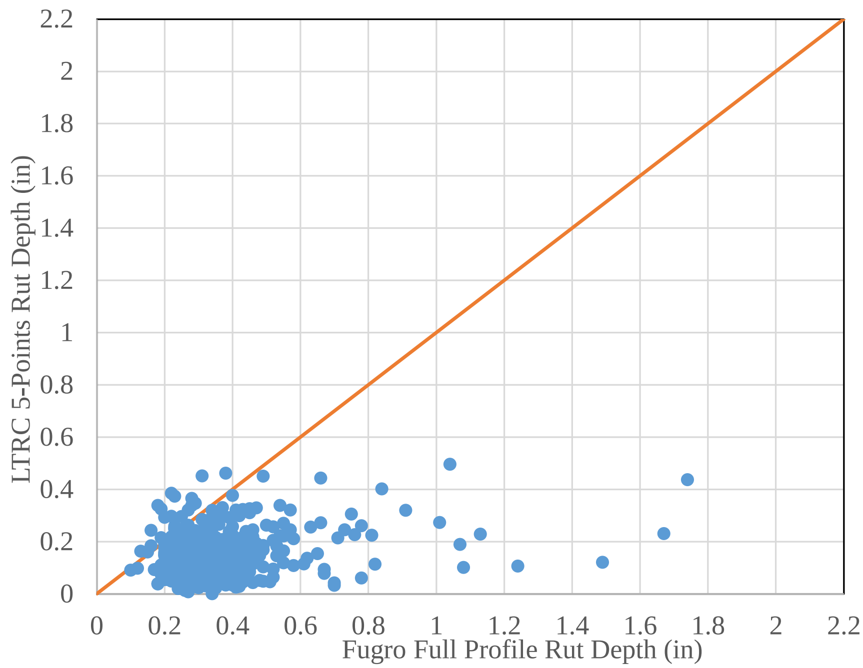

(b) RWP

Figure 103. Scatterplot of Fugro's full profile rut depth vs. LTRC's 5-point rut depth for CS244-01

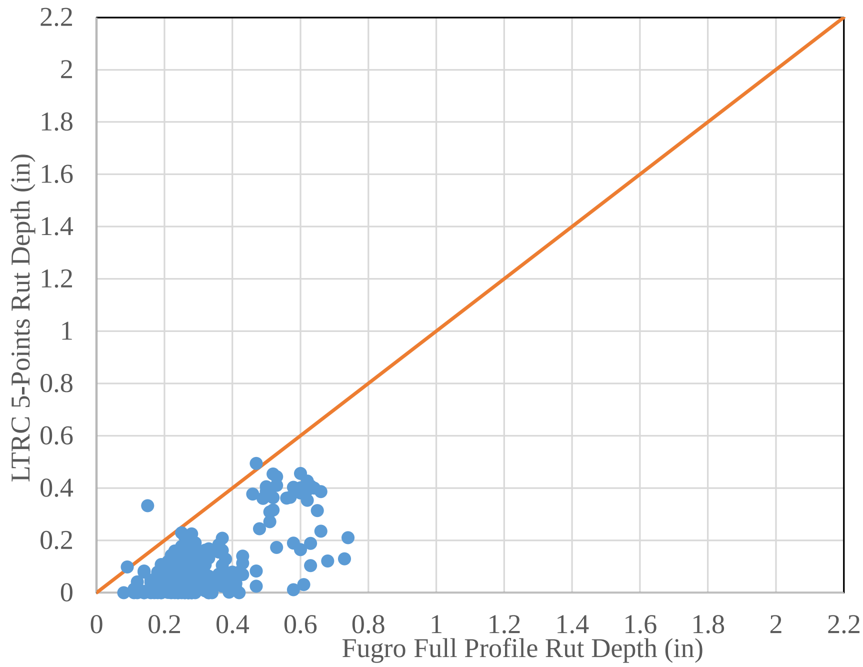

(a) LWP

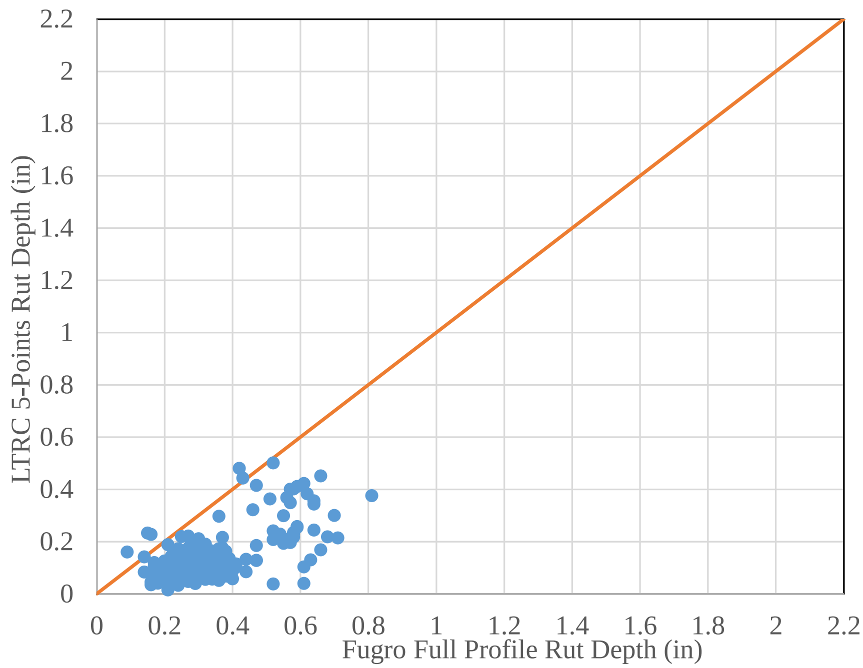

(b) RWP

Figure 104. Scatterplot of Fugro's full profile rut depth vs. LTRC's 5-point rut depth for CS424-07

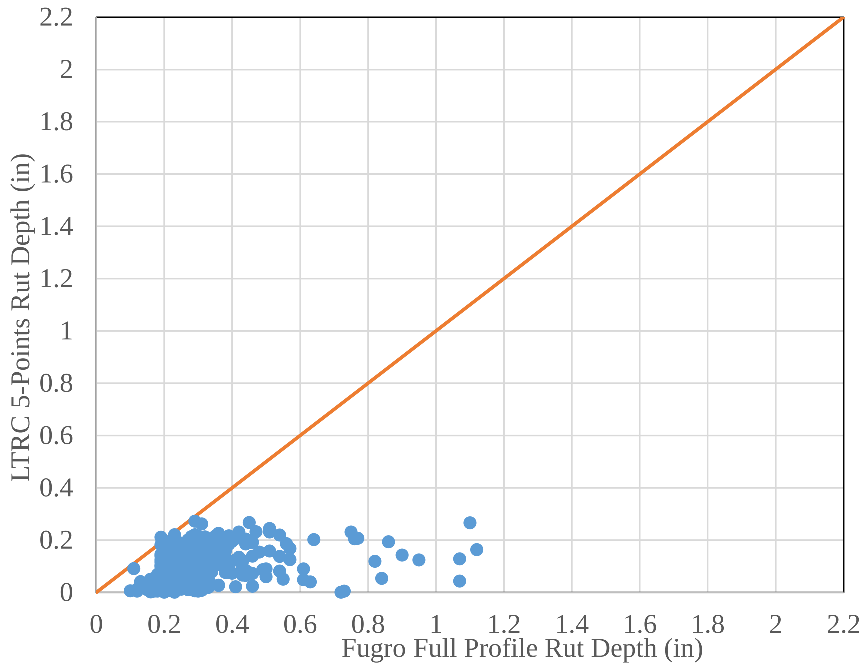

(a) LWP

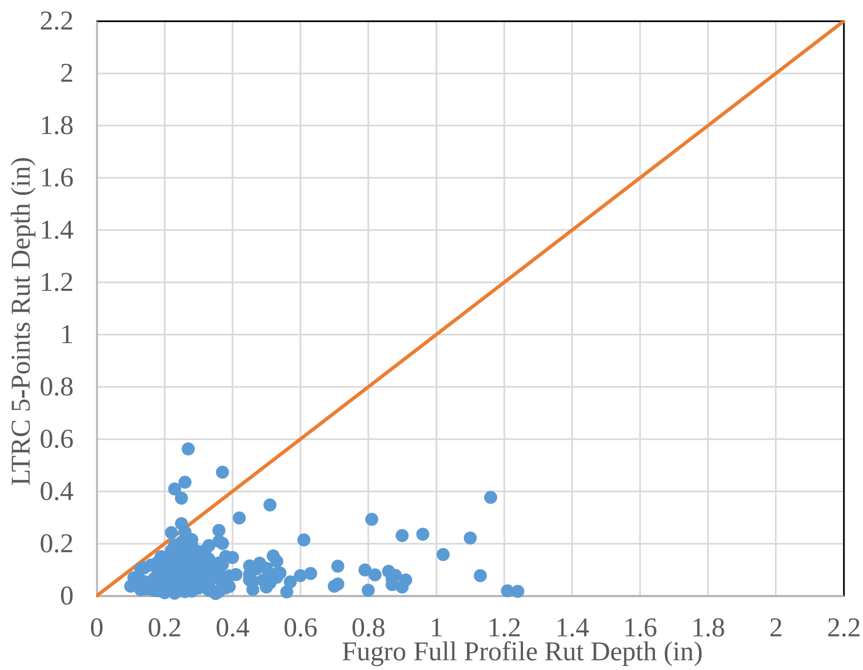

(b) RWP

Figure 105. Scatterplot of Fugro's full profile rut depth vs. LTRC's 5-point rut depth for CS450-12

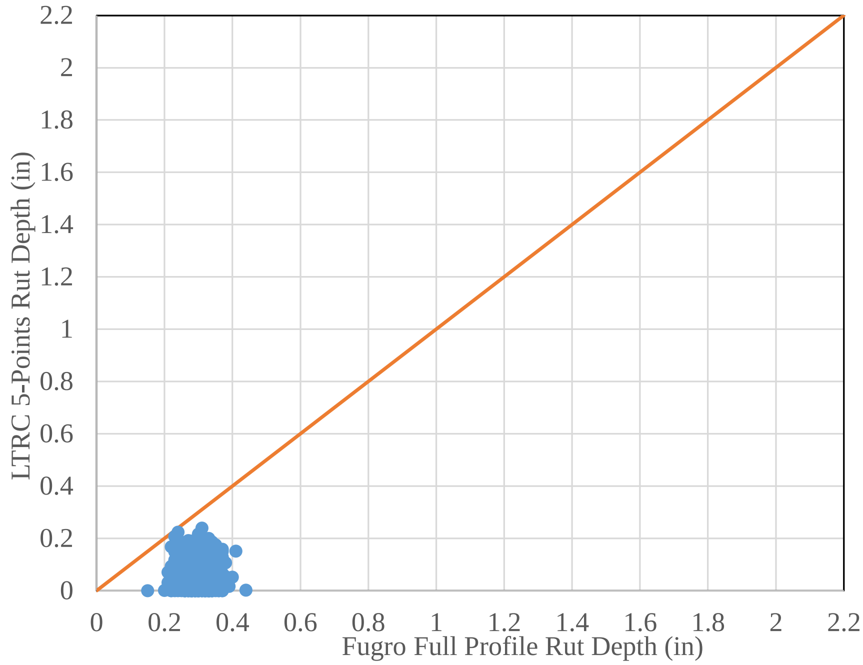

(a) LWP

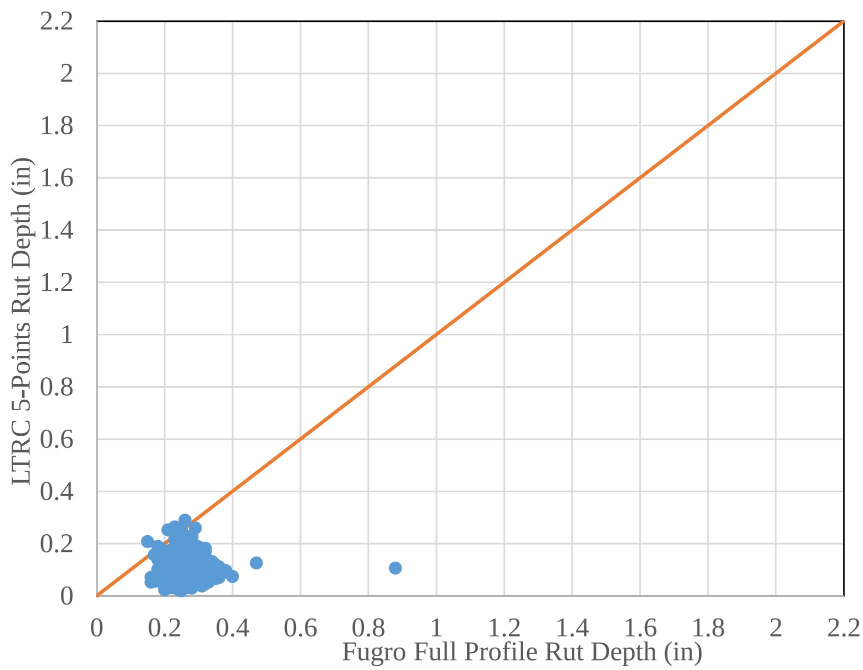

(b) RWP

Figure 106. Scatterplot of Fugro's full profile rut depth vs. LTRC's 5-point rut depth for CS455-01

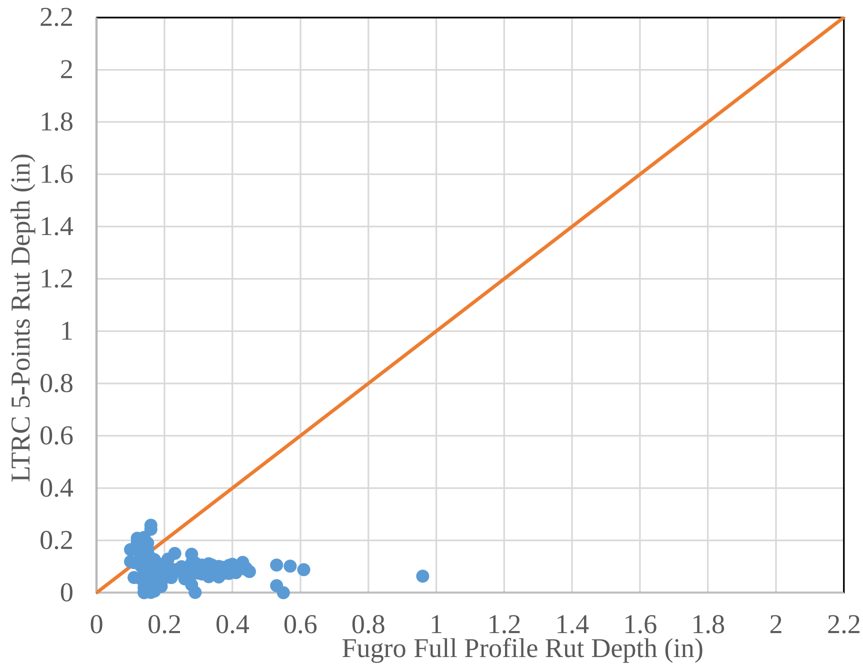

(a) LWP

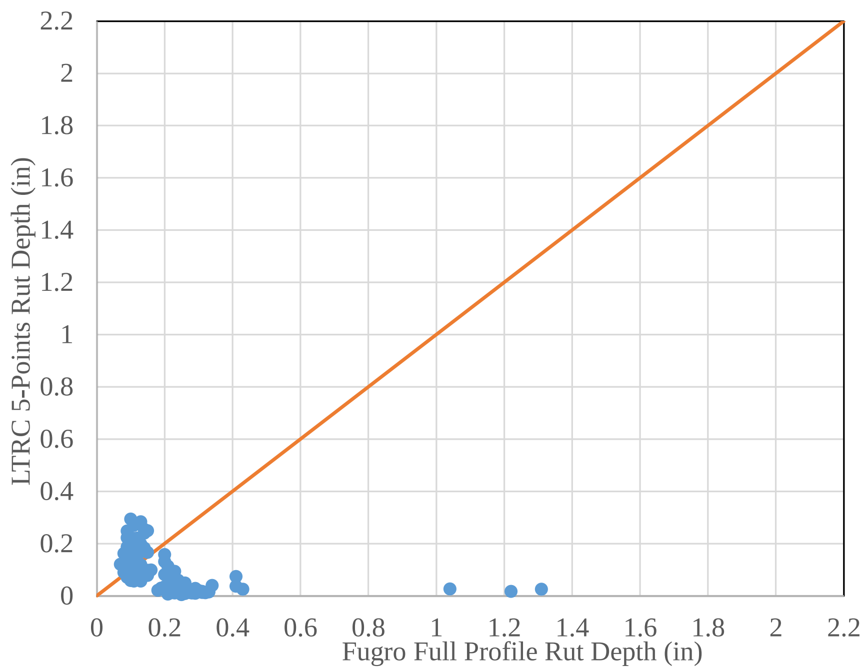

(b) RWP

Figure 107. Scatterplot of Fugro's full profile rut depth vs. LTRC's 5-point rut depth for CS081-01

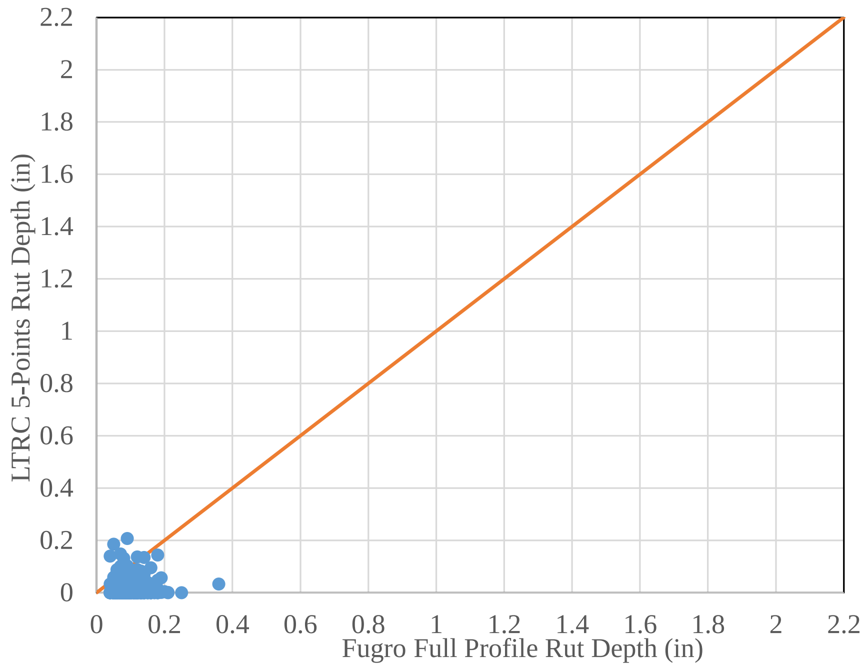

(a) LWP

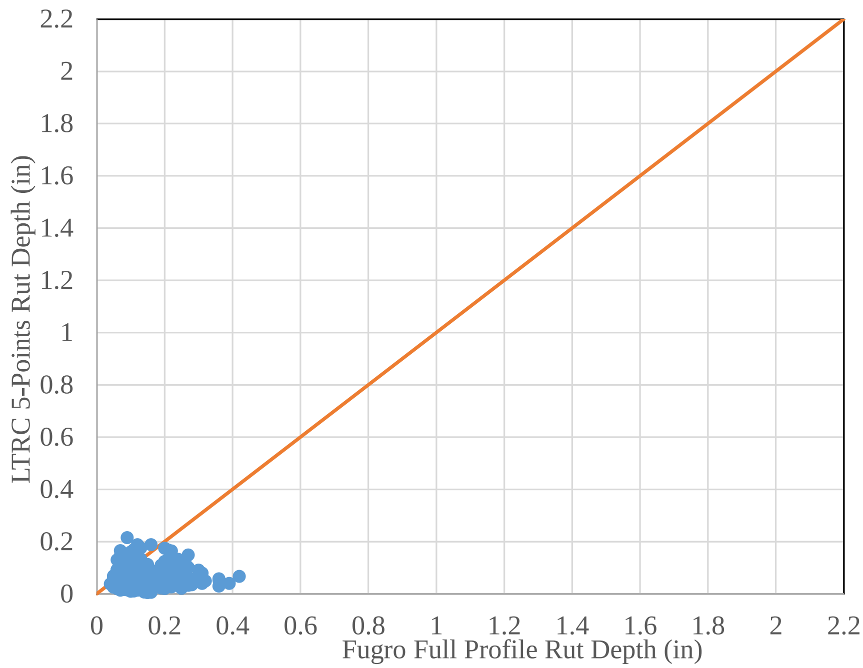

(b) RWP

Figure 108. Scatterplot of Fugro's full profile rut depth vs. LTRC's 5-point rut depth for CS060-01

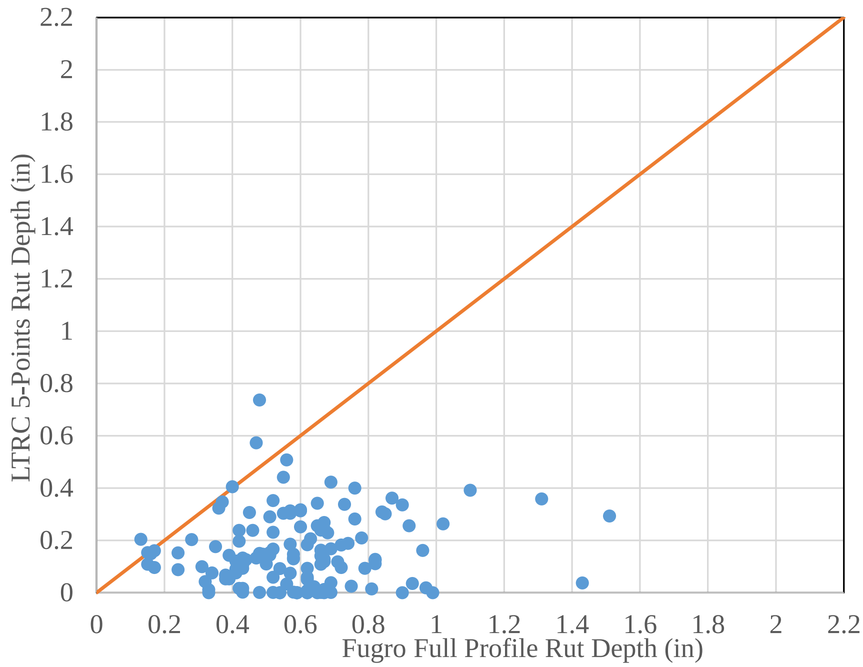

(a) LWP

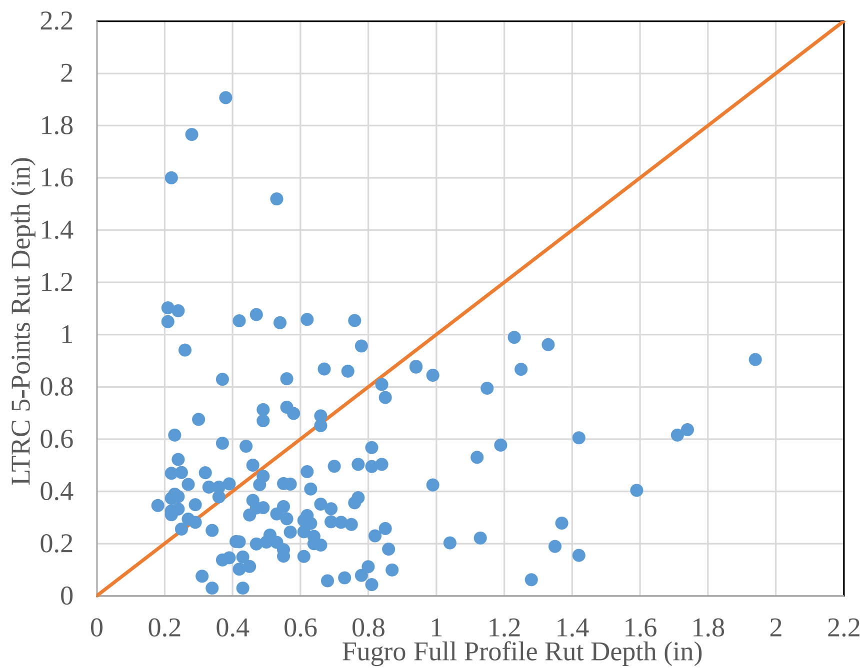

(b) RWP

Figure 109. Scatterplot of Fugro's full profile rut depth vs. LTRC's 5-point rut depth for CS203-01

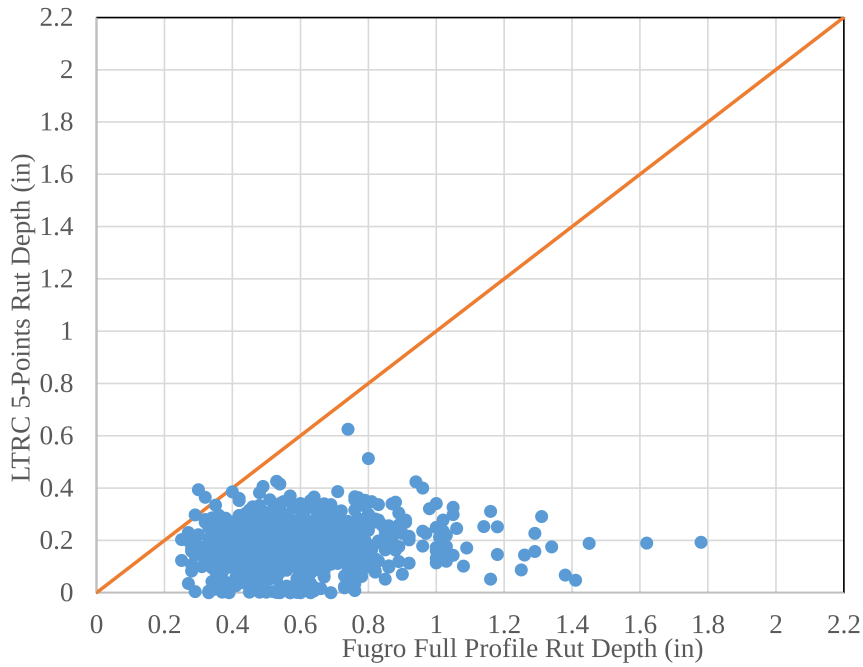

(a) LWP

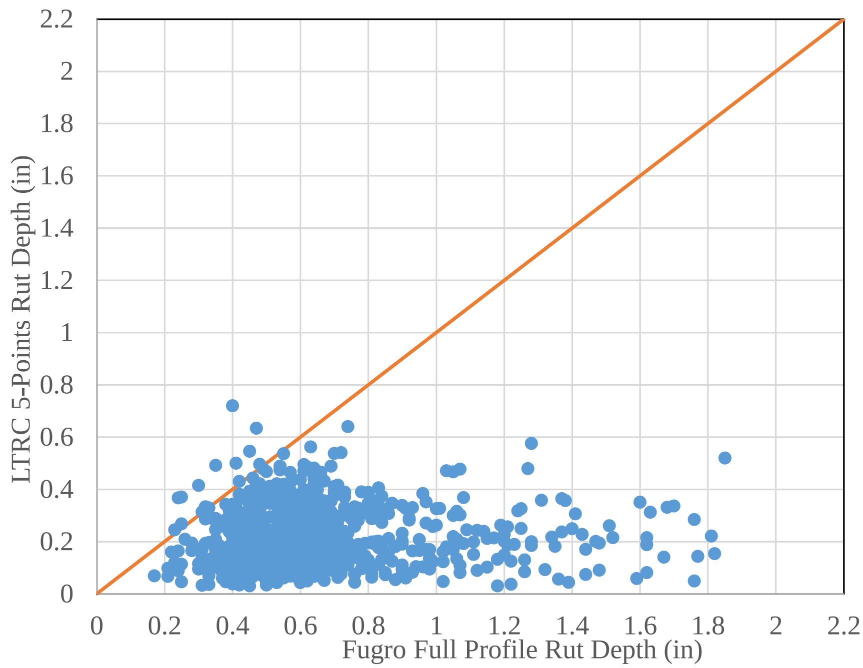

(b) RWP

Figure 110. Scatterplot of Fugro's full profile rut depth vs. LTRC's 5-point rut depth for CS419-01

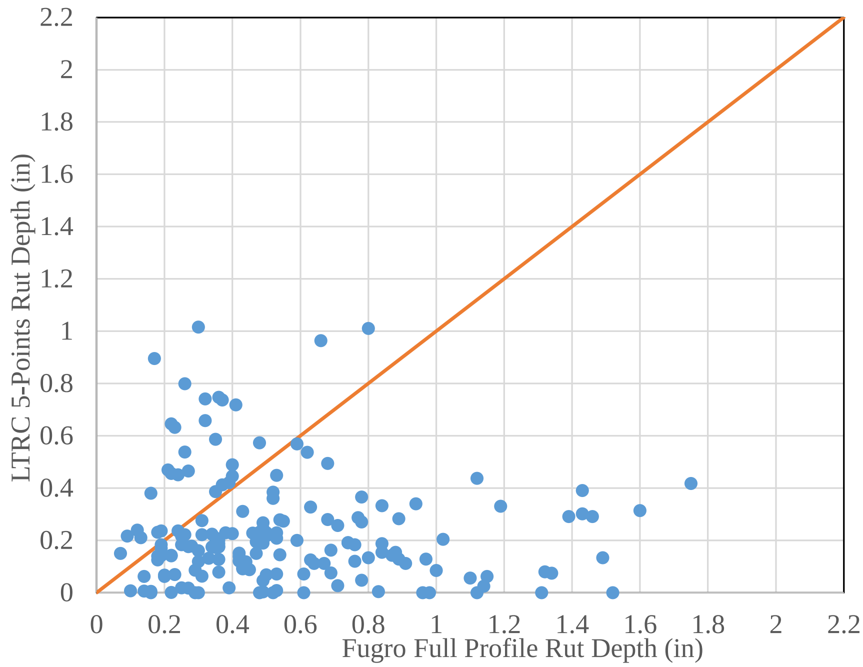

(a) LWP

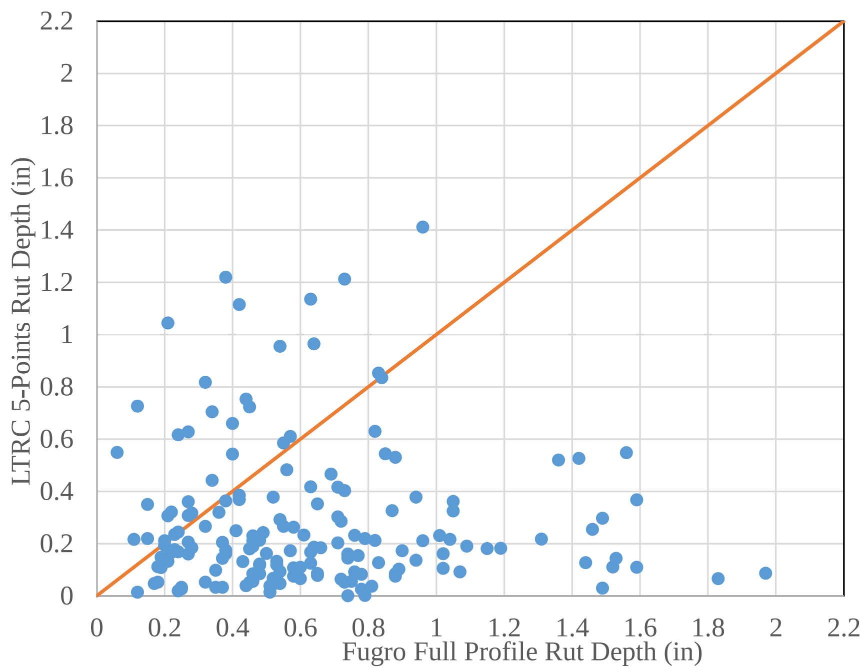

(b) RWP

Figure 111. Scatterplot of Fugro's full profile rut depth vs. LTRC's 5-point rut depth for CS849-10

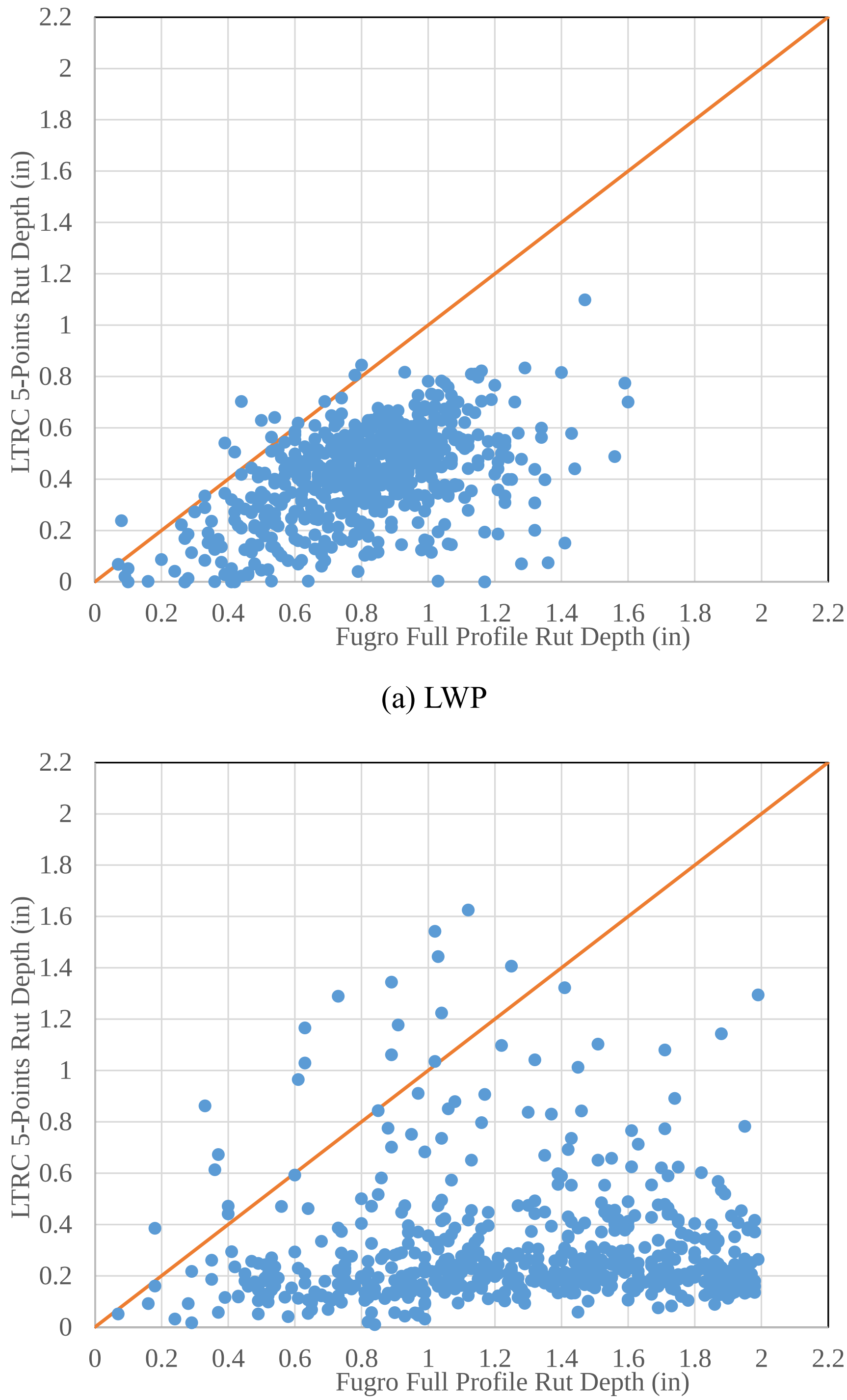

(a) LWP

(b) RWP

Figure 112. Scatterplot of Fugro's full profile rut depth vs. LTRC's 5-point rut depth for CS849-23

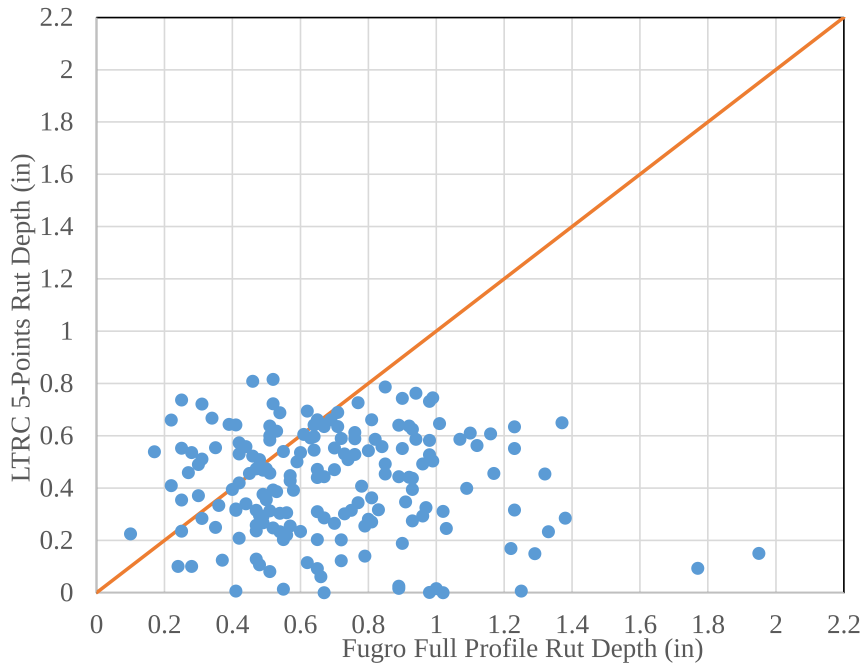

(a) LWP

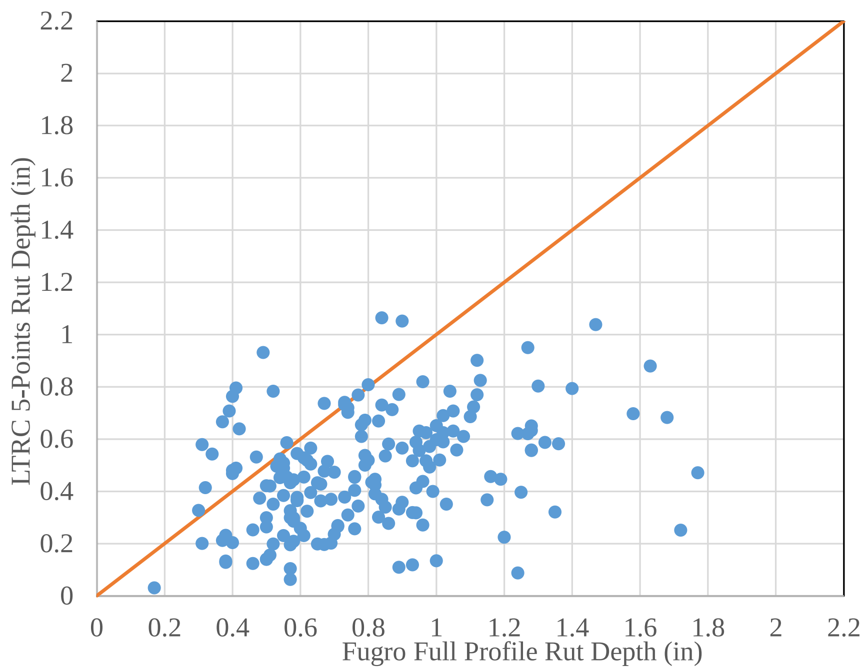

(b) RWP

Figure 113. Scatterplot of Fugro's full profile rut depth vs. LTRC's 5-point rut depth for CS208-01

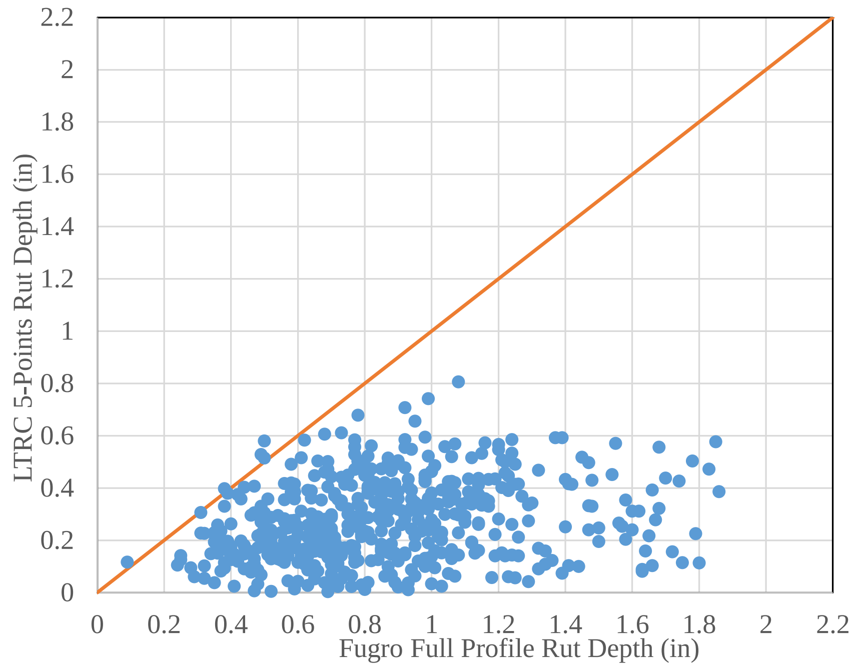

(a) LWP

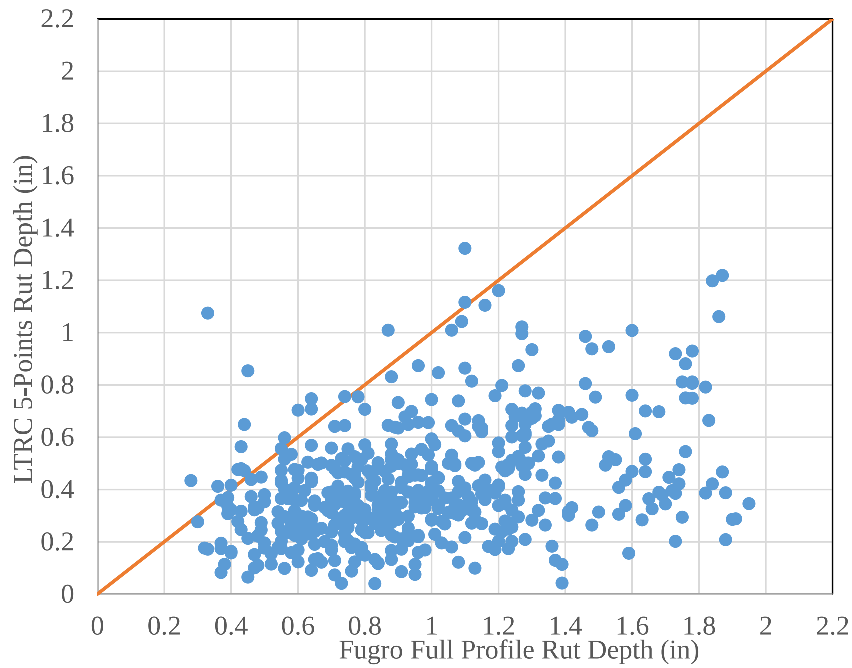

(b) RWP

Figure 114. Histograms of Fugro's full profile rut depths (0.1-mile average) for all selected sites

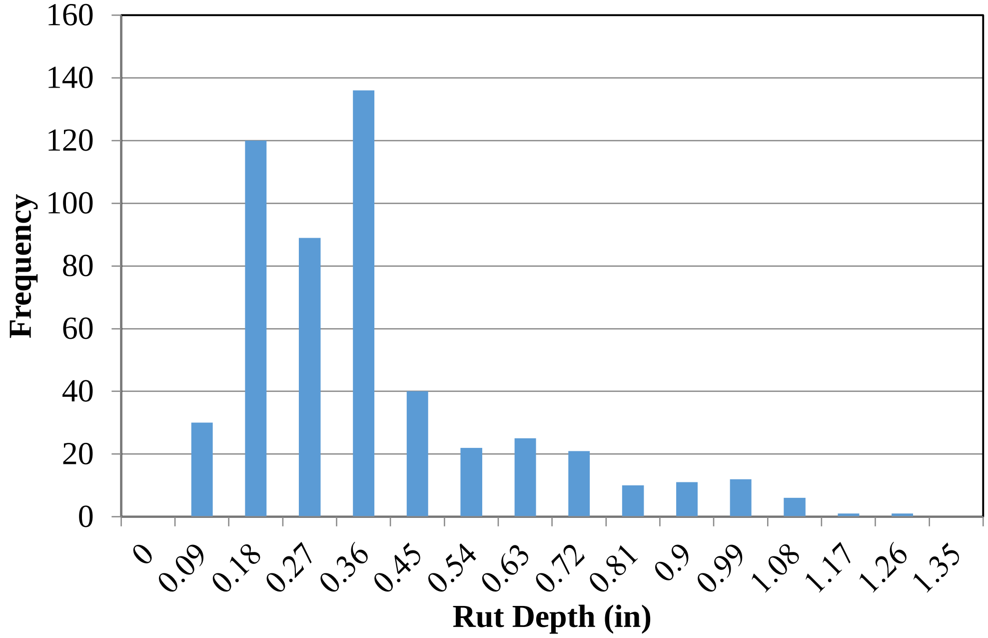

(a) LWP

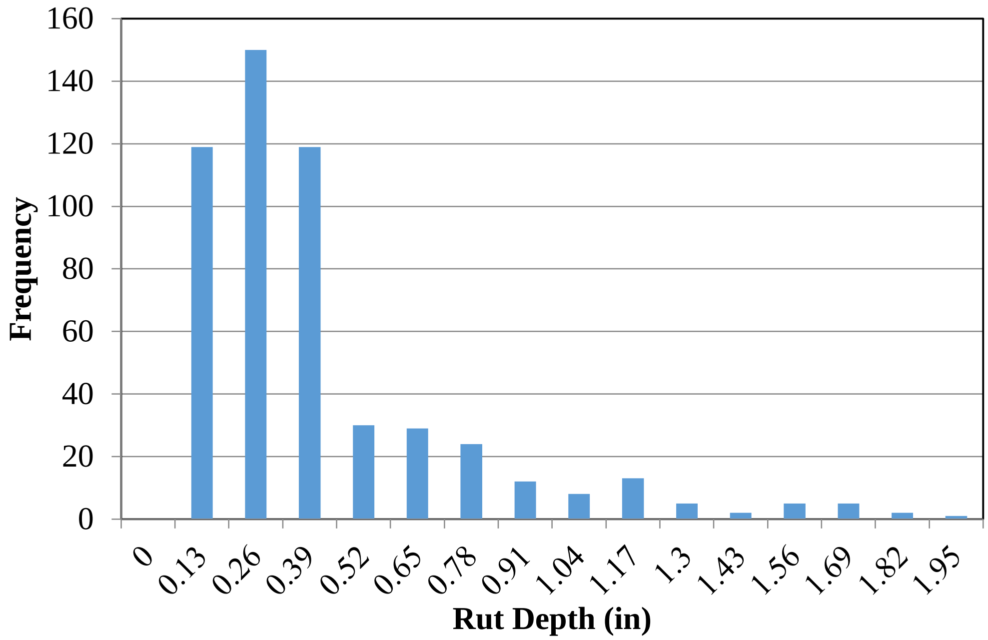

(b) RWP

Figure 115. Histograms of LTRC's 5-point rut depths (0.1-mile average) for all selected sites

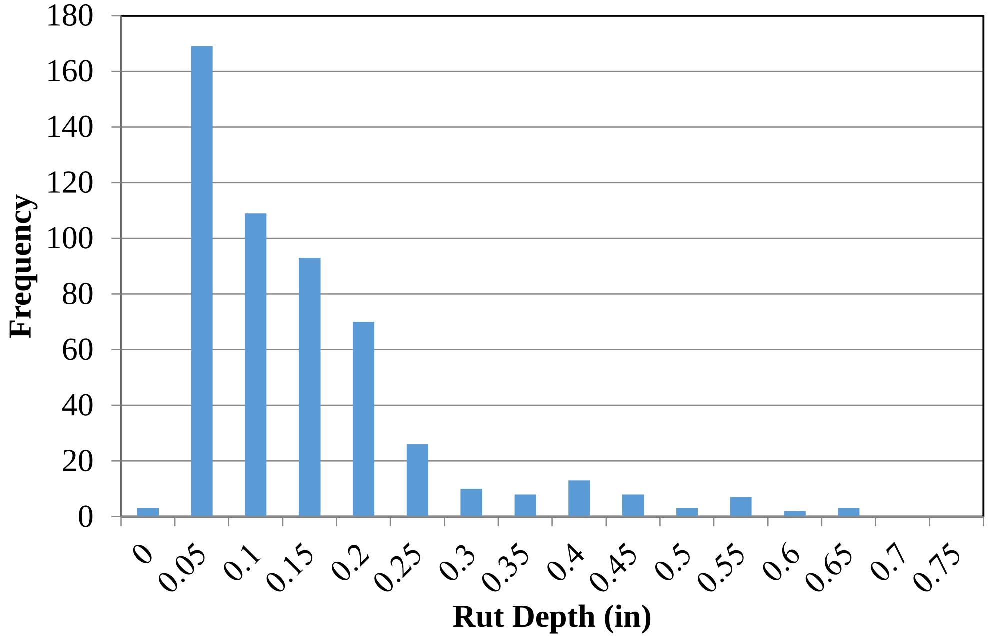

(a) LWP

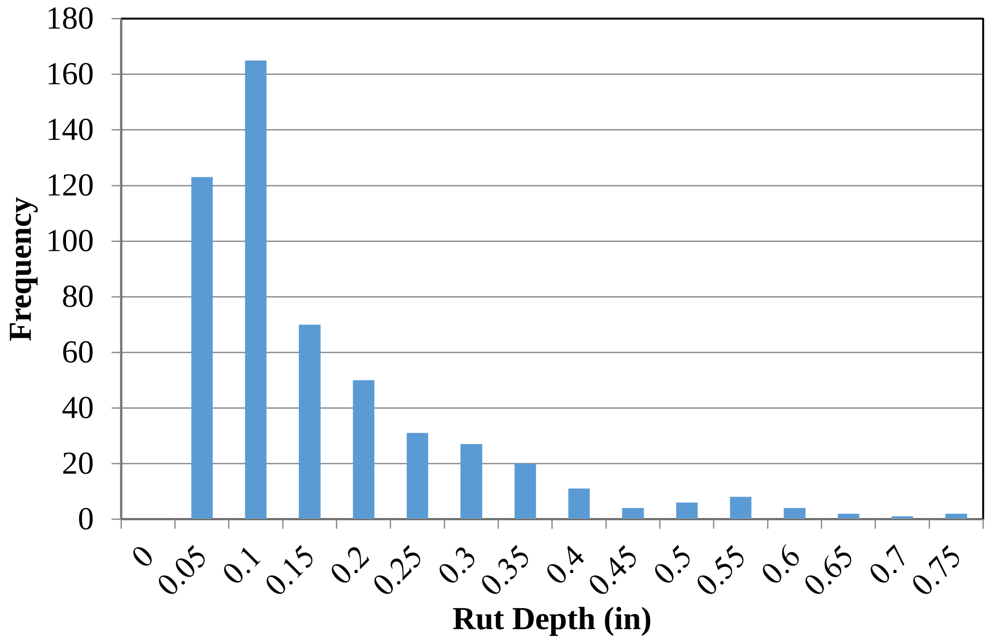

(b) RWP